LBL-9945

WASTE ISOLATION SAFETY ASSESSMENT PROGRAM

TASK 4: COLLECTION AND GENERATION OF TRANSPORT DATA

THEORETICAL AND EXPERIMENTAL EVALUATION OF WASTE TRANSPORT IN SELECTED ROCKS

ANNUAL PROGRESS REPORT

OCTOBER 1, 1978 - SEPTEMBER 30, 1979

R. J. SILVA, L. V. BENSON, A. W. YEE
and G. A. PARKS (STANFORD UNIVERSITY)

SEPTEMBER 30, 1979

BATTELLE/ONWI SUBCONTRACT NO. 45901AK

LAWRENCE BERKELEY LABORATORY
UNIVERSITY OF CALIFORNIA
BERKELEY, CALIFORNIA 94720

This report was prepared by Lawrence Berkeley Laboratory under Subcontract 45901AK with Battelle Memorial Institute, Project Management Divsion, under Contract EY-76-C-06-1830 with the Department of Energy. The subcontract was administered by the Office of Nuclear Waste Isolation.

NOTICE

TABLE OF CONTENTS

LIST OF FIGURES

LIST OF TABLES

THEORETICAL AND EXPERIMENTAL EVALUATION OF WASTE TRANSPORT IN SELECTED ROCKS

R. J. Silva
L. V. Benson
A. W. Yee
G. A. Parks

ABSTRACT

The objective of the program is to establish a basis for the prediction of radionuclide sorption in geologic environments. In FY 79, experimental and theoretical efforts were concentrated on a study of the sorption of cesium on the solid substrates Min-u-sil (quartz) and Belle Fourche clay (montmorillonite).

Cesium sorption isotherms were obtained for the two substrates at 26°C as a function of initial Cs concentration in solution (10^{-3}M to 10^{-9}M), pH (5 to 10) and supporting electrolyte concentration (0.002M, 0.01M, 0.1M, and 1M NaCl and a simulated basalt groundwater in batch-type experiments using crushed material. Characterization of the solid phases included measurements of chemical compositions, particle sizes, surface areas, and cation-exchange capacities. In addition, potentiometric acid/base titrations of the solid phases were conducted in order to determine the acid dissociation and electrolyte exchange constants of the surfaces. Preliminary analysis of the sorption data indicated that while the clay data could be explained by simple mass-action expressions, the quartz data could not.

Theoretical efforts were aimed at developing and testing an electrolyte binding electrical double-layer model to predict sorption isotherms. A computerized version of the model, MINEQL, which simultaneously considers surface and solution chemical equilibria, was brought to operational status. Input parameters required by MINEQL were determined and sorption isotherms for Cs on the Belle Fourche clay were calculated over the same range of parameters as the experimental measurements. Comparisons showed that the model was able to simulate the isotherms quite well except at the lowest pH values for the 0.002M and 0.01M NaCl solutions.

INTRODUCTION

The licensing procedure for the storage of nuclear waste in underground geologic media will involve a safety assessment of the proposed site. Since the time scale being considered is one hundred thousand to a million years, predictions based on realistic modeling studies provide the main avenue of assessment. Modeling studies are only as reliable as the data on which they are based. For the prediction of radionuclide migration in geologic media, it is essential that the systems involved be well understood. Without this information, arguments regarding subsurface storage lack credibility.

The specific goal of Task 4 is the development of quantitative data and methods to describe the radionuclide-geologic media interactions that control the aqueous transport of radionuclides. The method must quantify the relationships of the independent variables to the observed sorption phenomena and develop into a predictive model which is capable of estimating the interaction (i.e., distribution coefficients) of any given radionuclide with a variety of geologic materials and groundwater types. The resultant predictive model can then be incorporated into a more general radionuclide transport model (WISAP Task 3), which includes hydrologic, geosphere and biosphere transport. The general model will be used for the hazards assessment of subsurface storage for any proposed site.

This report covers the FY 79 activities of the Geosciences Group of the Earth Sciences Division, Lawrence Berkeley Laboratory, by R. J. Silva, L. V. Benson, and A. W. Yee in support of Task 4 of the Waste Isolation Safety Assessment Program with contributions from Professor G. A. Parks, consultant from Stanford University.

OBJECTIVE OF PROGRAM

The objective of the program is to develop quantitative data and methods to describe the interactions that control the transport of radionuclides in geologic environments anticipated for terminal radioactive waste storage facilities. It covers a theoretical and experimental evaluation of the physical and chemical processes which govern the sorption phenomena with the goal of

establishing a basis on which distribution coefficients might be reliably predicted for any given radionuclide with a variety of geologic materials and groundwater types.

The migration behavior of a radionuclide is strongly dependent on its chemical properties. Therefore, the effects of oxidation state, speciation and concentration of the radionuclide on the rock-nuclide interactions, i.e., distribution coefficients, need to be determined and any realistic model should include them as input parameters. This means reliable data on the solubilities of radionuclide compounds and complexation constants of radionuclide ions that might form under geologic conditions, e.g., carbonates, hydroxides, phosphates, etc., is needed. In addition, the conditions for oxidation and reduction should be considered.

Further, the chemical and physical properties of the sorbing substrates need to be known in detail since the sorptive properties depend on sorption site densities, effective areas, surface charges, pH, concentration of radionuclide in the liquid phase, concentration and nature of the supporting electrolyte, etc. The effects of these parameters on the rock-nuclide interaction need also to be studied and should be included in the model.

It was concluded that the most effective means of securing information relevant to the migration of radionuclides was to proceed with a study aimed at defining the principle controls on the migration of any radionuclde, including the properties of the substrates as well as the radionuclides, and to attempt to develop a model for predicting distribution coefficients, k_d's based on these relationships. It is believed that by focusing the research effort, results in a usable form will be available in time to meet the licensing requirements of a high level waste terminal storage repository.

PROGRESS REPORTED PREVIOUSLY

The first year of this program, fiscal 1977, was devoted to a review of the literature on the thermodynamic data for aqueous complexes and solid phases of Pu, Np, Am and Cm likely to form in the natural environment and on the transport mechanisms of radionuclides in water-saturated rocks. An

assessment of factors influencing the radionuclide-rock interactions for conditions expected in a terminal storage facility was made. This work was reported in the WISAP Task 4 Contractor Information Meeting Proceedings, September 20-23, 1977 (Apps et al., 1977).

During FY 78, a theoretical and experimental program was developed with the purpose of identifying the most important parameters governing the transport of five actinides (U, Np, Pu, Am and Cm) in the three rock types Umtanum basalt (Hanford), Eleana shale (NTS), and Climax quartz monzonite (NTS). The work demonstrated that the behavior of the actinides in groundwater and their sorption on rocks was dependent on the oxidation state of the actinide and on the solubility of stable precipitates such as oxides, hydroxides, and carbonates. Furthermore, it was determined that secondary alteration phases such as clays and zeolites, appeared to sorb actinides preferentially over other rock-forming minerals such as silica and feldspars. This work was reported in detail in the WISAP Task 4 Contractor Information Meeting Proceedings, October 2-5, 1978 (Silva et al., 1978).

OBJECTIVES FOR FY 79

In FY 79, experimental and theoretical efforts were concentrated on a study of the sorption of cesium on the substrates quartz and montmorillonite - two representative geologic materials that are widely distributed and frequently coat weathered surfaces - in order to begin to delineate the principle parameters in sorption processes. Cesium was chosen for these beginning studies because it exhibits rather simple chemical behavior under most solution conditions. Thermodynamic data (Sillen and Martell 1964; Smith and Martell 1976; Seidell and Linke 1958) indicate that the compounds of cesium likely to form under geologic conditons, i.e., carbonates, hydroxides, chlorides, sulfates, etc., are quite soluble and it is not expected to hydrolize or complex to any extent, except at very high ligand concentrations, and should exist mainly as Cs^+ ion in solution.

The experimental effort was aimed at (1) characterization of the solid phases, (2) a study of the surface chemistry of the solid phases, and (3) the

measurement of Cs sorption isotherms on the two substrates over a wide range of Cs concentrations, pH, and concentration of supporting electrolyte. Sodium chloride was selected as the supporting electrolyte because of the current interest in salt domes as a waste repository. In addition, one mixed electrolyte of a composition similar to the groundwaters from Columbia River basalts was selected to simulate a natural system.

The theoretical effort was aimed at developing and testing an advanced sorption model to predict K_d values. This model is reasonably complete in that physical and chemical interactions are considered simultaneously in the calculation of surface and solution equilibria for major electrolyte ions and dilute solutes and has been successfully used to describe the uptake of metal ions and complexes on solid surfaces. The model requires a rather complete knowledge of the thermodynamic properties of the solid surfaces as well as the solute, e.g., sorption site density, solute solubility and complexation constants, sorption isotherms, etc. However, once a system has been characterized, the model can be used to quantitatively predict sorption effects for other aqueous systems having different compositions for the solute and substrate. It was desired that a computerized version of the model, called MINEQL, be brought to full operational status at LBL. Data from the experimental effort could then be input to the computer code, the sorption isotherms for Cs on the two substrates simulated, and the ability of the model to predict K_d values for this system tested. Discrepancies between the simulated and measured quantities would provide the basis for corrections to the model.

THE ELECTROLYTE BINDING ELECTRICAL DOUBLE LAYER MODEL

INTRODUCTION

Electrical charge acquired by colloid or solid surfaces in aqueous systems plays a significant role in determining the properties of the surfaces. Therefore, methods for predictively modelling the behavior of charged surfaces are important for an understanding of adsorption behavior.

A particle or surface which acquires charge, or an electrical potential different from the solution, accumulates counter charges in order to preserve electrical neutrality. The countercharge may consist simply of a rather loosely bound, diffuse atmosphere of counter ions or a compact layer of bound charge near or at the surface plus a diffuse atmosphere. The surface, compact and diffuse charges together have been called the electrical double layer (e.d.l.). The compact layer counterions are unlikely to approach the surface more closely than some distance, β, probably close to the ionic radii of anions and the hydrated radii of cations (James and Parks 1979). For calculational purposes, the surface charge, σ_0, is taken to be at the surface (s-plane), the compact charge, σ_β, at some distance β from the surface (β-plane) and the diffuse charge, σ_d, at the boundary between the compact and diffuse regions (d-plane).

Gouy and Chapman (Gouy 1910; Chapman 1913; Gouy 1917) derived equations for describing the diffuse distribution of counter ions accumulated near a charge surface; Stern and Grahame (Grahame 1947) extended the model to include specific adsorption or binding of counter ions close to the surface, i.e., the compact layer in addition to the diffuse layer. In recent years, several lines of research and model development involving a variety of surfaces as different as metallic mercury, insoluble oxides, silver halides, proteins, polystyrene latexes, and clays (James and Parks 1979), have converged. For colloids and hydrosols which contain acidic, basic, and amphoteric functional groups at their surfaces, a single, conceptually simple model capable of predictively modeling the development of surface charge and potential, electrolyte adsorption densities and other related properties has emerged, the electrolyte binding electrical double layer model (Yates, Levine and Healy 1974; Davis, James and Leckie 1978).

DESCRIPTION OF MODEL

In order to develop a description of the e.d.l., it is necessary to formulate the reactions for the development of surface charge on the solid surfaces. A variety of acidic, basic, and amphoteric hydroxyl groups are present on oxides, hydroxides, and silicates. It is generally considered that the

surface charging mechanism for oxides is the adsorption of protons or hydroxyl ions by ionizable surface groups to form positive or negative sites. The resulting surface charge, which depends on an excess of one type of charge site or the other, is a function of the solution pH. For this reason, H^+ and OH^- are considered the potential determining ions, p.d.i.

Clays and zeolites contain OH sites, but, in addition, their surface charge properties may be dominated by less localized charge distributions. The structure consists of SiO_4, AlO_6 and AlO_4 groups, bonded together by varying degrees of oxygen sharing. In many resulting structures, there is a net deficiency of positive charges which may be associated with a particular AlO_4 group but not with any particular oxygen ion. Such charge may not be best described as an ionizable site, in the same sense as a particular OH group, but this interpretation has been applied with reasonable success (James and Parks 1979).

As part of the development of the model, it is customary to write local equilibrium reactions and intrinsic (thermodynamic) constants for simple ionization reactions of the surface sites (S), i.e.,

$$SOH_2^+ \rightleftharpoons SOH + H_s^+; \quad K_{a_1}^{int} = \frac{(SOH)(H^+)_s}{(SOH_2^+)} \tag{1}$$

$$SOH \rightleftharpoons SO^- + H_s^+; \quad K_{a_2}^{int} = \frac{(SO^-)(H^+)_s}{(SOH)} \tag{2}$$

where the subscript, s, denotes at the surface. The first reaction dominates at high acid concentrations while the second dominates in near neutral and alkaline solutions.

In addition to reactions involving protons and hydroxyl ions, electrolyte counter ions could interact directly with the surface and adsorb to neutralize specific sites. The formation of surface complexes readjust the acid-base equilibrium and affects the proton balance. To account for specific adsorption

of electrolyte ions, e.g., Na^+ and Cl^-, the formation of ion pairs or surface complexes at the charged sites is assumed, i.e.,

$$SO^- + Na_s^+ \rightleftharpoons SO^-Na^+; \quad K_{Na^+}^{int} = \frac{(SO^-Na^+)}{(SO^-)(Na^+)_s} \tag{3}$$

$$SOH_2^+ + Cl_s^- \rightleftharpoons SOH_2^+Cl^-; \quad K_{Cl^-}^{int} = \frac{(SOH_2^+Cl^-)}{(SOH_2^+)(Cl^-)_s} \tag{4}$$

The protons involved in the surface reactions are assumed to be in the surface plane and the electrolyte ions to lie in the compact layer at a distance β from the surface. The protons in the suface plane and the Na^+ and Cl^- ions in the β plane are distinguished from those in the bulk solution because the difference in the electrical potentials between the surface and bulk solution, Ψ_0, and the β plane and solution, Ψ_β, result in a difference in the chemical potential of the ions. Their activities are modified by the electrical work necessary to bring them from the bulk solution to the plane in which they react. Hence, the activities at the surface are related to the activities in solution by (Stumm and Morgan 1970),

$$(H^+)_s = (H^+)_{aq}\exp(-e\Psi_0/kT) \tag{5}$$

$$(Na^+)_s = (Na^+)_{aq}\exp(-e\Psi_\beta/kT) \tag{6}$$

$$(Cl^-)_s = (Cl^-)_{aq}\exp(+e\Psi_\beta/kT) \tag{7}$$

where the subscripts s and aq refer to activities at the surface and in the bulk solution, respectively, e is the unit electronic charge, k is the Boltzmann constant, and T is the absolute temperature.

The intrinsic constants are related to operational reaction quotients, Q, through the modification of equations (1)-(4) using equations (5)-(7), i.e.,

$$Q_{a_1} = \frac{(SOH)(H^+)_{aq}}{(SOH_2^+)} = K_{a_1}^{int} \exp(+e\Psi_o/kT) \tag{8}$$

$$Q_{a_2} = \frac{(SO^-)(H^+)_{aq}}{(SOH)} = K_{a_2}^{int} \exp(+e\Psi_o/kT) \tag{9}$$

$$Q_{Na^+} = \frac{(SO^-Na^+)}{(SO^-)(Na^+)_{aq}} = K_{Na^+}^{int} \exp(-e\Psi_\beta/kT) \tag{10}$$

$$Q_{Cl^-} = \frac{(SOH_2^+Cl^-)}{(SOH_2^+)(Cl^-)_{aq}} = K_{Cl^-}^{int} \exp(+e\Psi_\beta/kT) \tag{11}$$

These latter reactions, 10 and 11, may be written as exchange reactions which are more useful for analyses of surface charge data, i.e.,

$$SOH + Na_s^+ \rightleftarrows SO^-Na^+ + H^+_s \tag{12}$$

The corresponding intrinsic exchange constants, ${}^*K^{int}$, and exchange reaction quotients, ${}^*Q$, are:

$${}^*Q_{Na^+} = \frac{(SO^-Na^+)(H^+)_{aq}}{(SOH)(Na^+)_{aq}} = {}^*K_{Na^+}^{int} \exp \frac{e\Psi_o - e\Psi_\beta}{kT} \tag{13}$$

and

$${}^*Q_{Cl^-} = \frac{(SOH)(H^+)_{aq}(Cl^-)_{aq}}{(SOH_2^+Cl^-)} = {}^*K_{Cl^-}^{int} \exp \frac{e\Psi_o - e\Psi_\beta}{kT} \tag{14}$$

Thus, because of the surface charge and double layer potential, the distribution of ions between surface and solution are not given by a simple equilibrium constant but by a variable activity or concentration quotient. This quotient is the product of an intrinsic constant applicable when the surface charge and potential are zero and a variable Boltzman term which depends on the state of

charge or potential of the surface. In principle, the intrinsic constants and reaction quotients are determined by the activities of the reacting species. However, since there is no theory for calculating the activity coefficient of the surface species SOH, SO^-, SO^-Na^+, and $SOH_2^+Cl^-$, the practice has been to substitute the concentrations of these species for their activities in calculations (see for example, equations 22, 25, 27, and 30).

Additional solute ions are handled in a similar manner as for NaCl with similar sets of equilibrium equations and intrinsic exchange constants. The solute cations are allowed to compete with H^+ and Na^+ for surface sites. It is also possible to include simultaneously in the model other ionizable adsorption sites which exhibit different intrinsic ionization and exchange constants. However, the relative amounts of the different types of sites need to be known.

SURFACE CHARGE

The surface charge, σ_0, represents the net number of protons released or consumed by all surface reactions including electrolyte ion binding reactions as well as ionization of the surface to form the species SO^- and SOH_2^+. Hence, surface charge is determined by the concentration of reacted sites,

$$\sigma_0 = B([SOH_2^+] + [SOH_2^+Cl^-] - [SO^-] - [SO^-Na^+]) \quad (15)$$

and the charge due to specific adsorption is given by,

$$\sigma_\beta = B([SO^-Na^+] - [SOH_2^+Cl^-]) \quad (16)$$

where B is a factor for conversion from concentrations, moles/liter, to surface charge, μ coulombs/cm^2.

$$B = \frac{10^6 F}{A}$$

where F = Faraday constant and A = surface area (cm^2/ℓ) of the solid substrate

containing the sites. For the species (SO^-Na^+) and ($SOH_2^+Cl^-$), the SO^- and SOH_2^+ are considered to be at the surface and contribute charge to the S-plane, while the Na^+ and Cl^- are in the compact layer and contribute charge to the β-plane.

The surface species are distributed among the total number of sites available. The total number of sites is then

$$N_s = [SOH] + [SOH_2^+] + [SOH_2^+Cl^-] + [SO^-] + [SO^-Na^+] \tag{17}$$

Electrical neutrality requires that

$$\sigma_o + \sigma_\beta + \sigma_d = 0 \tag{18}$$

The generalized relationship between diffuse layer charge and Ψ_d for a $z_+ : z_-$ electrolyte at 25°C is (Hunter and Wright 1971),

$$\sigma_d = -0.0587\sqrt{C}\left[\frac{\Psi_d}{|\Psi_d|}\right]\left[\frac{1}{z_+}\left(\exp\left(-z_+e\frac{\Psi_d}{kT}\right)-1\right)-\frac{1}{z_-}\left(\exp\left(-z_-e\frac{\Psi_d}{kT}\right)-1\right)\right]^{1/2} \tag{19}$$

where

C = electrolyte concentration

Ψ_d = mean potential at the start of the diffuse layer

e = unit electronic charge

There are two planes of fixed charge, the surface plane, σ_o, and the plane of bound counter ions, σ_β. The separation of charge allows the use of conventional molecular capacitor models (Grahame 1947) to relate charge density to potential gradient, i.e.,

$$\Psi_o - \Psi_\beta = \frac{\sigma_o}{C_1} \qquad \Psi_\beta - \Psi_d = -\frac{\sigma_d}{C_2} \tag{20}$$

where C_1, and C_2 are the integral capacitances of the surface to β and the β to d portions of the compact layer, respectively.

DETERMINATION OF INTRINSIC SURFACE IONIZATION AND EXCHANGE CONSTANTS

The intrinsic acid ionization and exchange constants needed for the model are not amenable to direct measurement since the surface activities of the reacting ions, e.g., $(H^+)_s$ and $(Na^+)_s$, are not directly measurable. However, the constants can be estimated from experimental acid-base titration data obtained on aqueous suspension of the solid material over a wide range of pH at several different electrolyte concentrations.

During acid and/or base titrations, a surface charge may be acquired by the solid surfaces if the transfer of positive and negative potential determining ions, e.g., $[H^+]$ and $[OH^-]$, is nonstoichiometric. The total net surface charge is the difference in the concentrations of the positive and negative sites, i.e.,

$$\sigma_o = B([C_A - C_B] - [C_H - C_{OH}]) \qquad (21)$$

C_A and C_B are the total hydrogen ion and/or hydroxyl ion concentrations added to reach a point on the titration curve and C_H and C_{OH} are the measured concentrations of H^+ and OH^- at that point. For amphoteric surfaces, a point of zero charge (PZC) should be observed corresponding to zero net charge on the solid surface. Curves of pH versus amount of acid and/or base added for each of several electrolyte concentrations should intersect at a unique pH, the pH of the PZC. At lower pH values, the next charge is positive corresponding to the formation of an excess of positively charged surface sites, e.g., SOH_2^+ and $SOH_2^+Cl^-$, while at higher pH values the net charge is negative corresponding to an excess of negatively charged sites, e.g., SO^- and SO^-Na^+. At the PZC, the concentration of positive and negative sites are equal. Their concentrations are usually small but depend on the actual ionization and exchange constants of the sites. Furthermore, σ_o is dominated by uncomplexed species when the electrolyte concentration is very low and by complexed species when the electrolyte concentration is high. Thus, by selection of the appropiate range of pH and electrolyte concentrations, the experimental σ_o provides an estimate of the surface concentrations of one of four possible species that is dominant.

Surface Ionization Constants

At low electrolyte concentrations, the surface charge may be approximated as being due to simple acid dissociation, i.e., reactions (1) and (2). For pH values less than the PZC, the positive sites, SOH_2^+, are dominant and

$$(SOH_2^+) \cong \frac{\sigma_o}{B}, \quad (SOH) \cong \frac{N_s - \sigma_o}{B} \tag{22}$$

where total number of sites, N_s, is expressed in terms of charge/cm^2. Substitution in equation (8) gives

$$K_{a_1}^{int} \cong \frac{\frac{N_s - \sigma_o}{B} (H^+)_{aq}}{\frac{\sigma_o}{B}} \exp(-e\psi_o/kT) \cong Q_{a_1} \exp(-e\psi_o/kT) \tag{23}$$

In negative logarithmic form

$$pK_{a_1}^{int} = pH + \log \frac{\alpha_+}{1 - \alpha_+} + \frac{e\psi_o}{2.3kT} = pQ_{a_1} + \frac{e\psi_o}{2.3kT} \tag{24}$$

where

α_+ = fractional ionization of the positive site $\cong \frac{\sigma_o}{N_s}$

Since the surface ionization constants are functions of both the surface ionization (or degree of ionization) and the electrolyte concentration, plots of pQ_{a_1} versus σ_o (or α_+) for each electrolyte concentration are first made. Smooth curves through the experimental points can be extrapolated to $\sigma_o = \alpha_+ = 0$ and provisional $pK_{a_1}^{int}$ values obtained for each electrolyte concentration. These provisional $pK_{a_1}^{int}$ values are then plotted as a function of electrolyte concentration, C, and extrapolation to C = 0 results in an estimate of $pK_{a_1}^{int}$.

As previously mentioned, zero surface charge does not mean zero concentration of charged sites but only equal concentrations of positively and

negatively charged sites, e.g., $SOH_2^+ = SO^-$. Thus, the approximation,

$$\left[SOH_2^+\right] \cong \frac{\sigma_o}{B}$$

is not valid for small values of σ_o and the calculated pQ_{a_1} diverges to infinity. Extrapolation to $\sigma_o = 0$ is made assuming a smooth, continuous variation of pQ_{a_1} with σ_o and the sharp divergence of the calculated pQ_{a_1} at small σ_o is ignored. This is a reasonable assumption since the function,

$$pK_{a_1}^{int} = pQ_{a_1} + \frac{e\Psi_o}{kT}$$

is a well behaved and a slowly varying linear function of σ_o at small values of σ_o.

Similar considerations for the region pH > PZC, where σ_o is negative, give

$$(SO^-) \cong \frac{|\sigma_o|}{B}, \quad (SOH) \cong \frac{N_s - |\sigma_o|}{B}, \text{ and } \alpha_- \cong \frac{|\sigma_o|}{N_s} \tag{25}$$

yields

$$pK_{a_2}^{int} \cong pH - \log \frac{\alpha_-}{1 - \alpha_-} + \frac{e\Psi_o}{2.3kT} \cong pQ_{a_2} + \frac{e\Psi_o}{2.3kT} \tag{26}$$

Again plots of pQ_{a_2} versus σ_o or α_- can be extrapolated to zero surface charge and electrolyte concentration to estimate $pK_{a_2}^{int}$

Exchange Constants

At high electrolyte concentrations, surface complexes dominate the contribution to surface charge formation, i.e, $SOH_2^+Cl^-$ and SO^-Na^+. For the region pH > PZC, SO^-Na^+ is assumed dominant and

$$(SO^-Na^+) \cong \frac{|\sigma_o|}{B}, \quad (SOH) \cong \frac{N_s - |\sigma_o|}{B} \quad \alpha_- \cong \frac{|\sigma_o|}{N_s} \tag{27}$$

Substitution of these equations into equation (13) yields

$$ {}^{*}K^{int}_{Na^+} \cong \frac{(H^+)_{aq}(\alpha_-)}{(Na^+)_{aq}(1-\alpha_-)} \exp \frac{e\Psi_\beta - e\Psi_o}{kT} \cong {}^{*}Q_{Na^+} \exp \frac{e\Psi_\beta - e\Psi_o}{kT} \qquad (28) $$

In negative logarithmic form,

$$ p^{*}K^{int}_{Na^+} \cong pH - \log \frac{\alpha_-}{1-\alpha_-} + \log(Na^+) + \frac{e(\Psi_o - \Psi_\beta)}{2.3kT} \qquad (29) $$

$$ \cong p^{*}Q_{Na^+} + \frac{e(\Psi_o - \Psi_\beta)}{2.3kT} $$

Similar considerations for the region pH < PZC at high electrolyte concentration, where

$$ (SOH_2^+Cl^-) \cong \frac{\sigma_o}{\beta}, \quad (SOH) \cong \frac{N_s - \sigma_o}{\beta}, \quad \text{and} \quad \alpha_+ \cong \frac{\sigma_o}{N_s}, \qquad (30) $$

give

$$ p^{*}K^{int}_{Cl^-} \cong pH + \log \frac{\alpha_+}{1-\alpha_+} - \log(Cl^-) + \frac{e(\Psi_o - \Psi_\beta)}{2.3kT} \qquad (31) $$

$$ \cong p^{*}Q_{Cl^-} + \frac{e(\Psi_o - \Psi_\beta)}{2.3kT} $$

Again, plots of $p^{*}Q_{Na^+}$ and $p^{*}Q_{Cl^-}$ versus σ_o (or α_- and α_+) can be extrapolated to zero surface charge (or α) and high electrolyte concentration (usually taken as 1M) and the intrinsic exchange constants estimated.

THE COMPUTER PROGRAM MINEQL

DESCRIPTION

The components of water solutions are more often than not distributed among many species. The calcium in hard water, for instance, is likely to be present as bicarbonate and sulfate complexes in addition to free $Ca^{2+}(aq)$.

In an unsaturated solution of $CaSO_4$, exposed to atmospheric CO_2, for example, the components of the solution and species among which they are distributed are

H_2O: $H^+ OH^-$

Ca^{2+}: Ca^{2+}, $CaHCO_3^+$, $CaCO_3^o$ (aq), $CaSO_4^o$ (aq)

SO_4^{2-}: SO_4^{2-}, HSO_4^-, $CaSO_4^o$ (aq)

CO_3^{2-}: CO_3^{2-}, HCO_3^-, $H_2CO_3^o$ (aq), $CaHCO_3^+$, $CaCO_3^o$ (aq)

If the analytical concentration of each component is known, the concentration of all eleven species can be calculated, since all are related through mass balances for each component, stability constants for each complex, and dissociation constants for water and the weak acids. Even in this simple system, simultaneous solution of the set of constraining equations is tedious.

MINEQL is a computer code designed to accept a list of components of a solution and their total analytical concentrations, solve the appropriate set of mass balance and equilibrium constant expressions, and produce a list of the identities and concentrations of all species formed by interaction among the components and between them and/or water.

An internal data set, THRM.DAT, contains the compositions and stability constants for most complexes (and solid precipitates) likely to form from commonly encountered components. MINEQL scans for possible interactions and searches THRM.DAT to select those for which stability constants are available. It is not

necessary to instruct the program that complexes will form if the data exist in THRM.DAT. (It is a simple matter to add new complexes or to edit stability constants through the input data set as well.)

The minimum essential input data set includes the list of components and total concentrations, a measure of total hydrogen and hydroxyl ions and the fixed pH and an ionic strength (assumed fixed in most current versions of MINEQL). Data processing involves reading the input solution composition, identifying the complexes expected, fetching the required stability constants, connecting the stability constants to the ionic strength imposed, and deriving the appropriate mass balance expressions. The resulting set of stability and mass balance expressions is solved by the Newton Raphson method, using satisfaction of the mass balances as the criterion of successful solution. The mathematical methods have been described in detail (Westall, Zachary and Morel 1976)

Precipitation and dissolution of solids can be included by extending the mass balance expressions to include solids. The output then includes the mass of precipitates formed or dissolved. Redox reactions are included as well by including the electron as a "component". Changes in computational constraints appropriate for the presence of solids or occurrence of redox reactions are part of the program; they are triggered by flags entered with the input information.

Simple sorption can be incorporated by writing the reaction as complexation with a surface site, or more specifically, if S: represents an sorption site, adsorption of $Hg^{++}(aq)$ could be represented as

$$Hg^{++}(aq) + S: = Hg:S \qquad (32)$$

If Hg actually adsorbs the dihydroxo complex, the reaction would be written

$$Hg(OH)_2(aq) + S: = Hg(OH)_2 : S \qquad (33)$$

For convenience in programming, this reaction would be written in the equivalent form,

$$Hg^{++}(aq) + 2\ H_2O + S: = S:Hg(OH)_2 + 2\ H^+ \qquad (34)$$

Any reaction can be incorporated into MINEQL if the reaction stoichiometry and equilibrium constants are known.

Ion exchange by clay can be introduced by treating the clay surface as a weak acid, SOH, which can dissociate,

$$SOH \rightleftharpoons SO^- + H_s^+; \quad K_{a_2}^{int} = \frac{(SO^-)(H^+)_s}{(SOH)} \qquad (2)$$

or adsorb Na^+ in exchange for H^+,

$$SOH + Na_s^+ \rightleftharpoons SO^-Na_s^+ + H_s^+; \quad {}^*K_{Na^+}^{int} = \frac{(SO^-Na^+)(H^+)_s}{(SOH)(Na^+)_s} \qquad (12)$$

$$SOH + Cs_s^+ \rightleftharpoons SO^-Cs^+ + H_s^+; \quad {}^*K_{Cs^+}^{int} = \frac{(SO^-Cs^+)(H^+)_s}{(SOH)(Cs^+)_s} \qquad (35)$$

The MINEQL input data includes a new component, SOH, and the total concentration of SOH in the system. This concentration is equivalent to the cation exchange capacity of the system. The input must also include the information in equations 2, 12, and 35 including stoichiometry and equilibrium constants, since THRM.DAT includes no adsorption or exchange information.

Through manipulation of the input information, any of the common modes of describing cation exchange can be simulated. If the clay is assumed totally saturated with either Na^+ or Cs^+ at all times (SO^- and SOH << SO^+Na^+ or SO^-Cs^+), $K_{a_2}^{int}$ can be set arbitrarily small (SOH made a strong acid) and ${}^*K_{Na^+}^{int}$ and ${}^*K_{Cs^+}^{int}$ set >> $K_{a_2}^{int}$ with the absolute values arbitrary but ${}^*K_{Cs^+}^{int}/{}^*K_{Na^+}^{int}$ equal to the Cs/Na exchange constant. The exchange constant which describes the reaction

$$SO^-Na_s^+ + Cs_{aq}^+ \rightleftharpoons SO^-Cs_s^+ + Na_{aq}^+$$

must be determined experimentally. For calculational purposes, the selectivity coefficient corrected for activities in solution, $K^{a}_{Cs/Na}$, is usually used.

Experimental values of $K^{a}_{Cs/Na}$ are often sensitive to pH and the ratio of Cs^+ to Na^+ on the clay, i.e.,

$$\frac{[SO^-Cs^+]}{[SO^-Na^+]} \quad \text{or} \quad \frac{[SO^-Cs^+]}{[SO^-Cs^+] + [SO^-Na^+]}$$

pH dependence can be introduced by experimental determination of $K^{int}_{a_2}$ as well as of $^*K^{int.}_{Na+}$.

Sensitivity to loading requires a solid-state activity correction which is beyond the state-of-the-art. A regular solution model has been described (Truesdell and Christ 1968; Garrels and Christ 1956) through which a semi-empirical solid state activity coefficient is introduced. This has not yet been used in MINEQL (to our knowledge).

Particles in water are electrically charged through partial dissociation of SiOH or AlOH groups or release of exchangeable ions. A correction for the effect of surface charge on the equilibrium constants of reactions near surfaces has been incorporated into MINEQL (Davis, James and Leckie 1978), i.e., the electrical double layer model.

Surface Charge Effects

If surface charge is finite, there must be a potential difference between the surface and the bulk solution. The resulting difference in activities of the ions near the surface and far from the surface is the work that must be done to bring the ion from zero potential to the surface potential, i.e. $Z_i e^{\Psi}_0/kT$, where Z_i is the charge on the ion. These corrections have been discussed previously, e.g., equations 5, 6 and 7.

Equation 8 can be written:

$$K^{int}_{a_1} = \frac{(SOH)(H^+)_{aq}}{(SOH_2^+)} \exp(-e^{\Psi}_0/kT)$$

The exponential term plays the same algebraic role as do the chemical species, thus the surface charge correction can be incorporated into MINEQL by including $\exp(-Ze\psi_o/kT)$ as a component and including that "component" in defining the composition of complexes. A positive site produced by adsorption of H^+ onto SOH would be composed of one each of three components,

$$(SOH),\ (H^+),\ \left(\exp \frac{e\psi_o}{kT}\right),$$

for example.

In the version of MINEQL developed by Davis, James and Leckie, to incorporate the surface charge correction, the Gouy-Chapman-Stern Grahame model of electrical double layer development is adopted. The equation relating surface charge, area, and potential are added to the chemical constraints and solved simultaneously. Charge is assumed to develop by ionization of surface sites; and potential develops in response to charge as required by the electrical double layer constraints. Adsorbing ions are assumed to approach the surface less closely than protons and a smaller potential is used in the exponential term which corrects for their altered chemical potential.

Input for computations involving electrochemical adsorption must include surface area, total site concentration, and the reaction and equilibrium constants responsible for charge development and adsorption in addition to the composition of the solution phase (Davis, James and Leckie 1978).

EXPERIMENTAL METHODS AND RESULTS

PREPARATION OF SOLUTIONS AND SOLID PHASES

Solutions

In order to investigate the effects of pH and supporting electrolyte concentration on the Cs sorption process, four solutions were first prepared with concentrations of 0.002M, 0.01M, 0.1M, and 1M in NaCl. In addition, a synthetic groundwater (SGW) was prepared with the chemical composition given

in Table 1 and had an ionic strength of 0.003M. The composition was similar to the groundwaters within Columbia River basalts and allowed a comparison of the effects of a mixed electrolyte of a more natural composition with the NaCl.

TABLE 1. Chemical Composition of Synthetic Groundwater

Component	Na	K	Ca	Mg	Fe	Al	HCO_3	Cl	SO_4	SiO_2
Concentration (mg/l)	30.0	5.0	10.0	5.0	0.1	0.01	65.0	27.8	24.0	25.0

Care was taken in the preparation of solutions so as not to introduce contaminants. All solutions were prepared with doubly-distilled deionized water from which CO_2 had been removed by boiling for about one hour followed by flushing with Ar. Ultrapure salt, obtained from Alfa Division of Ventron Corp., was used for preparing the NaCl solutions; analytical grade $NaHCO_3$, $CaSO_4 \cdot 2H_2O$, $CaCl_2$, KCl, $MgSO_4 \cdot 7H_2O$, $AlCl_3 \cdot 6H_2O$, $FeCl_2 \cdot 4H_2O$, and H_4SiO_4, from Mallinckrodt Inc., were used to prepare the synthetic groundwater.

Six portions of each of the five electrolyte solutions had their pH adjusted to 5, 6, 7, 8, 9, or 10 with ultrapure NaOH, from Alfa Division of Ventron, and were placed in an argon filled, inert atmosphere box. Since the effect of dissolved CO_2, i.e., HCO_3^- and CO_3^{2-} ions, on the sorptive properties of the solid substrates was unknown, it was decided to exclude CO_2 from the system. A final pH adjustment was made in the inert box just prior to use in the Cs sorption experiments.

Solid Phases

Min-u-sil

The Min-u-sil (SiO_2) was obtained from the Pennsylvania Glass Sand Corporation in the form of a fine powder (nominal 5 micron particle size). It was prepared from natural quartz sand from Berkeley Springs, West Virginia, by grinding in a silica lined ball mill using silica pebbles. Selection of

particle size was by air separation in a cyclone separator. The silica was first boiled twice in a 6M HNO_3-HCl mixture to dissolve and remove any iron contaminant introduced in the manufacturing process. After settling each time, the very finely suspended material was decanted off. The remaining leached material was filtered out on a fine glass frit and washed repeatedly with first 0.1M HCl and then deionized-distilled water. The material was then washed with 2M NaOH followed by 0.5M NaCl to produce the sodium form and repeatedly washed with deionized-distilled water to remove the excess salt. Each water wash was tested for residual chloride by adding $AgNO_3$. The washing was continued until no AgCl precipitate formed. The purified silica was then dried in an oven at 110°C, heated to 450°C for 12 hours to destroy organic material, and stored in a desiccator.

Belle Fourche Clay

The Belle Fourche clay (montmorillonite #27) was obtained from Ward's Natural Science Establishment, Inc., Rochester, N. Y. Three hundred grams of clay were first soaked in 8 liters of deionized water overnight with gentle stirring using an electric stirrer. The suspension was then filtered through a 350 mesh stainless steel screen to remove the coarse particles. The viscous filtrate was then diluted to a total volume of 16 liters and divided equally into four 4-liter beakers. The clay suspension was allowed to stand undisturbed for 48 hours. At the end of 48 hours the unsettled clay suspension was carefully decanted and the settled material discarded. The clay suspension was placed in 8-oz plastic bottles and centrifuged at 5,000 rpm for ten minutes using a Sorval high-speed preparative centrifuge. Particles less than 1 micron remained in the supernatant and were discarded (Jackson 1975, p.110).

To remove the iron and aluminum oxides on the clay, extraction with acid ammonium oxalate was selected (McKeague and Day 1966). This method was used in preference to the citrate-dithionite method because of less possible structural alteration of the clay. The clay particles were stirred in 8 liters of 0.2M ammonium oxalate solution and the pH adjusted to 4.0 using 1.0N HCl. At the end of 24 hours, the clay suspension was centrifuged and rinsed twice with deionized water. To remove the amorphous silica imbedded between the layers

of the clay particles, hot caustic extraction was employed (Jones and Bower 1977, p.197). To each of the plastic centrifuge bottles containing the clay, 0.5M NaOH was added. The mixtures were stirred and placed in a 95°C water bath for 1 hour. At the end of the extraction period, they were centrifuged and washed. To fully convert the clay particles into the sodium form, the solid phase was rinsed twice with 0.5M NaCl and then once with deionized water to remove the excess salt before dialysis. The sodium clay, still containing large amounts of salt, was placed in a cellulose acetate dialysis bag and dialyzed against deionized water in a 4-liter beaker with constant agitation (Keren, Gast and Barnhisel 1977). To shorten the dialysis time, frequent 30-minute water changes were necessary. The silver nitrate method was used to monitor the progress of dialysis. When no cloudy precipitate was formed on addition of 0.1N $AgNO_3$ to the dialysate, dialysis was considered to be complete. The purified clay suspension was then removed from the dialysis bag and diluted with deionized water and stored in a plastic container for subsequent experiments.

Characterization of Solid Phases

Chemical Analyses

In order to check the purity of the samples, both the Min-u-sil and the Belle Fourche clay were sent to John Husler of the University of New Mexico for chemical analyses.

Sili a was determined gravimetrically by fusion with Na_2CO_3, dehydration with HCl, and weighing as SiO_2. Sulfur was determined on the filtrate by precipitation with $BaCl_2$ and weighing as $BaSO_4$ (Koltoff, Sandell, Meeham and Bruckenstein 1969, p.602). Total Fe, Al, Mg, Ca, Na, K, Ti, Mn, and Sr were determined by atomic absorption spectrophotometry by a method developed by Husler (Husler 1972). The P was determined by a colorimetric method (Husler 1972). The H_2O^- was determined by weight loss at 110°C and the loss on ignition, H_2O^+, was determined by weight loss from 110°C to 1000°C. The Fe^{2+} was determined by volumetric titration with standardized $K_2Cr_2O_7$ (Koltoff, Sandell,

Meeham and Bruckenstein 1969, p.839). In addition, trace element analysis of the clay was done by Helen Michels of LBL by neutron activation analysis. The results of the analyses are given in Table 2.

The chemical composition of the clay was typical for a smectite and very similar to a reported composition of smectite from Upon, Wyoming (Grim 1968, p.578). The K concentration in our sample was considerably less than the Upon clay (0.6%) however, probably due to replacement by Na during the processing of our clay. There was no evidence for Cs of sufficient concentration to interfere with the subsequent sorption measurements.

The Min-u-sil contained considerably larger amounts of Fe, Mg, Ca, Na, K, and Al than is usually found in pure quartz; these elements are usually present in the few parts per million range (Deer, Howie, and Zussman 1963. p.191). Our results are consistent with the analyses supplied by the manufacturer, i.e., 99.6% SiO_2, 0.10% Al_2O_3, 0.019% TiO_2, and 0.023% Fe_2O_3. Apparently most of the iron was surface or particulate contamination and was removed during our processing. The proportions of the cations suggest the presence of a small amount (a few tenths of a percent) of other silicate minerals.

Particle Size

Scanning electron microscopy was used by Barry Scheetz of Pennsylvania State University to measure the particle sizes and size distributions of the Min-u-sil and Belle Fourche clay samples. Summarizing the data, the average particle size for the Belle Fourche clay was 1.14 microns with 90% of the particle sizes in the range 0.5 - 2.0 microns; the average size for the Min-u-sil was 2.42 microns with 90% in the range 0.28 - 4.56 microns.

Surface Areas

Total surface area is required in the calculation of layer charges and potentials. Surface area measurements of the purified clay and quartz were performed by the nitrogen adsorption technique, i.e., the BET method (Jackson 1975, p.335). For the clay, approximately 2 milliliters of the stock suspension

TABLE 2. Chemical Composition of Solid Substrates.

Component[1]	Chemical Analysis (%) Min-u-sil	Belle Fourche Clay	Component	Activation Analysis[2] Belle Fourche Clay
SiO_2	98.92	55.73	Al	11.0 ± 0.1 %
Al_2O_3	0.20	22.17	Mg	2.2 ± 0.7 %
Fe_2O_3	0.006	3.71	Ca	< 1.0 %
FeO	--	0.02	Ti	700 ± 320
MgO	0.007	2.18	V	< 37
CaO	0.004	0.65	Dy	2.37 ± 0.05
Na_2O	0.006	2.70	Mn	8.0 ± 0.6
K_2O	0.014	0.023	Na	1.99 ± 0.03 %
H_2O^+	0.22	6.08	K	0.17 ± 0.13 %
H_2O^-	0.04	6.61	Sr	82 ± 36
TiO_2	< 0.05	0.14	U	1.03 ± 0.03
P_2O_5	< 0.01	< 0.01	Th	3.62 ± 0.18
MnO	<0.001	0.002	Sm	3.42 ± 0.02
SrO	<0.003	0.013	La	18.4 ± 0.02
SO_3	<0.1	--	Nd	16.1 ± 1.0
			Mo	1.1 ± 0.5
Total	99.42	100.03	W	2.8 ± 1.4
			Ba	< 12
			Co	0.50 ± 0.06
			Sc	6.12 ± 0.03
			Fe	2.62 ± 0.04 %
			Cr	2.41 ± 0.59
			Rb	3.5 ± 2.4
			Cs	< 0.28
			Ce	32.9 ± 0.7
			Hf	7.56 ± 0.09
			Ta	2.56 ± 0.03
			Yb	1.17 ± 0.02
			Eu	0.23 ± 0.01

1 Reported as shown.
2 ppm except when stated %.

were carefully introduced into a weighed sample holder with the aid of a syringe fitted with teflon tubing. The sample was then freeze-dried. After drying, the sample tube was kept in a 100°C oven overnight to prevent surface adsorption of moisture. The tube was weighed and the actual weight of the clay obtained by subtracting the weight of the sample holder. The surface area determined by this method was 18.1 m^2/gram. For the quartz, 0.5 g samples of the dried material were used. The measured surface area for the Min-u-sil by this method was 3.03 m^2/g.

The value obtained for the clay was considerably lower than the theoretical value of ~800 m^2/g from unit cell dimensions (Grim 1968, p.464; van Olphen 1977, p.254). However, the BET method measures only the exposed external surface area of the particles and not the interlayer surface areas (Grim 1968, p.464). Further, the exposed external surface area of the clay varies with the degree of aggregation, i.e., face-to-face association. Therefore, surface areas obtained by the BET method show a wide variation for clay, e.g., values in the range of 30 - 150 m^2/g (Alymore 1977, p.148). Water vapor adsorption methods are thought to measure both internal and external surface areas for montmorillonite and give values of 150 - 250 m^2/g (Grim 1968, p.265). Aggregation seems also to effect the values. Alternative methods to determine total internal and external surface areas are based on the adsorption of polar organic compounds from the liquid phase, e.g., adsorption of cetyl pyridinium bromide has been used and gave 800 m^2/g (Greenland and Quirk 1962) while ethylene glycol adsorption has been found to give values of 700 - 800 m^2/g for montmorillonite (Morin and Jacobs 1964). Methods based on adsorption of negative ions yielded values of 470 - 560 m^2/g (Edwards and Quirk 1962). With these methods, difficulties are encountered due to surface changes produced by heating and drying, surface contamination, and in obtaining only monolayers of adsorbed molecules. For our modeling calculations, the theoretical value of 800 m^2/g is probably the most appropriate and reliable.

The B.E.T. method does appear to be reliable for the measurement of external surface areas of simple materials such as silica. In fact, some form of silica is frequently used as a standard for calibration.

Cation Exchange Capacities

Cation exchange capacities, CEC, are needed for calculating loading fractions used in data evaluation as well as for measurement of site density for modeling calculations. The Na, K, Ca, Cs, and NH_4 cation exchange capacities were determined for the Belle Fourche smectite and the Min-u-sil. For the clay, the procedure of M. L. Jackson (Jackson 1975, p.253) was closely followed. The method involved washing an accurately weighed sample in a tared centrifuge tube with a 0.5M solution of the chloride salt of the cation to be loaded on the clay. This was followed by five washings with 0.01M salt solution. After centrifugation and removal of the solution phase, the excess 0.01M solution remaining with the sample was determined by again weighing the tube. To desorb Na, K, or Cs, the sample was rinsed with 0.5M NH_4Cl five times with centrifugation between rinsings. For Ca and NH_4 desorption, 0.5M $MgCl_2$ and 0.5M NaCl solutions, respectively, were used. The combined rinse was diluted and the concentration of Na, K, Cs, or Ca determined by atomic absorption using a Perkin Elmer model 306 spectrophotometer. To determine ammonia, three methods were tested. For samples with high cation exchange capacities and therefore high concentrations of ammonium ion, a simple macro-kjeldahl determination could be used directly on the mineral sample. For samples with low exchange capacities, either Nessler's method (Hawk, Oser, and Summerson 1965, p.878) or the Ninhydrin method (Hawk, Oser, and Summerson 1965, p.892) could be used. Nessler's method is about thirty times more sensitive than the Kjeldahl method and can detect NH_3 down to the 1 ppm level. The Ninhydrin method is even more sensitive and can detech NH_3 down to the 10^{-9}M level. Both Nessler's and the Ninhydrin methods involve the formation of colored complexes that can be quantitatively detected spectrophotometrically.

In order to avoid the loss of particles during decantation in processing of the Min-u-sil, the procedure was modified to placement of the samples in a column with a glass fritted disk at the outlet. The weight of the column was determined by weighing. The salt solution used to load the sample with the appropriate cation was poured through the column slowly (~30 ml/hr). The saturated solid was then rinsed with the 0.01M salt solution and the excess solution remaining on the column determined by weighing as before. To elute the

cations, the appropriate desorption solution (given above) was passed through the column. The eluate was collected and the concentrations of cations determined as before. The results of the cation exchange capacity measurements for duplicate samples are given in Table 3.

TABLE 3. Cation Exchange Capacities (meq/100g)

Cation	Na^+	K^+	Ca^{2+}	Cs^+	NH_4^+
Min-u-sil	0.22	0.26	1.25	0.45	0.95 (N)
Belle Fourche Clay	120	131	146	119	91.4 (NH) 97.2 (K)

N = Nessler, K = Kjeldahl, NH = Ninhydrin

Cation exchange capacities of a given mineral vary with a number of factors, e.g., source, pretreatment, etc. A range of 80 - 150 milliequivalents (meq) per 100 g has been reported (Grim 1968, p.189) for smectite. It was expected that all of the cations used in the CEC determinations would give about the same value for the clay (van Olphen 1977, p.255) i.e., 90 - 95 meq/100 g. The discrepancy between NH_4 and the other monovalent ions is bothersome since it was originally felt that the methods for determining ammonia were more reliable than those for the other ions.

The total surface site concentration, N_S, is an input parameter for the calculations using MINEQL, e.g., equations 22, 25, 27, and 30. In the case of clays, the experimental CEC appears to be a good measure of N_S, i.e., nearly all of the hydrogen on the sites has been exchanged for the electrolyte cations (James and Parks 1979). However, for SiO_2, standard methods for measuring CEC underestimate the total number of sites considerably (Allen, Matijevic and Meites 1971). For example, at pH 7 and 1M NaCl electrolyte concentration (typical conditions for loading cations in CEC measurements), only about 10% of the sites may have been converted from the hydrogen form to the sodium form. Calculated site concentrations based on measured surface areas appear to give

a more accurate estimate for N_s (Yates 1975) and it is N_s that is needed as input to MINEQL. Yates has estimated a site density for SiO_2 of 5 sites/nm^2 from structural considerations. Using this value and our measured surface of 3.03 m^2/g, a site concentration of 2.52 meq/100 g was calculated assuming one equivalent is equal to Avogadro's number of sites.

DETERMINATION OF INTRINSIC SURFACE IONIZATION AND EXCHANGE CONSTANTS

Potentiometric Titrations

Potentiometric acid/base titration of a sol provides a direct measure of surface charge, σ_0, through equation 21. From a mass balance of the potential determining hydrogen and hydroxyl ions added to the sol compared to the measured amounts in the solution, the concentration of excess or the deficiency of H^+ ions on the surface can be calculated. As described in the section on the electrolyte binding electrical double layer model, σ_0 can be used to approximate the concentrations of different surface species, i.e., SO^-, SO^-Na^+, SOH_2^+, and $SOH_2^+Cl^-$ under certain conditions of pH and supporting electrolyte concentration. Using this information and the total site density, estimates of the intrinsic surface ionization and exchange constants can be made for input to the computer program MINEQL. Since the surface charge is a function of surface ionization itself, as well as supporting electrolyte concentration, a series of titrations over a wide range of pH and electrolyte concentrations are needed.

Procedures

Titrations were carried out on the acid forms of the Min-u-sil and the Belle Fourche clay. The acid form of the quartz was prepared by washing a few grams in a glass column with 0.1M HCl followed by doubly distilled deionized water to remove the excess acid. In the case of clay, it has been reported that it is nearly impossible to prepare a clay in which all the exchange sites are occupied by hydrogen ions, since Al^{3+} moves from the lattice to exchange positions before saturation with H^+ is completed (Grim 1968, p.210). It was suggested that a better method for preparing the hydrogen form of the clay is by

cation exchange with the hydrogen form of an organic ion exchange resin (Grim 1968, p.210). In our case, an aqueous suspension of the clay (0.02 g/ml) was passed through a 2.5 cm diameter by 14 cm long column of 100 - 200 mesh Dowex 50 x 8 cation exchange resin.

A small polyethylene cell (~200 ml capacity) was used to carry out the titrations under an inert atmosphere of argon and at a temperature of 26°C. Acid/base titrations of the purified water and the NaCl solutions to be used in the quartz and clay titrations were first made in order to detect and eliminate any contaminants in the system that could produce titration errors, e.g., carbon dioxide or acid-base impurities from the reagents. Cyclic titrations with first 0.05M HCl followed by 0.05M NaOH were conducted for two cycles over the pH region 3 - 11. A shift in the equivalence point between cycles of less than the volume of titrant used between successive titration points, 50 microliters, was considered adequate. It was found that the argon (99.998%) obtained from the standard manufacturer's cylinders needed to be purified. The purification system consisted of a CO_2 trap, dilute H_2SO_4 scrubber, a water scrubber, and a drying trap. Slightly improved results were also obtained when ultrapure grades of acid, base, and NaCl were used.

The first step in the titration of the sol was the determination of the pH of 100 ml of CO_2-free, purified water or salt solution, i.e., the initial H^+ ion concentration of the aqueous phase. Then, either 1 gram of clay or 10 grams of quartz was added to the aqueous phase and the pH again measured after stirring for ~ 5 minutes with a magnetic stirrer. For Min-u-sil, small portions, usually 50 microliters, of 0.05M HCl were added in steps until the pH was reduced to about 3.5. The suspension was then back-titrated in steps with 0.05M NaOH until the pH reached 8 - 9. At each step in the titration the resulting pH was measured. It usually required from 5 - 20 minutes for the readings to stabilize after stirring was stopped.

After addition of the clay to the water or NaCl solutions, the pH dropped to 3 or less. Because of the danger of structural alteration, further reduction of the pH with acid was omitted. Therefore, the clay was titrated only with base from the starting pH to pH ~ 11.

Results.

The results of a series of titrations of the Min-u-sil for 6.5×10^{-5}M, 0.001M, 0.01M, and 0.1M concentrations of NaCl are shown in Figure 1. The first value was the residual Na concentration in the sample with no sodium chloride added as determined by atomic absorption. For clarity, only the back titrations with base are shown. The curves for the four electrolyte concentrations converge at low pH values and cross at a pH of about 3.9, i.e., the point of zero charge.

The results obtained for the Belle Fourche clay at several electrolyte concentrations are shown in Figure 2. The residual Na concentration in the clay sample with no sodium chloride added was 0.0002M. A PZC was not observed in the pH range investigated. The titration curves appear to be made up of more than one component. One site being neutralized from the initial pH to pH ~ 5.5 and the other from pH ~ 5.5 to ~ 11. To distinguish between the two sites, the first is frequently called SOH sites and the second TOH sites. This is typical behavior for montmorillonite and is usually interpreted as resulting from the successive neutralization of two energetically different exchange sites with differing acid constants (Garrels and Christ 1956).

Figure 3 shows the surface charge as a function of pH calculated for Min-u-sil from the titration data, while Figure 4 is a similar plot for the Belle Fourche clay. The surface charge was calculated for each titration point using equation 21, i.e.,

$$\sigma_o = \frac{10^6 F}{A}\left[(H^+)_o - (OH^-)_o\right]\frac{V_o}{\gamma_o} + C_A V_A - C_B V_B - \left[(H^+)_1 - (OH)_1\right]\frac{V_1}{\gamma_1} \quad \mu C/cm^2. \tag{36}$$

F = Faraday constant, coulombs/equivalent

A = total surface area of sample, cm^2

$(H^+)_o$, $(OH^-)_o$ = measured H^+ and OH^- ion activities of the starting electrolyte solution of starting volume V_o (liters)

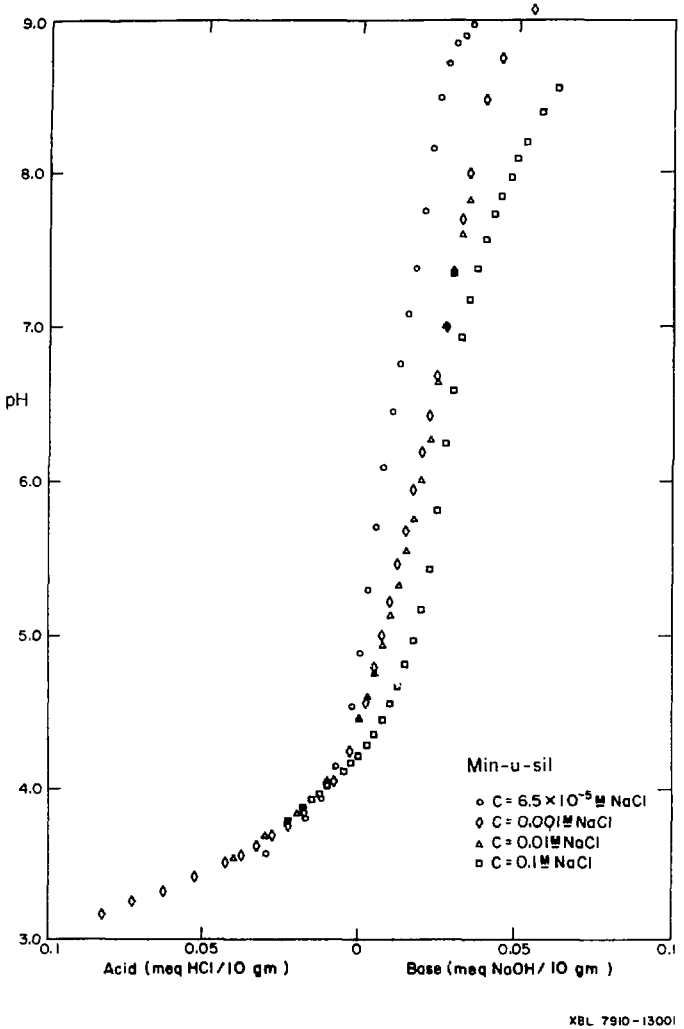

FIGURE 1. Potentiometric acid/base titration curves for Min-u-sil in aqueous suspension as a function of NaCl electrolyte concentration.

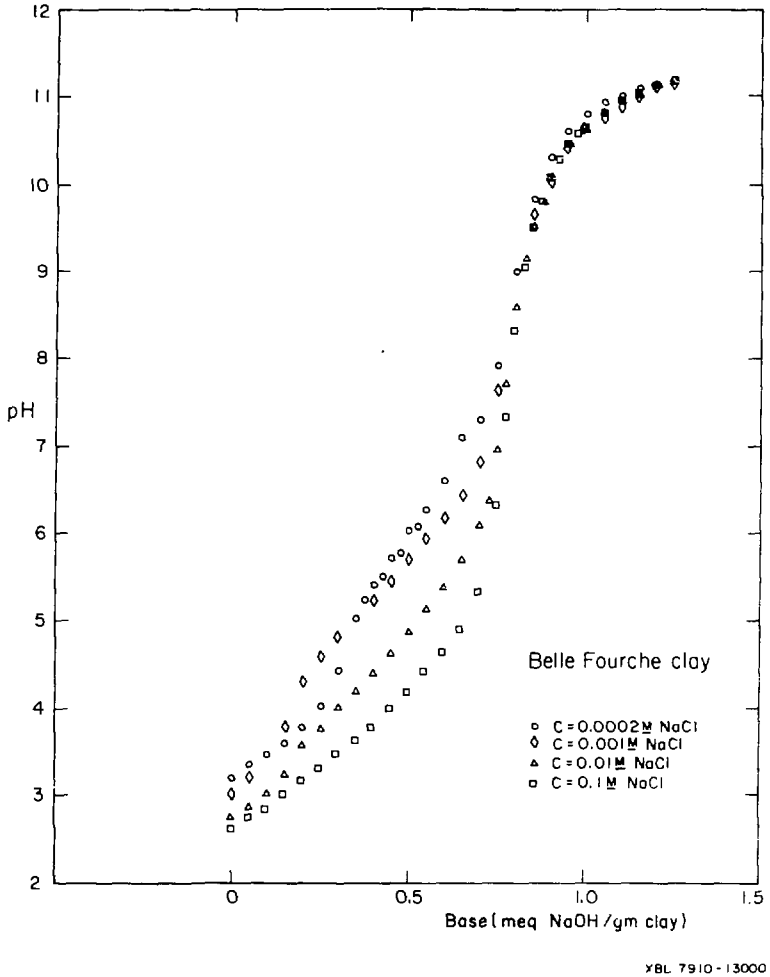

FIGURE 2. Potentiometric base titration curves for Belle Fourche clay in aqueous suspension as a function of NaCl electrolyte concentration.

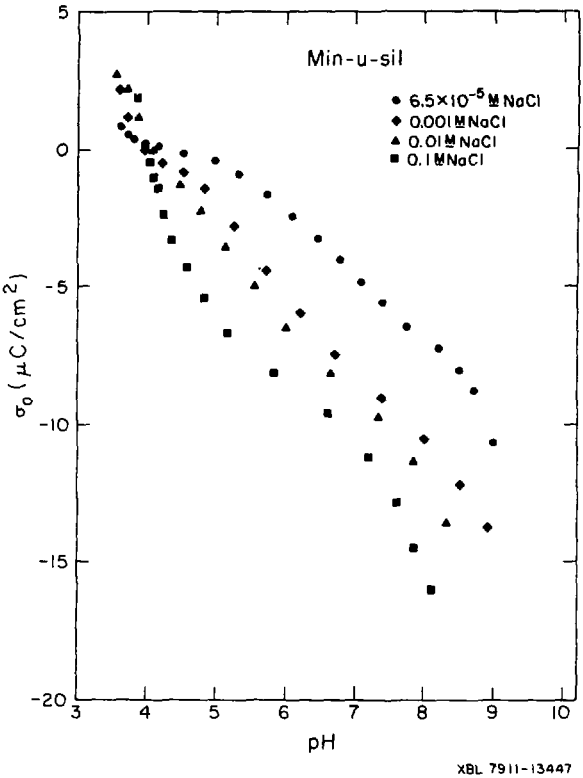

FIGURE 3. The surface charge, σ_0, of Min-u-sil in aqueous suspension as a function of pH and NaCl electrolyte concentration. Calculated from titration data.

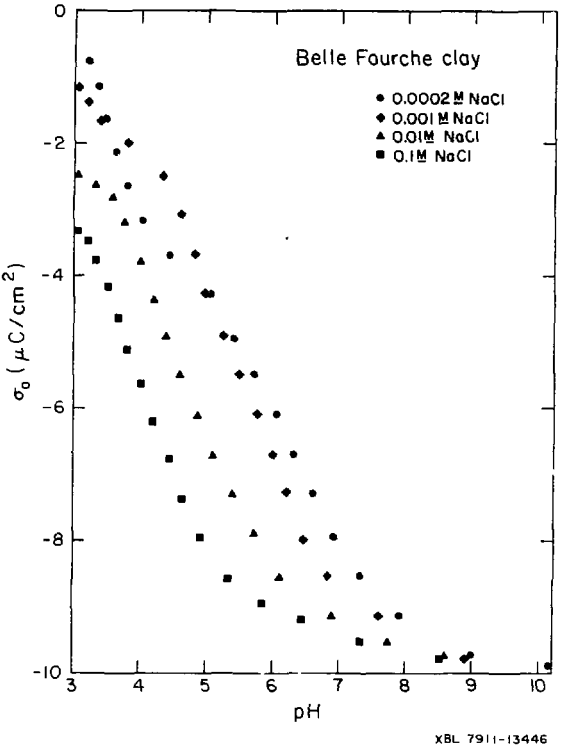

FIGURE 4. The surface charge, σ_0, of Belle Fourche clay in aqueous suspension as a function of pH and NaCl electrolyte concentration. Calculated from titration data.

C_A, C_B = molar concentration of acid and base used for titration

V_A, V_B = volume of acid and/or base used to reach a given point 1 on titration curve, liters

$(H^+)_1$, $(OH^-)_1$ = measured H^+ and OH^- ion activities at a given point on titration curve

V_1 = total volume at a given point on titration curve, $V_o+V_A+V_B$

γ_o, γ_1 = activity coefficients of H^+ and OH^- used to convert activities to concentrations. Calculated using Davies equation (Butler 1964, p.437).

Estimates of Intrinsic Constants by Double Extrapolation

Estimates of the intrinsic surface ionization and exchange constants can be made using the surface charge information derived from the titration data. Since the Cs sorption isotherms were measured over a pH range of 5 - 10, i.e., pH >> PZC, the surface charge is always negative and the constants of interest are $K_{a_2}^{int}$ and $^*K_{Na^+}^{int}$. The approximations that are used and the appropriate equations, 25, 26, 27 and 29, were given previously in the section describing the e.d.l. model. Since the intrinsic constants are functions of both the degree of ionization of the surface or surface charge and the concentration of supporting electrolyte, C, a double extropolation procedure has been developed (James, Davis and Leckie 1978). For the estimates of $pK_{a_2}^{int}$, pQ_{a_2} is plotted versus $\alpha_- + \sqrt{C}$. The square root of C is used rather than C itself to spread the data more evenly and conveniently for graphic extrapolations. The shapes of the curves depend upon α_-. The $\sqrt{C}$ only shifts the curves relative to each other.

Figure 5 shows plots of the pQ_{a_2} versus $\alpha_- + \sqrt{C}$ for Min-u-sil for the several different electrolyte concentrations. The fractional ionizations, α_-, for Min-u-sil were calculated using the estimated value of 0.0252 meq/g for the total site concentration, N_s, or 80.2 $\mu C/cm^2$ in terms of charge. For each NaCl concentration, a smooth curve through the experimental points is drawn and the nearly linear, decreasing portion at low values of α_- is extrapolated to intersect the vertical line $\alpha + \sqrt{C} = \sqrt{C}$. At this point α_o is zero. These

extrapolations produce the open symbols in Figure 5. A smooth curve is then drawn through these points and extrapolated to $\alpha_- + \sqrt{C} = 0$, where both α_0 and C are zero. This intercept is taken as an estimate for $pK_{a_2}^{int}$.

For an estimate of $p^*K_{Na^+}^{int}$, it is convenient to plot $p^*Q_{Na^+}$ versus $\alpha_- - 1/10 \log C$. Figure 6 shows such plots for Min-u-sil for the different electrolyte concentrations. Extrapolation of smooth curves through the points to $\alpha_- - 1/10 \log C = -1/10 \log C$ yields the open symbols. Extrapolation of a smooth curve through the open symbols to $\alpha_- - 1/10 \log C = 0$ yields a value for $p^*Q_{Na^+}$ for C = 1M. This value is customarily taken as an estimate for $p^*K_{Na^+}^{int}$

There is some arbitrariness involved in the extrapolations. However, this method is useful for obtaining a first-estimate for the intrinsic constants. These values can then be starting values for input to MINEQL. By fitting calculated titration curves using MINEQL with the experimentally determined ones, refinements in the values of the intrinsic constants can be made.

Application of the double extrapolation method to the clay did not produce reliable results. At the starting point of the titration, the SOH sites are already 20 to 30% ionized depending on the salt concentration, i.e., $\alpha_- = 0.2$ to 0.3. Plots of pQ_{a_2} or $p^*Q_{Na^+}$ versus a_- (or a_- plus the appropriate function of C) did not produce regions of points where a smooth curve could be drawn and extrapolated to $\alpha_- = 0$ with any confidence as for Min-u-sil. As an example, a plot of pQ_{a_2} versus $\alpha_- + \sqrt{C}$ for the SOH sites is shown in Figure 7. For the TOH sites, a similar problem in the extrapolations occurs. A surface charge builds up during the titration of the SOH sites and the effect on the subsequent ionization of the TOH is not known. Extrapolation to $\alpha_- = 0$ in this case does not mean $\sigma_0 = 0$. Plots of pQ_{a_2} or $p^*Q_{Na^+}$ versus some function of σ_0 seem appropriate, however, extrapolation from the data points for the TOH sites to $\sigma_0 = 0$ is quite long, from 4 - 5 $\mu c/cm^2$ to 0, and rather meaningless. Therefore, estimates of the intrinsic constants from fitting curves calculated by MINEQL to the experimental titration curves is probably the best recourse. Simpler methods of reliably estimating the intrinsic constants from the titration data are being explored.

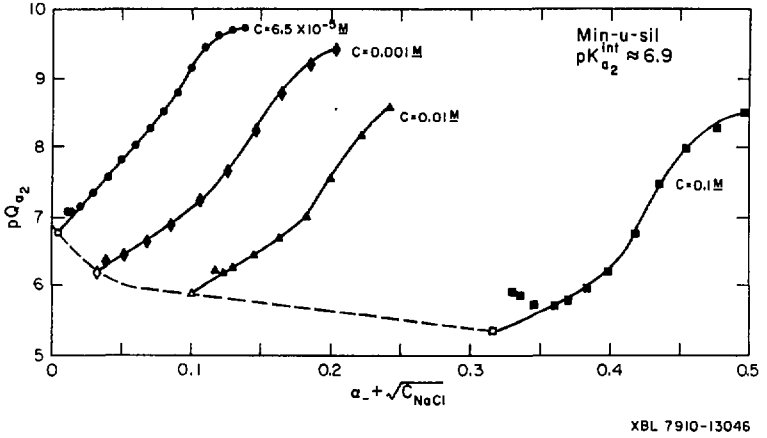

FIGURE 5. Double extrapolation plot for the estimation of pK_{a2}^{int} showing the variation of the surface acidity quotient, pQ_{a2}, for the dissociation of the negative sites on Min-u-sil in aqueous suspension at 26°C with the fractional ionization, α_-, and the NaCl electrolyte concentration.

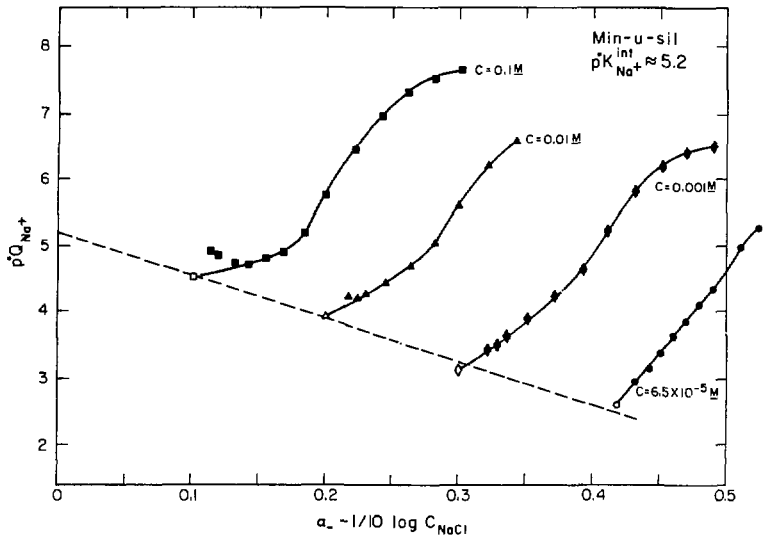

XBL 7910-13048

FIGURE 6. Double extrapolation plot for the estimation of $p^* K^{int}_{Na^+}$ showing the variation of the Na exchange quotient, $p^*Q_{Na^+}$, for the negative sites on Min-u-sil in aqueous suspension at 26°C with the fractional ionization, α_-, and the NaCl electrolyte concentration.

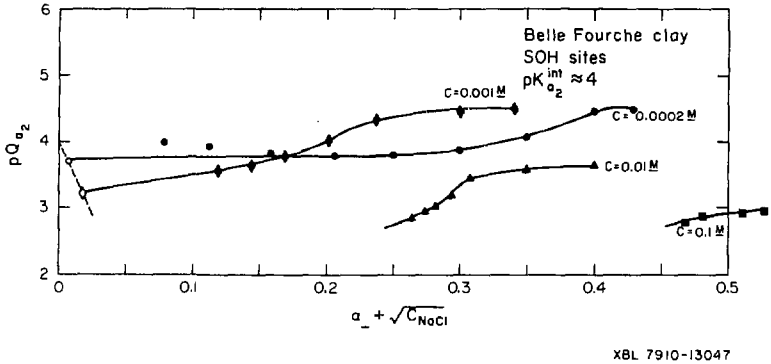

FIGURE 7. Double extrapolation plot for the estimation of pK^{int}_{a2} showing the variation of surface acidity quotient, pQ_{a2}, for the dissociation of the negative SOH-type sites on Belle Fourche clay in aqueous suspension at 26°C with the fractional ionization, α_-, and the NaCl electrolyte concentration.

DETERMINATION OF Cs SORPTION ISOTHERMS

Procedures

Cesium sorption isotherms using the sodium form of the Belle Fourche clay and Min-u-sil were obtained as a function of Cs concentration, pH, and supporting electrolyte concentration in batch-type experiments. The initial Cs concentrations ranged from 10^{-3}M to 10^{-9}M for the clay and 10^{-4}M to 10^{-9}M for the quartz; pH values were 5, 6, 7, 8, 9, and 10; electrolyte solutions were 0.002M, 0.01M, 0.1M, and 1M NaCl and the simulated groundwater.

Clay and quartz suspensions of approximately 500 ml volumes were made up to each of the five different electrolyte concentrations. The pH of 75 ml portions of each of these suspensions was adjusted to a given value with microliter amounts of 0.05M HCl or 0.05M NaOH and the solutions were transferred to the inert box. Just prior to the sorption measurements, the pH of the solutions were checked and readjusted if necessary. Ten ml portions of each of these solutions of a given pH were placed in polyethylene bottles and 10 microliter aliquots of different concentrations of stock Cs solutions, "spiked" with ^{137}Cs tracer, were also added. The solutions were agitated for 15 - 20 minutes. The sorption of Cs as a function of time was investigated in separate experiments and no detectable increase in sorption was measured after 15 minutes. Approximately 3 ml of the suspensions were then centrifuged for 3 minutes at 12,000 rpm. The supernates were filtered through 0.2 micrometer pore size filters. Exactly one ml portions of the filtrates were analyzed for ^{137}Cs content by γ-ray counting using a 3" x 3" NaI crystal.

Results

Since the concentration (and radioactivity) of the influent Cs solutions had previously been measured, the determinations of the ^{137}Cs radioactivities (and thus total Cs concentrations) in the effluent solutions allowed the calculation of K_d's.

$$K_d = \frac{1 - f}{f} \cdot \frac{v}{w} \tag{37}$$

where

f = fraction of influent Cs remaining in solution
v = volume of solution (ml)
w = weight of clay or quartz (g)

The results of the Cs sorption isotherm measurements at 26 ± 2°C are summarized in Tables 4 - 15. Also shown are the final Cs concentrations in solution, C_f, and on the substrate, L_{Cs}. The assigned errors result from a consideration of errors associated with counting and sampling. Duplicates were run on only about 10% of the samples and agreements were within the estimated error.

The equation for the exchange of the monovalent cations Cs^+ and Na^+ between the solid surface, s, and the aqueous solution, a, may be written as

$$SO^-Na_s^+ + Cs_a^+ \rightleftharpoons SO^-Cs_s^+ + Na_a^+ \tag{38}$$

The mass action expression for the thermodynamic equilibrium constant is

$$K_{Cs/Na} = \frac{[SO^-Cs^+]_s[Na^+]_a}{[SO^-Na^+]_s[Cs^+]_a} \cdot \frac{\gamma_{Na^+}\ \gamma_{SO^-Cs^+}}{\gamma_{Cs^+}\ \gamma_{SO^-Na^+}} \tag{39}$$

where the first term is expressed in concentrations of ions on the surface and in the solution phases and the second term contains the corresponding activity coefficients. The latter equation can be written as (Helfferich 1962, p.154)

$$K_{Cs/Na} = K^a_{Cs/Na}\ \frac{\gamma_{SO^-Cs^+}}{\gamma_{SO^-Na^+}} \tag{40}$$

The Cs/Na selectivity coefficient corrected for activities in solution, $K^a_{Cs/Na}$, can be determined experimentally since it is made up of quantities that can be measured or estimated. In logarithmic form with rearrangement,

$$\log\frac{(SO^-Cs^+)_s}{(SO^-Na^+)_s} = \log K^a_{Cs/Na} + \log\frac{(Cs^+)_a}{(Na^+)_a} \cdot \frac{\gamma_{Cs^+}}{\gamma_{Na^+}} \tag{41}$$

TABLE 4. Cs SORPTION ISOTHERM DATA ON BELLE FOURCHE CLAY AT 26 ± 2°C

Supporting Electrolyte / Final Cs Conc.(M), C_f / Cs Loading (moles/gm), L_{Cs} / Distribution Coefficient (ml/gm), K_d	pH = 5 Initial Cs Concentration (M) 0.93×10^{-3}	1.00×10^{-4}	1.00×10^{-5}	1.01×10^{-7}	1.04×10^{-9}
0.002M NaCl					
C_f	$5.48\pm0.27\times10^{-5}$	$5.26\pm0.26\times10^{-6}$	$4.25\pm0.21\times10^{-7}$	$4.26\pm0.22\times10^{-9}$	$4.65\pm0.24\times10^{-11}$
L_{Cs}	$8.79\pm0.46\times10^{-2}$	$9.48\pm0.50\times10^{-3}$	$9.58\pm0.50\times10^{-4}$	$9.67\pm0.50\times10^{-6}$	$9.94\pm0.53\times10^{-8}$
K_d	1606±92	1801±102	2253±127	2271±179	2138±121
0.01M NaCl					
C_f	$1.05\pm0.05\times10^{-4}$	$8.77\pm0.44\times10^{-6}$	$9.11\pm0.46\times10^{-7}$	$9.11\pm0.46\times10^{-9}$	$1.11\pm0.06\times10^{-10}$
L_{Cs}	$8.29\pm0.46\times10^{-2}$	$9.12\pm0.50\times10^{-3}$	$9.00\pm0.50\times10^{-4}$	$9.19\pm0.50\times10^{-6}$	$9.30\pm0.53\times10^{-8}$
K_d	790±47	1040±61	988±59	1009±59	843±50
0.1M NaCl					
C_f	$4.69\pm0.23\times10^{-4}$	$4.80\pm0.24\times10^{-5}$	$4.09\pm0.20\times10^{-6}$	$4.30\pm0.22\times10^{-8}$	$4.44\pm0.22\times10^{-10}$
L_{Cs}	$4.66\pm0.46\times10^{-2}$	$5.25\pm0.50\times10^{-3}$	$5/92\pm0.50\times10^{-4}$	$5.81\pm0.50\times10^{-6}$	$5.96\pm0.52\times10^{-8}$
K_d	99.2±10.2	108±11	145±13	135±12	134±12
1M NaCl					
C_f	$8.85\pm0.44\times10^{-4}$	$9.04\pm0.45\times10^{-5}$	$8.61\pm0.43\times10^{-6}$	$8.93\pm0.45\times10^{-8}$	$9.67\pm0.49\times10^{-10}$
L_{Cs}	$4.93\pm4.78\times10^{-3}$	$9.55\pm5.00\times10^{-5}$	$1.39\pm0.50\times10^{-4}$	$1.17\pm0.51\times10^{-6}$	$7.34\pm5.22\times10^{-9}$
K_d	5.6 ±5.3	10.6 ±5.5	16.1 ±5.8	13.1 ±5.7	7.6 ±5.4
Sum					
C_f	$6.91\pm0.35\times10^{-5}$	$5.59\pm0.28\times10^{-6}$	$5.08\pm0.26\times10^{-7}$	$4.66\pm0.24\times10^{-9}$	$5.30\pm0.27\times10^{-11}$
L_{Cs}	$8.65\pm0.47\times10^{-2}$	$9.44\pm0.50\times10^{-3}$	$9.49\pm0.50\times10^{-4}$	$9.65\pm0.50\times10^{-6}$	$9.88\pm0.53\times10^{-8}$
K_d	1251±72	1690±96	1867±106	2069±117	1863±106

TABLE 5. Cs SORPTION ISOTHERM DATA ON BELLE FOURCHE CLAY AT 26 ± 2°C

Supporting Electrolyte / Final Cs Conc.(M), C_f / Cs Loading (moles/gm), L_{Cs} / Distribution Coefficient (ml/gm), K_d	pH = 6 Initial Cs Concentration (M) 0.93×10^{-3}	1.00×10^{-4}	1.00×10^{-5}	1.01×10^{-7}	1.04×10^{-9}
0.002M NaCl					
C_f	$4.25\pm0.21\times10^{-5}$	$3.70\pm0.19\times10^{-6}$	$3.26\pm0.16\times10^{-7}$	$3.24\pm0.16\times10^{-9}$	$3.45\pm0.18\times10^{-11}$
L_{Cs}	$8.92\pm0.46\times10^{-2}$	$9.62\pm0.50\times10^{-3}$	$9.67\pm0.50\times10^{-4}$	$9.78\pm0.52\times10^{-6}$	$1.05\pm0.05\times10^{-7}$
K_d	2098±118	2602±146	2986±166	3022±169	2916±164
0.01M NaCl					
C_f	$1.04\pm0.05\times10^{-4}$	$1.00\pm0.50\times10^{-5}$	$9.81\pm0.49\times10^{-7}$	$8.59\pm0.43\times10^{-9}$	$9.53\pm0.21\times10^{-10}$
L_{Cs}	$8.30\pm0.41\times10^{-2}$	$9.00\pm0.50\times10^{-3}$	$9.02\pm0.50\times10^{-4}$	$9.24\pm0.50\times10^{-6}$	$8.75\pm0.53\times10^{-8}$
K_d	801±48	897±53	919±54	1076±63	997±58
0.1M NaCl					
C_f	$4.47\pm0.22\times10^{-4}$	$4.49\pm0.25\times10^{-5}$	$4.17\pm0.21\times10^{-6}$	$4.12\pm0.21\times10^{-8}$	$4.13\pm0.21\times10^{-10}$
L_{Cs}	$4.87\pm0.46\times10^{-2}$	$5.51\pm0.50\times10^{-3}$	$5.83\pm0.50\times10^{-6}$	$5.98\pm0.50\times10^{-6}$	$6.28\pm0.52\times10^{-8}$
K_d	109±11	123±11	140±12	145±13	152±13
1M NaCl					
C_f	$8.57\pm0.43\times10^{-4}$	$9.32\pm0.47\times10^{-5}$	$9.09\pm0.45\times10^{-6}$	$8.99\pm0.45\times10^{-8}$	$9.50\pm0.48\times10^{-10}$
L_{Cs}	$7.70\pm4.67\times10^{-3}$	$6.79\pm5.00\times10^{-4}$	$9.17\pm5.00\times10^{-5}$	$1.11\pm0.51\times10^{-6}$	$9.05\pm5.14\times10^{-9}$
K_d	9.0 ±5.5	7.3 ±5.4	10.1 ±5.5	12.3 ±5.6	9.5 ±5.5
Sum					
C_f	$5.63\pm0.28\times10^{-5}$	$4.96\pm0.25\times10^{-6}$	$4.45\pm0.22\times10^{-7}$	$4.28\pm0.22\times10^{-9}$	$4.79\pm0.24\times10^{-11}$
L_{Cs}	$8.77\pm0.48\times10^{-2}$	$9.55\pm0.50\times10^{-3}$	$9.54\pm0.50\times10^{-4}$	$9.67\pm0.50\times10^{-6}$	$9.92\pm0.52\times10^{-8}$
K_d	1559±89	1917±109	2148±121	2260±127	2069±117

TABLE 6. Cs SORPTION ISOTHERM DATA ON BELLE FOURCHE CLAY AT 26 ± 2°C

Supporting Electrolyte	pH = 7				
Final Cs Conc.(M), C_f					
Cs Loading (moles/gm), L_{Cs}	Initial Cs Concentration (M)				
Distribution Coefficient (ml/gm), K_d	0.93×10^{-3}	1.00×10^{-4}	1.00×10^{-5}	1.01×10^{-7}	1.04×10^{-9}
0.002M NaCl					
C_f	$1.63\pm0.18\times10^{-5}$	$2.97\pm0.15\times10^{-6}$	$2.70\pm0.14\times10^{-7}$	$2.57\pm0.13\times10^{-9}$	$2.78\pm0.14\times10^{-11}$
L_{Cs}	$8.97\pm0.47\times10^{-2}$	$9.71\pm0.50\times10^{-3}$	$9.73\pm0.50\times10^{-4}$	$9.84\pm0.52\times10^{-6}$	$1.01\pm0.05\times10^{-7}$
K_d	2548±143	3267±182	3726±207	3839±214	3645±204
0.01M NaCl					
C_f	$9.36\pm0.47\times10^{-5}$	$9.49\pm0.48\times10^{-6}$	$8.16\pm0.41\times10^{-7}$	$8.52\pm0.43\times10^{-9}$	$8.06\pm0.41\times10^{-11}$
L_{Cs}	$8.40\pm0.47\times10^{-2}$	$9.05\pm0.50\times10^{-3}$	$9.16\pm0.50\times10^{-4}$	$9.25\pm0.50\times10^{-6}$	$9.60\pm0.53\times10^{-8}$
K_d	898±53	953±56	1126±65	1085±63	1190±69
0.1M NaCl					
C_f	$4.12\pm0.21\times10^{-4}$	$4.30\pm0.21\times10^{-5}$	$3.88\pm0.19\times10^{-6}$	$3.82\pm0.19\times10^{-8}$	$4.17\pm0.21\times10^{-10}$
L_{Cs}	$5.22\pm0.47\times10^{-2}$	$5.75\pm0.50\times10^{-3}$	$6.12\pm0.50\times10^{-4}$	$6.23\pm0.50\times10^{-6}$	$6.24\pm0.52\times10^{-8}$
K_d	127±12	133±12	157±13	161±13	150±13
1M NaCl					
C_f	$8.32\pm0.42\times10^{-4}$	$8.96\pm0.45\times10^{-5}$	$8.59\pm0.43\times10^{-6}$	$8.63\pm0.43\times10^{-8}$	$9.43\pm0.47\times10^{-10}$
L_{Cs}	$1.01\pm0.47\times10^{-2}$	$1.04\pm0.50\times10^{-3}$	$1.40\pm0.50\times10^{-4}$	$1.48\pm0.50\times10^{-6}$	$9.74\pm0.52\times10^{-8}$
K_d	12.5 ±5.6	11.7 ±5.6	16.6 ±5.8	17.7 ±5.9	10.3 ±5.5
Sea					
C_f	$4.79\pm0.24\times10^{-5}$	$3.81\pm0.19\times10^{-6}$	$3.71\pm0.19\times10^{-7}$	$3.48\pm0.18\times10^{-9}$	$3.63\pm0.18\times10^{-11}$
L_{Cs}	$8.86\pm0.47\times10^{-2}$	$9.62\pm0.50\times10^{-3}$	$9.62\pm0.50\times10^{-4}$	$9.76\pm0.52\times10^{-6}$	$1.00\pm0.05\times10^{-7}$
K_d	1851±105	2528±143	2594±146	2799±157	2765±155

TABLE 7. Cs SORPTION ISOTHERM DATA ON BELLE FOURCHE CLAY AT 26 ± 2°C

Supporting Electrolyte	pH = 8				
Final Cs Conc.(M), C_f					
Cs Loading (moles/gm), L_{Cs}	Initial Cs Concentration (M)				
Distribution Coefficient (ml/gm), K_d	0.93×10^{-3}	1.00×10^{-4}	1.00×10^{-5}	1.01×10^{-7}	1.04×10^{-9}
0.002M NaCl					
C_f	$3.12\pm0.16\times10^{-5}$	$2.55\pm0.13\times10^{-6}$	$2.23\pm0.11\times10^{-7}$	$2.22\pm0.11\times10^{-9}$	$2.25\pm0.12\times10^{-11}$
L_{Cs}	$9.02\pm0.47\times10^{-2}$	$9.74\pm0.50\times10^{-3}$	$9.78\pm0.50\times10^{-4}$	$9.86\pm0.52\times10^{-6}$	$1.02\pm0.05\times10^{-7}$
K_d	2891±162	3824±213	4384±244	4450±248	4529±254
0.01M NaCl					
C_f	$8.44\pm0.42\times10^{-5}$	$8.27\pm0.42\times10^{-6}$	$7.41\pm0.37\times10^{-7}$	$7.69\pm0.39\times10^{-9}$	$7.69\pm0.39\times10^{-11}$
L_{Cs}	$8.50\pm0.47\times10^{-2}$	$9.17\pm0.50\times10^{-3}$	$9.26\pm0.50\times10^{-4}$	$9.34\pm0.50\times10^{-6}$	$9.64\pm0.53\times10^{-8}$
K_d	1006±59	1109±65	1250±72	1250±72	1253±73
0.1M NaCl					
C_f	$4.02\pm0.20\times10^{-4}$	$4.09\pm0.21\times10^{-5}$	$3.98\pm0.20\times10^{-6}$	$3.83\pm0.19\times10^{-8}$	$3.92\pm0.20\times10^{-10}$
L_{Cs}	$5.32\pm0.47\times10^{-2}$	$5.92\pm0.50\times10^{-3}$	$6.01\pm0.50\times10^{-4}$	$6.28\pm0.50\times10^{-6}$	$6.43\pm0.52\times10^{-8}$
K_d	132±12	145±12	151±13	164±14	165±14
1M NaCl					
C_f	$8.12\pm0.41\times10^{-4}$	$9.09\pm0.46\times10^{-5}$	$8.59\pm0.43\times10^{-6}$	$8.52\pm0.43\times10^{-8}$	$9.71\pm0.49\times10^{-10}$
L_{Cs}	$1.21\pm0.47\times10^{-2}$	$9.12\pm5.00\times10^{-4}$	$1.40\pm0.50\times10^{-4}$	$1.58\pm0.50\times10^{-6}$	$1.39\pm0.53\times10^{-8}$
K_d	15.0 ±5.8	10.0 ±5.5	16.4 ±5.8	18.5 ±5.9	15.4 ±5.8
Sea					
C_f	$4.33\pm0.22\times10^{-5}$	$3.49\pm0.18\times10^{-6}$	$3.14\pm0.16\times10^{-7}$	$3.14\pm0.16\times10^{-9}$	$3.18\pm0.16\times10^{-11}$
L_{Cs}	$8.90\pm0.47\times10^{-2}$	$9.65\pm0.50\times10^{-3}$	$9.68\pm0.50\times10^{-4}$	$9.79\pm0.52\times10^{-6}$	$1.01\pm0.05\times10^{-7}$
K_d	2058±116	2767±155	3095±173	3157±174	3174±178

TABLE 8. Cs SORPTION ISOTHERM DATA ON BELLE FOURCHE CLAY AT 26 ± 2°C

Supporting Electrolyte	pH = 9				
Final Cs Conc.(M), C_f					
Cs Loading (mmoles/gm), L_{Cs}	Initial Cs Concentration (M)				
Distribution Coefficient (ml/gm), K_d	0.93×10^{-3}	1.00×10^{-4}	1.00×10^{-5}	1.01×10^{-7}	1.04×10^{-9}
0.002M NaCl					
C_f	$2.82\pm0.14\times10^{-5}$	$2.55\pm0.13\times10^{-6}$	$2.08\pm0.11\times10^{-7}$	$2.21\pm0.11\times10^{-9}$	$2.46\pm0.13\times10^{-11}$
L_{Cs}	$9.08\pm0.47\times10^{-2}$	$9.74\pm0.50\times10^{-3}$	$9.79\pm0.50\times10^{-4}$	$9.88\pm0.52\times10^{-6}$	$1.02\pm0.05\times10^{-8}$
K_d	3212±179	3826±212	5707±260	4451±246	4155±2??
0.01M NaCl					
C_f	$8.87\pm0.46\times10^{-5}$	$8.23\pm0.41\times10^{-6}$	$6.56\pm0.33\times10^{-7}$	$6.84\pm0.34\times10^{-9}$	$7.00\pm0.35\times10^{-11}$
L_{Cs}	$8.46\pm0.47\times10^{-2}$	$9.18\pm0.50\times10^{-3}$	$9.35\pm0.50\times10^{-4}$	$9.42\pm0.50\times10^{-6}$	$9.70\pm0.53\times10^{-8}$
K_d	953±56	1115±65	1429±82	1377±79	1386±80
0.1M NaCl					
C_f	$4.03\pm0.20\times10^{-4}$	$4.03\pm0.20\times10^{-5}$	$3.69\pm0.18\times10^{-6}$	$3.81\pm0.19\times10^{-8}$	$3.81\pm0.19\times10^{-10}$
L_{Cs}	$5.30\pm0.47\times10^{-2}$	$5.98\pm0.50\times10^{-3}$	$6.74\pm0.50\times10^{-4}$	$6.29\pm0.50\times10^{-6}$	$6.59\pm0.52\times10^{-8}$
K_d	132±12	148±13	171±14	165±14	173±14
1M NaCl					
C_f	$8.41\pm0.42\times10^{-4}$	$9.03\pm0.45\times10^{-5}$	$8.43\pm0.42\times10^{-6}$	$8.69\pm1.43\times10^{-8}$	$9.08\pm0.45\times10^{-10}$
L_{Cs}	$9.29\pm4.67\times10^{-3}$	$9.71\pm5.00\times10^{-4}$	$1.57\pm0.50\times10^{-4}$	$1.40\pm1.50\times10^{-6}$	$1.31\pm0.52\times10^{-8}$
K_d	11.1 ±5.6	10.8 ±5.5	18.6 ±5.9	16.2 ±?.8	14.4 ±5.?
Sum					
C_f	$4.11\pm0.21\times10^{-5}$	$3.36\pm0.17\times10^{-6}$	$3.37\pm0.17\times10^{-7}$	$3.19\pm0.16\times10^{-9}$	$3.01\pm0.15\times10^{-11}$
L_{Cs}	$8.93\pm0.47\times10^{-2}$	$9.66\pm0.50\times10^{-3}$	$9.66\pm0.50\times10^{-4}$	$9.78\pm0.50\times10^{-6}$	$1.01\pm0.05\times10^{-8}$
K_d	2174±122	2675±160	2869±160	3070±171	3352±188

TABLE 9. Cs SORPTION ISOTHERM DATA ON BELLE FOURCHE CLAY AT 26 ± 2°C

Supporting Electrolyte	pH = 10				
Final Cs Conc.(M), C_f					
Cs Loading (mmoles/gm), L_{Cs}	Initial Cs Concentration (M)				
Distribution Coefficient (ml/gm), K_d	0.93×10^{-3}	1.00×10^{-4}	1.00×10^{-5}	1.01×10^{-7}	1.04×10^{-9}
0.002M NaCl					
C_f	$2.73\pm0.14\times10^{-5}$	$2.55\pm0.13\times10^{-6}$	$2.19\pm0.11\times10^{-7}$	$2.06\pm0.10\times10^{-9}$	$2.08\pm0.11\times10^{-11}$
L_{Cs}	$9.07\pm0.47\times10^{-2}$	$9.74\pm0.50\times10^{-3}$	$9.78\pm0.50\times10^{-4}$	$9.90\pm0.50\times10^{-6}$	$1.02\pm0.05\times10^{-8}$
K_d	3327±185	3824±212	4474±247	4807±264	4899±275
0.01M NaCl					
C_f	$8.66\pm0.43\times10^{-5}$	$8.07\pm0.41\times10^{-6}$	$6.94\pm0.35\times10^{-7}$	$6.87\pm0.35\times10^{-9}$	$7.52\pm0.38\times10^{-11}$
L_{Cs}	$8.47\pm0.47\times10^{-2}$	$9.19\pm0.50\times10^{-3}$	$9.31\pm0.50\times10^{-4}$	$9.41\pm0.50\times10^{-6}$	$9.65\pm0.53\times10^{-8}$
K_d	979±58	1139±66	1341±77	1371±79	1284±74
0.1M NaCl					
C_f	$3.64\pm0.18\times10^{-4}$	$3.80\pm0.19\times10^{-5}$	$3.95\pm0.20\times10^{-6}$	$3.61\pm0.18\times10^{-8}$	$3.74\pm0.19\times10^{-10}$
L_{Cs}	$5.30\pm0.47\times10^{-2}$	$6.20\pm0.50\times10^{-3}$	$6.05\pm0.50\times10^{-4}$	$6.49\pm0.50\times10^{-6}$	$6.66\pm0.52\times10^{-8}$
K_d	145±13	163±14	153±13	180±14	176±14
1M NaCl					
C_f	$8.12\pm0.41\times10^{-4}$	$8.60\pm0.43\times10^{-5}$	$8.80\pm0.44\times10^{-6}$	$8.41\pm0.44\times10^{-8}$	$9.29\pm0.46\times10^{-10}$
L_{Cs}	$1.22\pm0.47\times10^{-4}$	$1.40\pm0.52\times10^{-3}$	$1.20\pm0.50\times10^{-4}$	$1.69\pm0.50\times10^{-6}$	$1.11\pm0.52\times10^{-8}$
K_d	15.1 ±5.8	16.3 ±5.8	13.6 ±5.7	20.1 ±6.0	12.0 ±5.6
Sum					
C_f	$4.03\pm0.20\times10^{-5}$	$3.10\pm0.16\times10^{-6}$	$3.09\pm0.16\times10^{-7}$	$2.75\pm0.14\times10^{-9}$	$3.12\pm0.16\times10^{-11}$
L_{Cs}	$8.94\pm0.47\times10^{-2}$	$9.70\pm0.50\times10^{-3}$	$9.67\pm0.50\times10^{-4}$	$9.83\pm0.50\times10^{-6}$	$1.01\pm0.05\times10^{-7}$
K_d	2219±125	3128±174	3132±174	3575±198	3.38±182

TABLE 10. Cs SORPTION ISOTHERM DATA ON Mln-u-Sil at 26 ± 2°C

Supporting Electrolyte	pH = 5					
Final Cs Conc.(M), C_f						
Cs Loading (moles/gm), L_{Cs}	Initial Cs Concentration (M)					
Distribution Coefficient (ml/gm), K_d	1.05×10^{-4}	1.05×10^{-5}	1.05×10^{-6}	1.06×10^{-7}	1.07×10^{-8}	1.09×10^{-9}
0.002M NaCl						
C_f	$8.29\pm0.41\times10^{-5}$	$6.24\pm0.62\times10^{-6}$	$3.16\pm0.16\times10^{-7}$	$4.06\pm0.21\times10^{-8}$	$8.77\pm0.44\times10^{-11}$	$9.74\pm0.49\times10^{-12}$
L_{Cs}	$2.10\pm0.50\times10^{-4}$	$4.05\pm0.51\times10^{-5}$	$6.97\pm0.51\times10^{-6}$	$9.68\pm0.51\times10^{-7}$	$1.01\pm0.05\times10^{-7}$	$1.03\pm0.06\times10^{-8}$
K_d	2.54±0.60	6.73±0.82	22.1 ±1.6	230±13	1150±66	1597±96
0.01M NaCl						
C_f	$8.77\pm0.44\times10^{-5}$	$7.62\pm0.38\times10^{-6}$	$4.95\pm0.25\times10^{-7}$	$1.28\pm0.06\times10^{-8}$	$3.40\pm0.19\times10^{-10}$	$2.45\pm0.13\times10^{-11}$
L_{Cs}	$1.65\pm0.50\times10^{-4}$	$2.75\pm0.51\times10^{-5}$	$5.28\pm0.51\times10^{-6}$	$8.84\pm0.51\times10^{-7}$	$9.83\pm0.53\times10^{-8}$	$1.01\pm0.06\times10^{-8}$
K_d	1.88±0.57	3.60±0.66	10.6 ±1.0	69.2 ±4.2	292±16	398±22
0.1M NaCl						
C_f	$9.89\pm0.49\times10^{-5}$	$9.59\pm0.48\times10^{-6}$	$7.60\pm0.38\times10^{-7}$	$4.05\pm0.20\times10^{-8}$	$2.93\pm0.15\times10^{-9}$	$1.13\pm0.06\times10^{-10}$
L_{Cs}	$5.76\pm4.97\times10^{-5}$	$8.65\pm4.97\times10^{-6}$	$2.77\pm0.51\times10^{-6}$	$6.20\pm0.51\times10^{-7}$	$7.37\pm0.51\times10^{-8}$	$9.28\pm0.53\times10^{-9}$
K_d	0.58±0.50	0.90±0.52	3.63±0.66	15.4 ±1.3	25.1 ±1.9	82.5 ±4.9
1M NaCl						
C_f	$1.00\pm0.05\times10^{-4}$	$1.02\pm0.06\times10^{-5}$	$9.73\pm0.49\times10^{-7}$	$7.35\pm0.37\times10^{-8}$	$5.43\pm0.27\times10^{-9}$	$5.65\pm0.28\times10^{-10}$
L_{Cs}	$4.44\pm4.97\times10^{-5}$	$3.26\pm4.97\times10^{-6}$	$7.37\pm4.97\times10^{-7}$	$3.10\pm0.44\times10^{-7}$	$5.02\pm0.44\times10^{-8}$	$4.97\pm0.46\times10^{-9}$
K_d	0.44±0.50	0.32±0.69	0.77±0.51	4.19±0.69	9.21±0.95	8.81±0.94
Sum						
C_f	$9.17\pm0.46\times10^{-5}$	$6.96\pm0.35\times10^{-6}$	$3.81\pm0.19\times10^{-7}$	$6.85\pm0.34\times10^{-9}$	$2.79\pm0.14\times10^{-10}$	$2.26\pm0.12\times10^{-11}$
L_{Cs}	$1.27\pm0.50\times10^{-4}$	$3.37\pm0.51\times10^{-5}$	$6.36\pm0.51\times10^{-6}$	$9.44\pm0.51\times10^{-7}$	$9.90\pm0.51\times10^{-8}$	$1.01\pm0.05\times10^{-8}$
K_d	1.38±0.55	4.83±0.72	16.7 ±1.4	137±08	354±20	446±25

TABLE 11. Cs SORPTION ISOTHERM DATA ON Mln-u-Sil at 26 ± 2°C

Supporting Electrolyte	pH = 6					
Final Cs Conc.(M), C_f						
Cs Loading (moles/gm), L_{Cs}	Initial Cs Concentration (M)					
Distribution Coefficient (ml/gm), K_d	1.05×10^{-4}	1.05×10^{-5}	1.05×10^{-6}	1.06×10^{-7}	1.07×10^{-8}	1.09×10^{-9}
0.002M NaCl						
C_f	$5.94\pm0.30\times10^{-5}$	$3.91\pm0.20\times10^{-6}$	$1.77\pm0.09\times10^{-7}$	$3.12\pm0.16\times10^{-9}$	$8.22\pm0.43\times10^{-11}$	$6.17\pm0.32\times10^{-12}$
L_{Cs}	$4.33\pm0.51\times10^{-4}$	$6.27\pm0.51\times10^{-5}$	$8.29\pm0.51\times10^{-6}$	$9.79\pm0.51\times10^{-7}$	$1.01\pm0.05\times10^{-7}$	$1.03\pm0.06\times10^{-8}$
K_d	7.30±0.85	16.0 ±1.3	46.9 ±3.0	313±17	1227±70	1669±103
0.01M NaCl						
C_f	$8.59\pm0.43\times10^{-5}$	$5.93\pm0.30\times10^{-6}$	$3.50\pm0.17\times10^{-7}$	$9.24\pm0.46\times10^{-9}$	$2.56\pm0.13\times10^{-10}$	$1.77\pm0.09\times10^{-11}$
L_{Cs}	$1.81\pm0.51\times10^{-4}$	$4.34\pm0.51\times10^{-5}$	$6.64\pm0.51\times10^{-6}$	$9.20\pm0.51\times10^{-7}$	$9.91\pm0.51\times10^{-8}$	$1.02\pm0.06\times10^{-8}$
K_d	2.12±0.58	7.32±0.74	19.0 ±1.5	99.5 ±6.1	391±22	577±37
0.1M NaCl						
C_f	$1.01\pm0.05\times10^{-4}$	$9.66\pm0.48\times10^{-6}$	$6.83\pm0.34\times10^{-7}$	$3.30\pm0.17\times10^{-8}$	$1.43\pm0.07\times10^{-9}$	$1.09\pm0.06\times10^{-10}$
L_{Cs}	$3.89\pm4.97\times10^{-5}$	$8.10\pm4.36\times10^{-6}$	$3.50\pm0.51\times10^{-6}$	$6.95\pm0.51\times10^{-7}$	$8.82\pm0.44\times10^{-8}$	$9.33\pm0.45\times10^{-9}$
K_d	0.39±0.49	0.83±0.52	5.09±1.74	21.0±1.6	62.7 ±3.9	85.6 ±5.1
1M NaCl						
C_f	$1.03\pm0.05\times10^{-4}$	$9.58\pm0.48\times10^{-6}$	$9.32\pm0.47\times10^{-7}$	$7.30\pm0.37\times10^{-8}$	$5.53\pm0.28\times10^{-9}$	$5.45\pm0.27\times10^{-10}$
L_{Cs}	$4.58\pm4.97\times10^{-5}$	$8.76\pm4.97\times10^{-6}$	$1.13\pm0.50\times10^{-6}$	$3.17\pm0.51\times10^{-7}$	$4.01\pm0.50\times10^{-8}$	$5.15\pm0.52\times10^{-9}$
K_d	0.15±0.48	0.91±0.52	1.21±0.54	4.29±0.70	8.84±0.94	9.45±0
Sum						
C_f	$8.35\pm0.42\times10^{-5}$	$5.96\pm0.35\times10^{-6}$	$3.01\pm0.15\times10^{-7}$	$5.41\pm0.27\times10^{-9}$	$2.38\pm0.12\times10^{-10}$	$2.09\pm0.11\times10^{-11}$
L_{Cs}	$2.01\pm0.50\times10^{-4}$	$4.31\pm0.44\times10^{-5}$	$7.11\pm0.51\times10^{-6}$	$9.55\pm0.51\times10^{-7}$	$9.92\pm0.51\times10^{-8}$	$1.02\pm0.05\times10^{-8}$
K_d	2.45±0.60	7.24±0.85	23.7 ±1.7	176±10	418±22	490±26

TABLE 12. Cs SORPTION ISOTHERM DATA ON Minus-Sil at 25 ± 2°C

Supporting Electrolyte	pH = 7					
Final Cs Conc. (M), C_f	Initial Cs Concentration (M)					
Cs Loading (moles/gm), L_{Cs}						
Distribution Coefficient (ml/gm), K_d	1.05×10^{-4}	1.05×10^{-5}	1.05×10^{-6}	1.06×10^{-7}	1.07×10^{-8}	1.08×10^{-9}
0.002M NaCl						
C_f	$5.60\pm0.78\times10^{-5}$	$2.32\pm0.12\times10^{-6}$	$1.15\pm0.06\times10^{-7}$	$2.13\pm0.11\times10^{-8}$	$6.62\pm0.33\times10^{-9}$	$4.13\pm0.21\times10^{-9}$
L_{Cs}	$4.73\pm0.51\times10^{-4}$	$7.77\pm0.51\times10^{-5}$	$8.85\pm0.51\times10^{-6}$	$9.86\pm0.51\times10^{-7}$	$1.01\pm0.05\times10^{-7}$	$1.04\pm0.05\times10^{-8}$
K_d	8.31±0.91	33.5 ±2.3	77.3 ±4.6	464±25	1549±86	2519±176
0.01M NaCl						
C_f	$8.47\pm0.42\times10^{-5}$	$5.10\pm0.26\times10^{-6}$	$3.05\pm0.15\times10^{-7}$	$7.34\pm0.37\times10^{-8}$	$2.27\pm0.12\times10^{-8}$	$1.80\pm0.10\times10^{-8}$
L_{Cs}	$1.93\pm0.50\times10^{-4}$	$5.15\pm0.51\times10^{-5}$	$7.08\pm0.51\times10^{-6}$	$9.37\pm0.51\times10^{-7}$	$9.97\pm0.51\times10^{-8}$	$1.02\pm0.05\times10^{-8}$
K_d	22.78±0.59	101 ±0.9	232 ±1.7	1284±7	4401±24	5714±36
0.1M NaCl						
C_f	$1.00\pm0.05\times10^{-4}$	$9.41\pm0.47\times10^{-6}$	$6.67\pm0.33\times10^{-7}$	$1.71\pm0.10\times10^{-8}$	$1.43\pm0.08\times10^{-8}$	$1.07\pm0.06\times10^{-8}$
L_{Cs}	$4.58\pm0.50\times10^{-4}$	$1.03\pm0.56\times10^{-5}$	$3.65\pm0.51\times10^{-6}$	$7.07\pm0.51\times10^{-7}$	$8.68\pm0.51\times10^{-8}$	$9.33\pm0.51\times10^{-8}$
K_d	0.46±0.50	1.10±0.53	5.46±0.76	21.9 ±1.6	55.8 ±3.4	84.1 ±6.1
1M NaCl						
C_f	$1.01\pm0.05\times10^{-4}$	$1.01\pm0.06\times10^{-5}$	$9.65\pm0.48\times10^{-7}$	$6.91\pm0.35\times10^{-8}$	$5.80\pm0.29\times10^{-8}$	$5.46\pm0.27\times10^{-8}$
L_{Cs}	$1.03\pm0.50\times10^{-4}$	$4.82\pm0.51\times10^{-5}$	$7.24\pm0.51\times10^{-6}$	$9.57\pm0.51\times10^{-7}$	$9.98\pm0.51\times10^{-8}$	$1.02\pm0.05\times10^{-8}$
K_d	0.36±0.49	0.35±0.59	0.84±0.52	5.08±0.74	8.04±0.89	9.45±0.97
Sun						
C_f	$8.19\pm0.41\times10^{-5}$	$5.42\pm0.27\times10^{-6}$	$2.88\pm0.14\times10^{-7}$	$5.37\pm0.27\times10^{-8}$	$2.36\pm0.12\times10^{-8}$	$1.89\pm0.10\times10^{-8}$
L_{Cs}	$1.03\pm0.50\times10^{-4}$	$4.82\pm0.51\times10^{-5}$	$7.24\pm0.51\times10^{-6}$	$9.57\pm0.51\times10^{-7}$	$9.94\pm0.51\times10^{-8}$	$1.02\pm0.05\times10^{-8}$
K_d	2.66±0.62	8.90±0.94	25.2±1.8	181±10	421±23	541±31

TABLE 13. Cs SORPTION ISOTHERM DATA ON Minus-Sil at 25 ± 2°C

Supporting Electrolyte	pH = 8					
Final Cs Conc. (M), C_f	Initial Cs Concentration (M)					
Cs Loading (moles/gm), L_{Cs}						
Distribution Coefficient (ml/gm), K_d	1.05×10^{-4}	1.05×10^{-5}	1.05×10^{-6}	1.06×10^{-7}	1.07×10^{-8}	1.08×10^{-9}
0.002M NaCl						
C_f	$5.67\pm0.28\times10^{-5}$	$1.81\pm0.09\times10^{-5}$	$8.14\pm0.41\times10^{-8}$	$1.65\pm0.08\times10^{-8}$	$6.43\pm0.32\times10^{-9}$	$4.13\pm0.21\times10^{-9}$
L_{Cs}	$4.58\pm0.51\times10^{-4}$	$8.27\pm0.51\times10^{-5}$	$9.20\pm0.51\times10^{-6}$	$9.90\pm0.50\times10^{-7}$	$1.01\pm0.05\times10^{-7}$	$1.04\pm0.05\times10^{-8}$
K_d	8.09±0.89	45.9 ±2.9	113±7	601±33	1573±98	2541±176
0.01M NaCl						
C_f	$8.12\pm0.41\times10^{-5}$	$4.57\pm0.23\times10^{-6}$	$2.64\pm0.13\times10^{-7}$	$6.48\pm0.33\times10^{-8}$	$2.34\pm0.12\times10^{-8}$	$1.84\pm0.10\times10^{-8}$
L_{Cs}	$2.27\pm0.51\times10^{-4}$	$5.63\pm0.51\times10^{-5}$	$7.48\pm0.51\times10^{-6}$	$9.46\pm0.51\times10^{-7}$	$9.98\pm0.51\times10^{-8}$	$1.02\pm0.05\times10^{-8}$
K_d	27.9±0.62	123 ±1.1	284 ±2.0	1460±9	4264±24	5544±37
0.1M NaCl						
C_f	$9.98\pm0.50\times10^{-5}$	$8.77\pm0.44\times10^{-6}$	$6.29\pm0.31\times10^{-7}$	$3.50\pm0.17\times10^{-8}$	$1.48\pm0.07\times10^{-8}$	$1.07\pm0.05\times10^{-8}$
L_{Cs}	$2.53\pm4.97\times10^{-5}$	$2.16\pm4.97\times10^{-3}$	$1.06\pm0.50\times10^{-6}$	$3.53\pm0.51\times10^{-7}$	$4.19\pm0.51\times10^{-8}$	$5.41\pm0.51\times10^{-8}$
K_d	0.52±0.50	1.87±0.57	6.35±0.80	19.3 ±1.6	55.1 ±3.4	77.0 ±4.3
1M NaCl						
C_f	$1.02\pm0.05\times10^{-4}$	$1.03\pm0.06\times10^{-5}$	$9.39\pm0.47\times10^{-7}$	$6.88\pm0.34\times10^{-8}$	$5.33\pm0.27\times10^{-8}$	$5.01\pm0.25\times10^{-8}$
L_{Cs}	$2.53\pm4.97\times10^{-5}$	$2.18\pm4.97\times10^{-3}$	$1.06\pm0.50\times10^{-6}$	$3.53\pm0.51\times10^{-7}$	$4.10\pm0.51\times10^{-8}$	$4.41\pm0.51\times10^{-8}$
K_d	0.25±0.49	0.21±0.58	1.13±0.53	5.13±0.74	7.69±0.89	8.8 ±1.0
Sun						
C_f	$8.10\pm0.42\times10^{-5}$	$5.45\pm0.27\times10^{-6}$	$2.57\pm0.13\times10^{-7}$	$6.84\pm0.34\times10^{-8}$	$2.14\pm0.11\times10^{-8}$	$1.89\pm0.09\times10^{-8}$
L_{Cs}	$2.04\pm0.50\times10^{-4}$	$4.80\pm0.51\times10^{-5}$	$7.55\pm0.51\times10^{-6}$	$9.44\pm0.51\times10^{-7}$	$9.93\pm0.51\times10^{-8}$	$1.02\pm0.05\times10^{-8}$
K_d	2.43±0.60	8.81±0.93	29.3 ±3.0	138±8	464±26	541±31

TABLE 14. Cs SORPTION ISOTHERM DATA ON Minu-Sil at 26 ± 2°C

Supporting Electrolyte	pH = 9					
[illegible]	Initial Cs Concentration (M)					
[illegible]	1.0x10^{-4}	1.0x10^{-5}	1.05x10^{-6}	1.06x10^{-7}	1.07x10^{-8}	1.09x10^{-9}
0.1 M $NaNO_3$						
[illegible]	4.2x10^{-6}	1.74±0.09x10^{-7}	7.42±0.37x10^{-8}	1.60±0.08x10^{-9}	4.51±0.25x10^{-11}	4.56±0.31x10^{-12}
[illegible]	5.4x10^{-4}	8.32±0.51x10^{-6}	9.28±0.51x10^{-6}	9.90±0.51x10^{-7}	1.02±0.05x10^{-7}	1.03±0.07x10^{-8}
[illegible]	[illegible]	47.7 ±3.5	125±7	621±35	2244±134	2267±161
0.01 M $NaNO_3$						
[illegible]	7.4x10^{-5}	3.88±0.19x10^{-6}	2.15±0.11x10^{-7}	6.03±0.30x10^{-9}	2.18±0.11x10^{-10}	1.71±0.09x10^{-11}
[illegible]	1.4x10^{-4}	8.29±0.51x10^{-5}	7.94±0.51x10^{-6}	9.50±0.61x10^{-7}	9.97±0.52x10^{-8}	1.02±0.05x10^{-8}
[illegible]	3.0 ±0.3	14.2 ±1.3	37.0 ±2.4	157±9	457±25	595±34
0.001 M $NaNO_3$						
[illegible]	9.0x10^{-5}	8.6±0.43x10^{-6}	6.07±0.30x10^{-7}	3.48±0.17x10^{-8}	1.41±0.07x10^{-9}	1.09±0.05x10^{-10}
[illegible]	1.4x10^{-4}	1.72±0.50x10^{-5}	4.20±0.51x10^{-6}	6.78±0.51x10^{-7}	8.82±0.51x10^{-8}	9.33±0.53x10^{-9}
[illegible]	1.0±0.50	1.99±0.58	6.93±0.83	19.5±1.5	62.5 ±3.8	94.8 ±5.6
0 M $NaNO_3$						
[illegible]	4.7x10^{-5}	1.00±0.06x10^{-5}	9.49±0.48x10^{-7}	7.03±0.35x10^{-8}	5.64±0.29x10^{-9}	4.96±0.25x10^{-10}
[illegible]	1.4x10^{-4}	4.55±4.97x10^{-6}	9.61±4.36x10^{-7}	3.39±0.51x10^{-7}	4.80±0.51x10^{-8}	5.45±0.53x10^{-9}
[illegible]	0.0±0.0	0.45±0.60	1.01±0.53	4.83±0.72	8.54±0.92	11.4 ±1.1
[illegible]						
[illegible]	4.3 ±0.3x10^{-4}	4.64±0.23x10^{-6}	2.35±0.12x10^{-7}	4.87±0.24x10^{-8}	2.17±0.11x10^{-10}	1.84±0.10x10^{-11}
[illegible]	1.4±0.51x10^{-4}	5.57±0.51x10^{-6}	7.74±0.51x10^{-6}	9.41±0.51x10^{-7}	9.9[illegible]±0.51x10^{-8}	1.02±0.05x10^{-8}
[illegible]	5.0±0.4	12.0 ±1.1	33.0 ±2.2	200±11	458±25	563±31

TABLE 15. Cs SORPTION ISOTHERM DATA ON Minu-Sil at 26 ± 2°C

[illegible]	pH = 10					
[illegible]	Initial Cs Concentration (M)					
[illegible]	1.0x10^{-4}	1.0x10^{-5}	1.05x10^{-6}	1.06x10^{-7}	1.07x10^{-8}	1.09x10^{-9}
[illegible]						
[illegible]	3.0±0.18x10^{-5}	1.92±0.10x10^{-6}	5.03±0.25x10^{-8}	1.30±0.07x10^{-9}	5.44±0.3 x10^{-11}	4.51±0.31x10^{-12}
[illegible]	1.4±0.51x10^{-4}	8.14±0.51x10^{-6}	9.50±0.51x10^{-6}	9.94±0.53x10^{-7}	1.01±0.05x10^{-7}	1.03±0.06x10^{-8}
[illegible]	16.1 ±1.4	42.6 ±2.7	169±11	768±42	1860±107	2286±143
[illegible]						
[illegible]	7.1x10^{-5}	5.0±0.25x10^{-6}	1.96±0.10x10^{-7}	6.27±0.31x10^{-9}	2.34±0.12x10^{-10}	1.92±0.10x10^{-11}
[illegible]	1.1x10^{-4}	5.15±0.51x10^{-5}	8.12±0.51x10^{-6}	9.48±0.51x10^{-7}	9.94±0.51x10^{-8}	1.02±0.05x10^{-8}
[illegible]	4.4±0.71	10.1 ±1.0	41.5 ±3.2	151±9	424±24	560±32
[illegible]						
[illegible]	9.5±0.48x10^{-5}	7.0±0.38x10^{-6}	5.37±0.27x10^{-7}	3.13±0.16x10^{-8}	1.3[illegible]±0.07x10^{-9}	8.6[illegible]±0.43x10^{-11}
[illegible]	1.4±4.97x10^{-5}	2.75±0.51x10^{-5}	4.88±0.51x10^{-6}	7.05±0.51x10^{-7}	8.93±0.51x10^{-8}	9.65±0.53x10^{-9}
[illegible]	1.4±0.52	3.61±0.66	9.08±0.95	22.7±1.7	68.5 ±4.1	111±7
[illegible]						
[illegible]	1.04±0.05x10^{-4}	9.69±0.58x10^{-6}	8.27±0.41x10^{-7}	5.91±0.30x10^{-8}	5.00±0.25x10^{-9}	4.32±0.22x10^{-10}
[illegible]	1.4±4.97x10^{-5}	7.70±4.97x10^{-6}	2.12±0.50x10^{-6}	4.40±0.51x10^{-7}	5.41±0.51x10^{-8}	6.2[illegible]±0.53x10^{-9}
[illegible]	0.10±0.4	0.79±0.61	2.56±0.61	7.37±0.86	10.8±1.0	14.6 ±1.3
[illegible]						
[illegible]	6.6±0.33x10^{-5}	4.89±0.25x10^{-6}	2.27±0.11x10^{-7}	5.24±0.26x10^{-9}	2.38±0.12x10^{-10}	2.05±0.11x10^{-11}
[illegible]	1.7±0.51x10^{-4}	5.32±0.51x10^{-5}	7.81±0.51x10^{-6}	9.51±0.51x10^{-7}	9.94±0.51x10^{-8}	1.02±0.05x10^{-8}
[illegible]	5.7±0.77	10.8 ±1.0	34.4 ±2.3	183±10	417±23	496±28

Plots of the first term versus the third term should produce straight lines of slope n = 1 for exchange of monovalent ions from which $K^a_{Cs/Na}$ can be obtained.

For low Cs loadings of the surface, $(SO^-Na^+)_s$ can be approximated by the sodium CEC and $(Na^+)_a$ by the electrolyte concentration. The concentrations of Cs on the surface can be calculated from the initial and final Cs concentrations in solution. The values of γ_{Cs^+} and γ_{Na^+} can be estimated for the different electrolyte solutions from extended Debye-Hückel theory (Butler 1964, p.438). Figures 8 - 19 show the logarithmic plots for the Belle Fourche clay and for Min-u-sil for the six pH values and the four NaCl solutions studied. The solid lines were calculated from a linear least squares fit to the points. The corresponding slopes, n, and Cs/Na exchange constants, $K^a_{Cs/Na}$, are also shown in the figures.

The plots of the clay data do result in straight lines of slope nearly equal to one. The $K^a_{Cs/Na}$ values increase slowly with pH from about 6 to 10. Apparently the sorption of Cs by the clay can be expressed as a simple exchange of Cs for Na and the mass-action equations are applicable over the range of pH and NaCl concentrations studied.

The plots of the Min-u-sil data also result in straight lines but slopes of from 0.55 to 0.64 were obtained with increasing pH. The values of $K^a_{Cs/Na}$ also varied over a factor of 6, from 0.78 to 5 with increasing pH. The simple mass action expression for the exchange of Cs for Na is not adequate to predict the Cs sorption. For the concentration of Na on the quartz, $(SO^-Na^+)_s$, we assumed the Na CEC value measured at pH 7 for all pH values in the analysis. Since the Na CEC may vary appreciably with pH for quartz (Allen, Matijevic and Meites 1971), using a constant value for $(SO^-Na^+)_s$ could cause the apparent variation of $K^a_{Cs/Na}$ with pH. Also, the results of the chemical analysis of the quartz suggest the presence of a small amount of a contaminating mineral or minerals. If this material has a high CEC, e.g., like mica or clay, it could make a measurable contribution to the sorption. The apparent slope, n, could then be the result of more than one component, one from the quartz and one or more from the contaminants, and thus the slope could differ from unity.

However, deviations from a single mass-action law expression were also observed by Allen et al. in investigations of the exchange of Na^+ for H^+ on silica (Allen, Matijevic and Meites 1971). They attempted to explain the deviations as being due to the presence of two distinct types of sites or silica phases with sufficiently different reactivities that one site nearly completely fills before the second site begins to fill. They also suggest that the apparent equilibrium constant for the exchange at a single type of site changes with the surface composition. It is not known at present whether the deviations from simple behavior we observe are due to experimental problems or are intrinsic to the quartz (or a combination of both).

Figures 20 - 25 show the variation of K_d with Cs loading, L_{Cs}, and electrolyte concentration for the clay for each of the pH values. The K_d values rapidly approach a constant value with decreasing loading for all pH values and electrolyte concentrations, as would be expected from the mass-action expression. The K_d values for the synthetic groundwater solutions behave similarly and the magnitudes are close to those of the NaCl solution of nearly the same ionic strength, i.e., the 0.002M NaCl solutions. An average K_d value was calculated for each electrolyte concentration over the range of loading where the K_d appears to be constant, i.e., L_{Cs} less than 10^{-3}, and these values are plotted as a function of pH in Figure 26. There does appear to be a small increase in K_d with decreasing hydrogen ion concentration, particularly for the lower electrolyte concentrations.

Figures 27 - 32 show the variation of K_d with Cs loading and electrolyte concentration for the quartz for each of the pH values. There is a rather large variation of K_d with loading for all electrolyte concentrations at all pH values, however, the K_d values appear to approach constant values at the lowest loadings. Figures 33, 34, and 35 show the variation of K_d with pH for the different electrolyte concentrations at fixed values of cesium loading of 2×10^{-4}, 2×10^{-6}, and 2×10^{-8}. The K_d values were estimated by drawing smooth curves through the points in the K_d versus L_{Cs} plots and slicing through the curves at the desired loading values. Except for L_{Cs} of 2×10^{-8}, the large errors in K_d values for the 1M NaCl solutions precluded a reliable

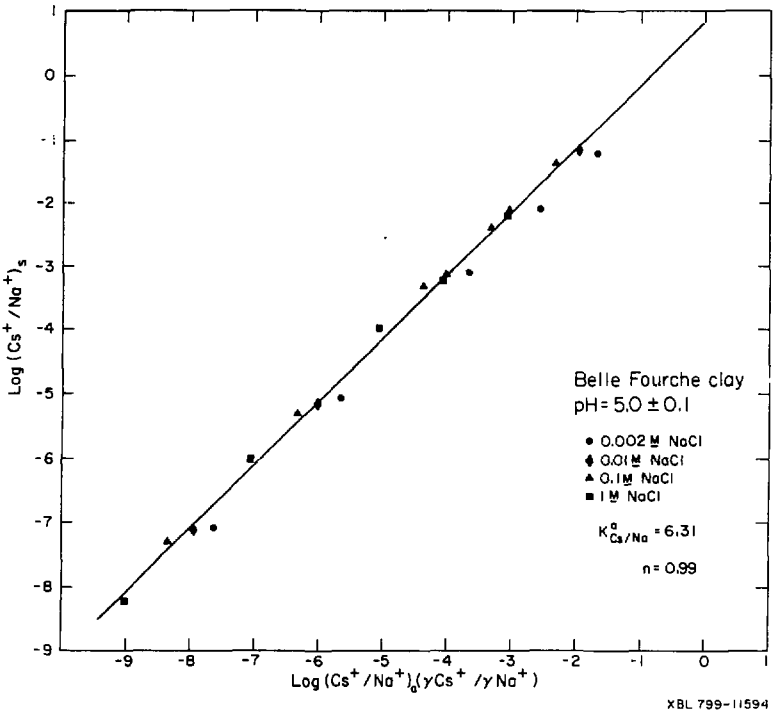

FIGURE 8. Mass-action law representation (equation 41) of the exchange of Cs^+ for Na^+ on the Belle Fourche clay at pH 5 and several NaCl electrolyte concentrations. The solid line is a least squares fit to the experiment points from which an estimate of the Cs/Na exchange constant, $K^a_{Cs/Na}$, can be obtained. The slope, n, should be 1 for the exchange of monovalent ions.

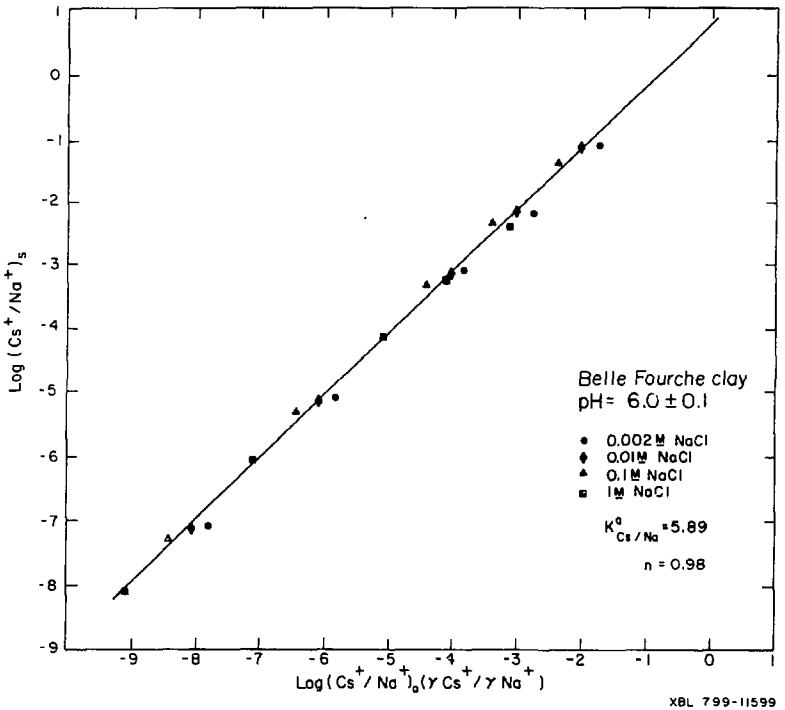

FIGURE 9. Mass-action law representation (equation 41) of the exchange of Cs^{+} for Na^{+} on the Belle Fourche clay at pH 6 and several NaCl electrolyte concentrations. The solid line is a least squares fit to the experimental points from which an estimate of the Cs/Na exchange constant, $K^{a}_{Cs/Na}$, can be obtained. The slope, n, should be 1 for the exchange of monovalent ions.

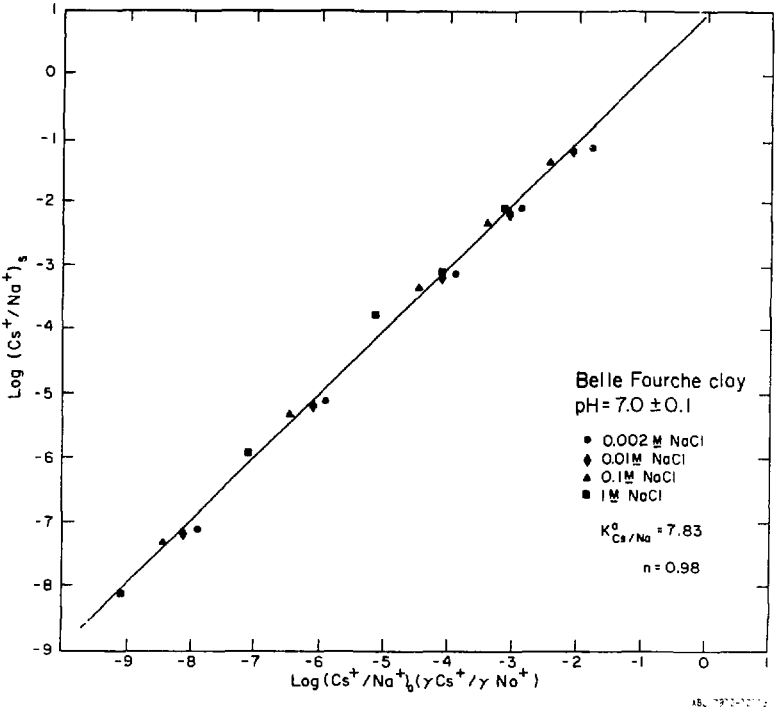

FIGURE 10. Mass-action law representation (equation 41) of the exchange of Cs^+ for Na^+ on the Belle Fourche clay at pH 7 and several NaCl concentrations. The solid line is a least squares fit to experimental points from which an estimate of the Cs/Na exchange constant, $K^a_{Cs/Na}$, can be obtained. The slope, n, should be 1 for the exchange of monovalent ions.

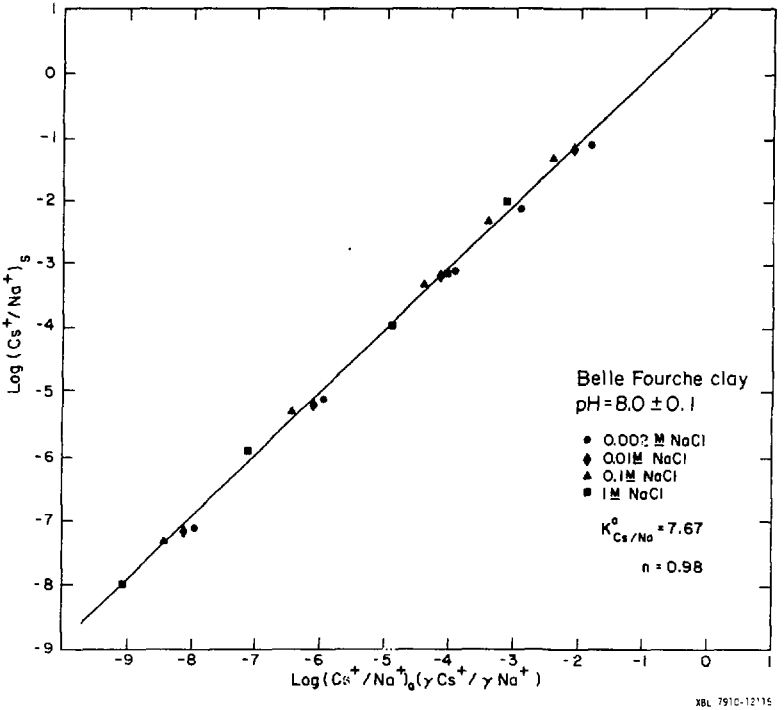

FIGURE 11. Mass-action law representation (equation 41) of the exchange of Cs^+ for Na^+ on the Belle Fourche clay at pH 8 and several NaCl concentrations. The solid line is a least squares fit to experimental points from which an estimate of the Cs/Na exchange constant, $K^{a}_{Cs/Na}$, can be obtained. The slope, n, should be 1 for the exchange of monovalent ions.

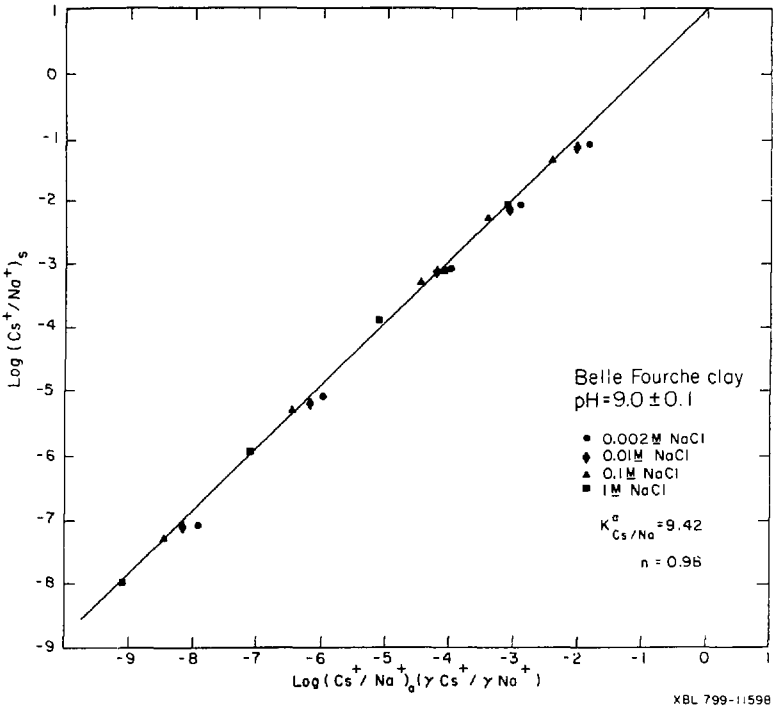

FIGURE 12. Mass-action law representation (equation 41) of the exchange of Cs^+ for Na^+ on the Belle Fourche clay at pH 9 and several NaCl concentrations. The solid line is a least squares fit to experimental points from which an estimate of the Cs/Na exchange constant, $K^{a}_{Cs/Na}$, can be obtained. The slope, n, should be 1 for the exchange of monovalent ions.

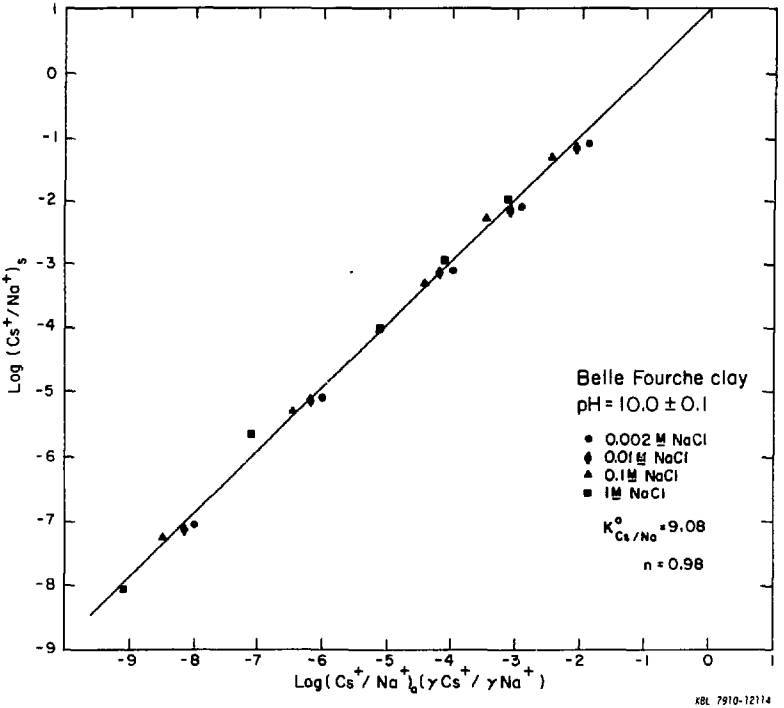

FIGURE 13. Mass-action law representation (equation 41) of the exchange of Cs^+ for Na^+ on the Belle Fourche clay at pH 10 and several NaCl concentrations. The solid line is a least squares fit to experimental points from which an estimate of the Cs/Na exchange constant, $K^{a}_{Cs/Na}$, can be obtained. The slope, n, should be 1 for the exchange of monovalent ions.

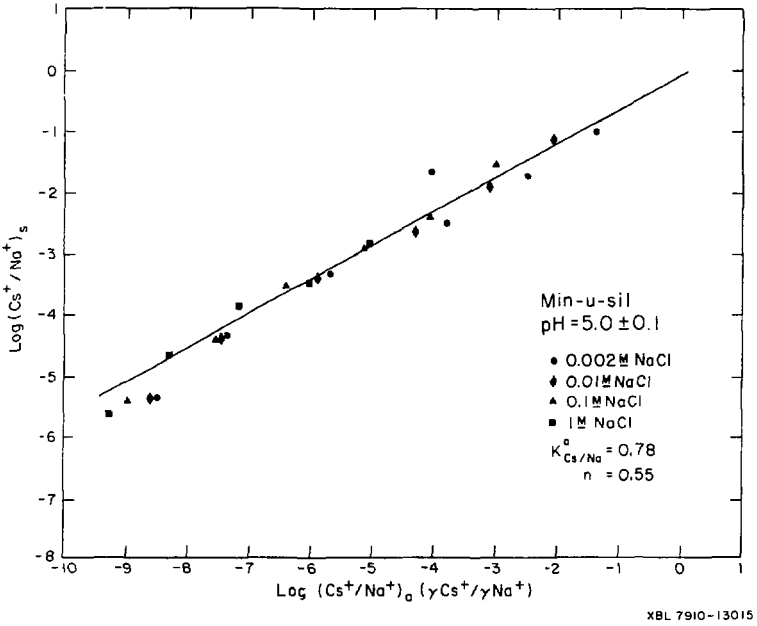

FIGURE 14. Mass-action law representation (equation 41) of the exchange of Cs^+ for Na^+ on the Min-u-sil at pH 5 and several NaCl concentrations. The solid line is a least squares fit to experimental points from which an estimate of the Cs/Na exchange constant, $K^{a}_{Cs/Na}$, can be obtained. The slope, n, should be 1 for the exchange of monovalent ions.

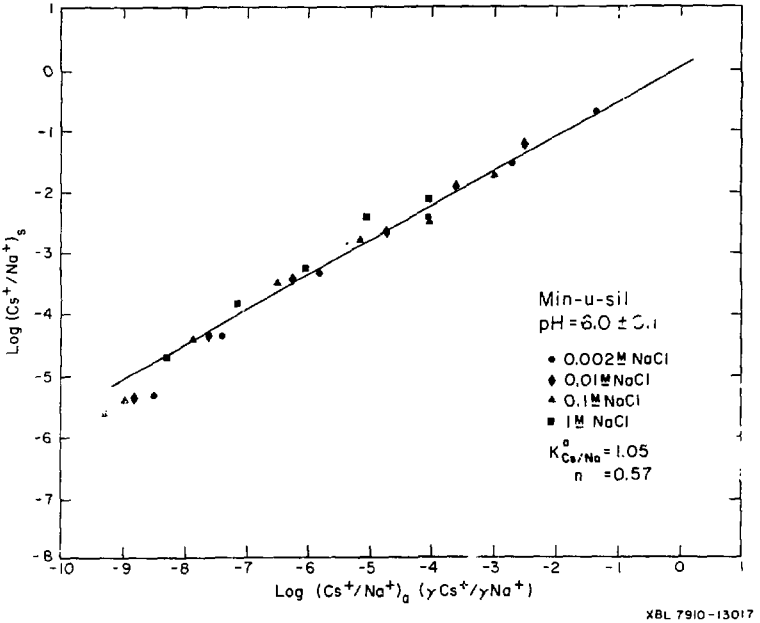

FIGURE 15. Mass-action law representation (equation 41) of the exchange of Cs^+ for Na^+ on the Min-u-sil at pH 6 and several NaCl concentrations. The solid line is a least squares fit to experimental points from which an estimate of the Cs/Na exchange constant, $K^{a}_{Cs/Na}$, can be obtained. The slope, n, should be 1 for the exchange of monovalent ions.

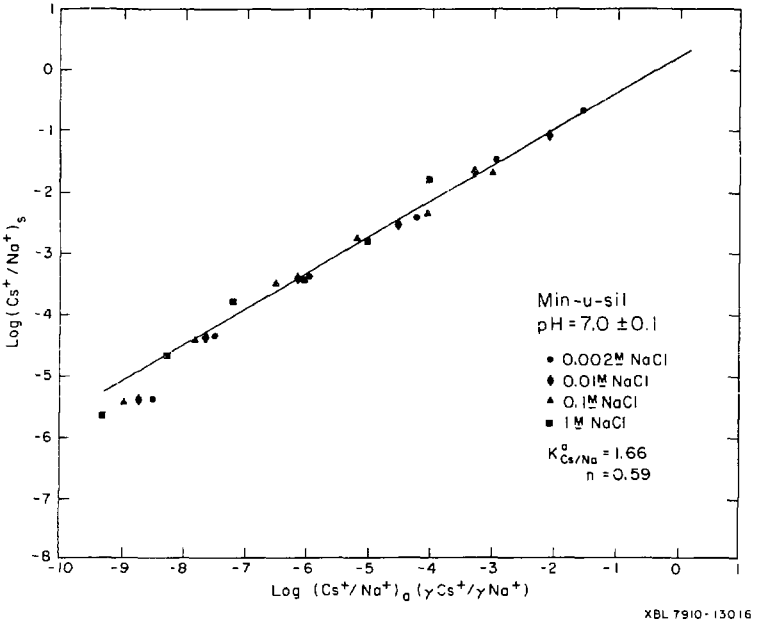

FIGURE 16. Mass-action law representation (equation 41) of the exchange of Cs^+ for Na^+ on the Min-u-sil at pH 7 and several NaCl concentrations. The solid line is a least squares fit to experimental points from which an estimate of the Cs/Na exchange constant, $K^{a}_{Cs/Na}$, can be obtained. The slope, n, should be 1 for the exchange of monovalent ions.

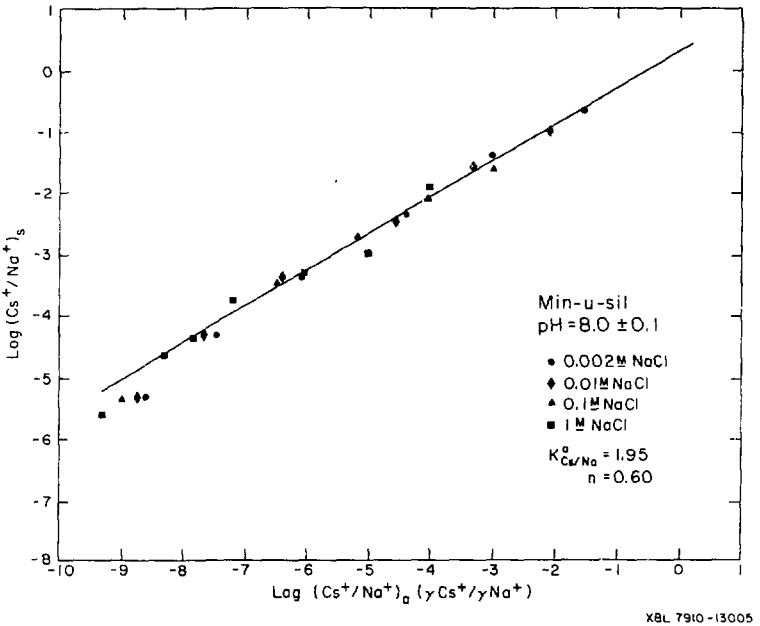

FIGURE 17. Mass-action law representation (equation 41) of the exchange of Cs^+ for Na^+ on the Min-u-sil at pH 8 and several NaCl concentrations. The solid line is a least squares fit to experimental points from which an estimate of the Cs/Na exchange constant, $K^{a}_{Cs/Na}$, can be obtained. The slope, n, should be 1 for the exchange of monovalent ions.

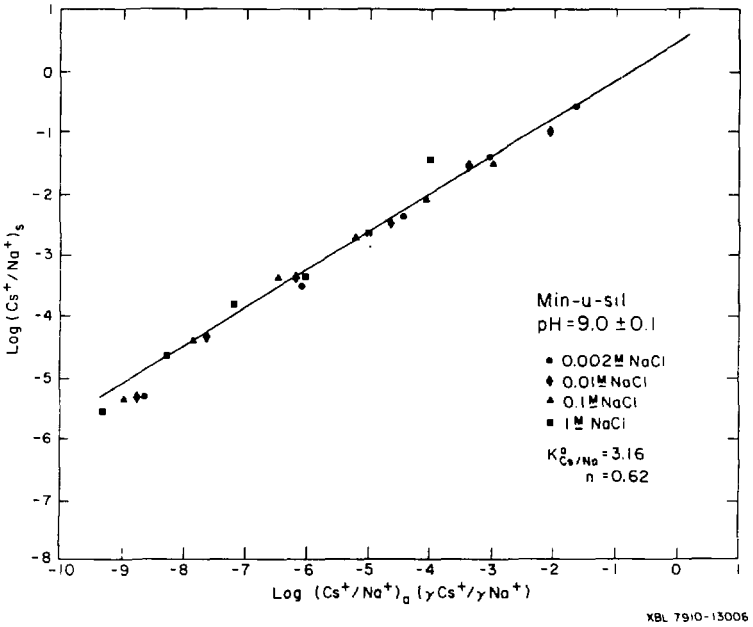

FIGURE 18. Mass-action law representation (equation 41) of the exchange of Cs^+ for Na^+ on the Min-u-sil at pH 9 and several NaCl concentrations. The solid line is a least squares fit to experimental points from which an estimate of the Cs/Na exchange constant, $K^a_{Cs/Na}$, can be obtained. The slope, n, should be 1 for the exchange of monovalent ions.

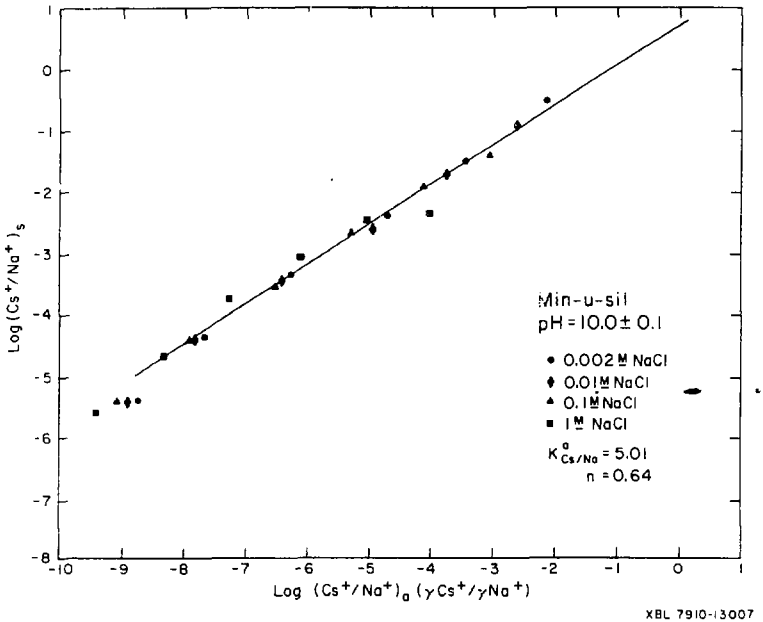

FIGURE 19. Mass-action law representation (equation 41), of the exchange of Cs^+ for Na^+ on the Min-u-sil at pH 10 and several NaCl electrolyte concentrations. The solid line is a least squares fit to the experimental points from which an estimate of the Cs/Na exchange constant, $K^a_{Cs/Na}$, can be obtained. The slope, n, should be 1 for the exchange of monovalent ions.

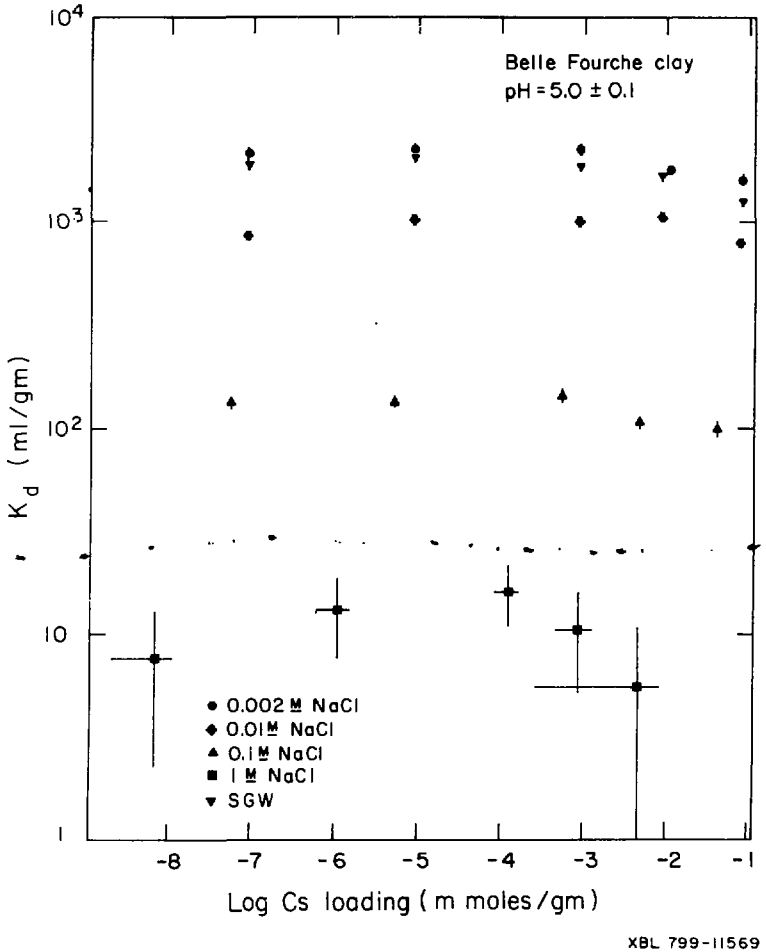

FIGURE 20. Distribution coefficients, K_d, for cesium measured at 26°C for the Na form of the Belle Fourche clay as a function of Cs loading at pH 5 for several electrolyte compositions. SGW = simulated basalt groundwater.

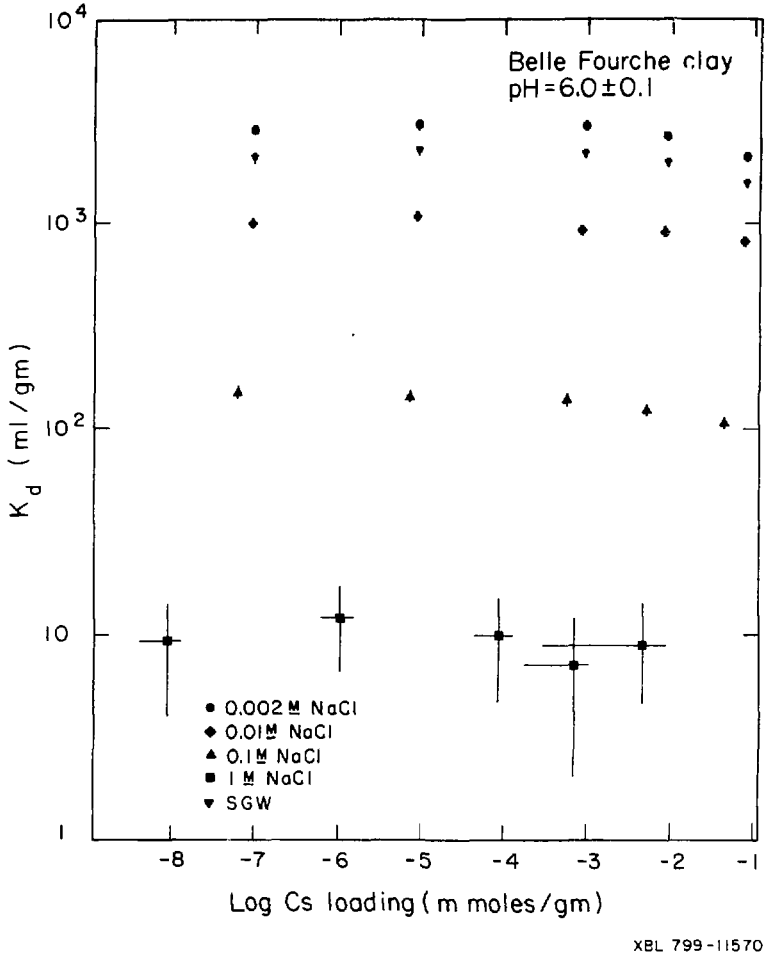

FIGURE 21. Distribution coefficients, K_d, for cesium measured at 26°C on the Na form of the Belle Fourche clay as a function of Cs loading at pH 6 for several electrolyte compositions. SGW = simulated basalt groundwater.

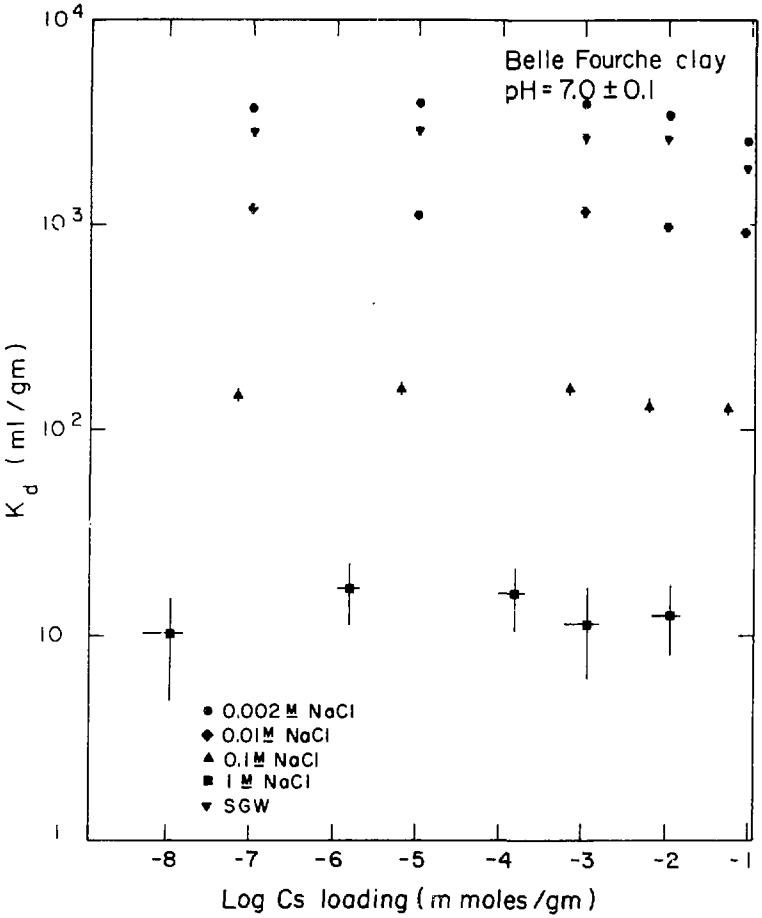

XBL 799-11576

FIGURE 22. Distribution coefficients, K_d, for cesium measured at 26°C on the Na form of the Belle Fourche clay as a function of Cs loading at pH 7 for several electrolyte compositions. SGW = simulated basalt groundwater.

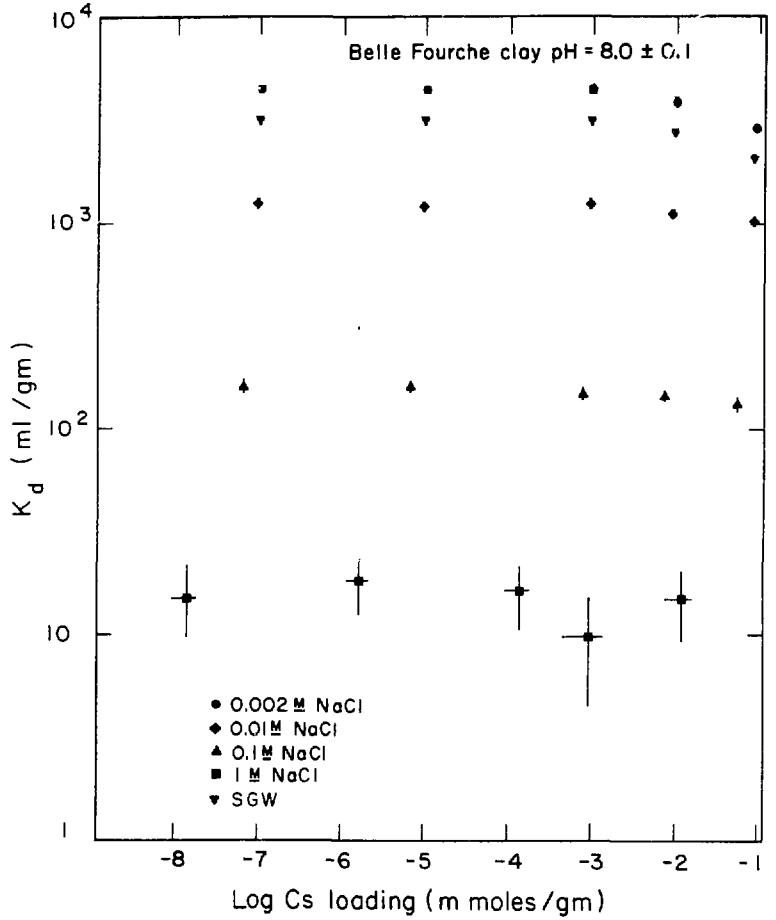

FIGURE 23. Distribution coefficients, K_d, for cesium measured at 26°C on the Na form of the Belle Fourche clay as a function of Cs loading at pH 8 for several electrolyte compositions. SGW = simulated basalt groundwater.

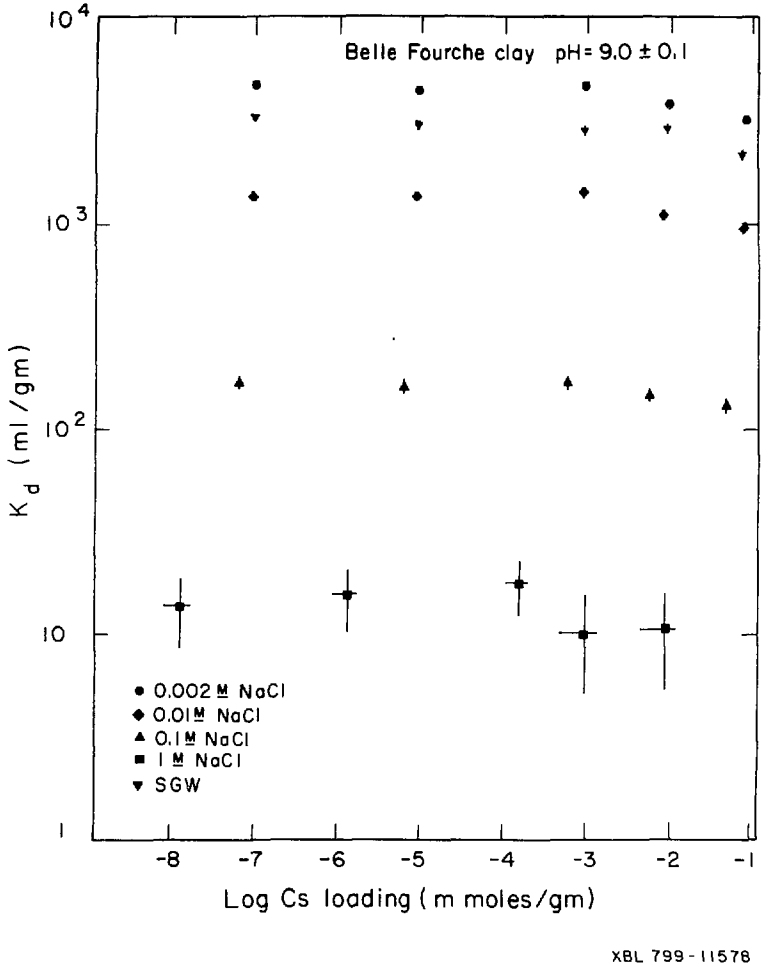

XBL 799-11578

FIGURE 24. Distribution coefficients, K_d, for cesium measured at 26°C on the Na form of the Belle Fourche clay as a function of Cs loading at pH 9 for several electrolyte compositions. SGW = simulated basalt groundwater.

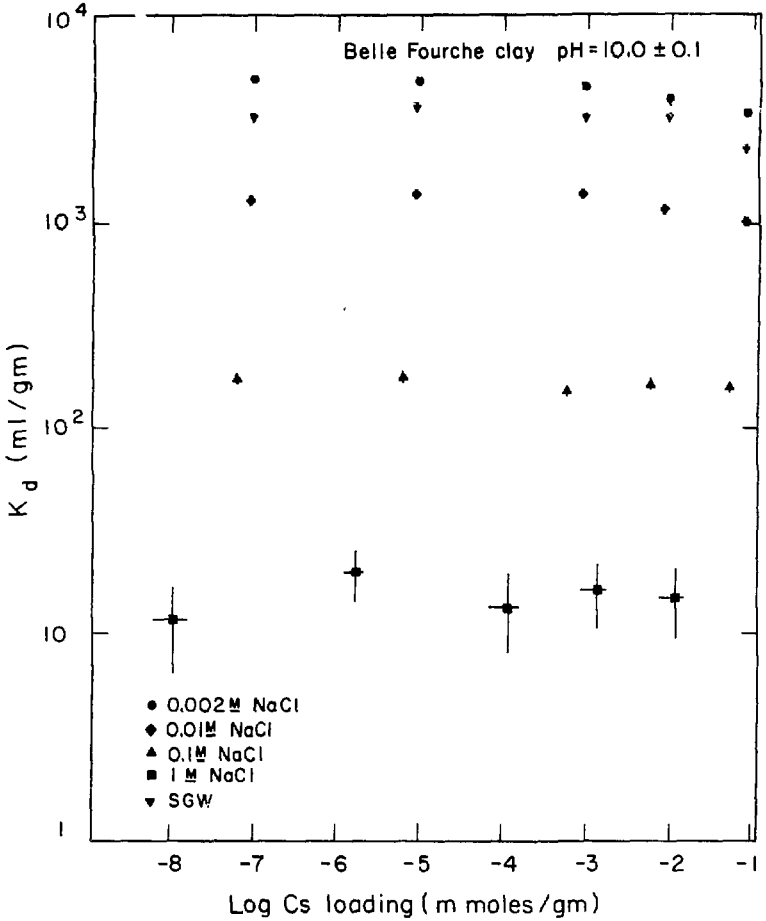

FIGURE 25. Distribution coefficients, K_d, for cesium measured at 26°C on the Na form of the Belle Fourche clay as a function of Cs loading at pH 10 for several electrolyte compositions. SGW = simulated basalt groundwater.

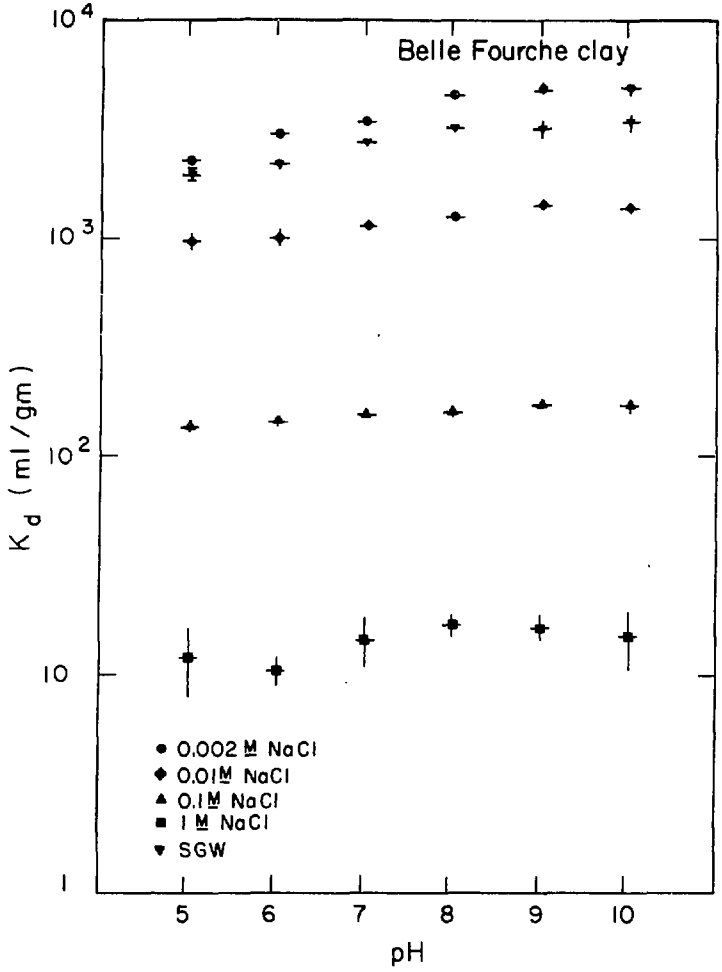

FIGURE 26. Average distribution coefficients, K_d, for cesium loadings less than 10^{-3} m moles/gm on the Belle Fourche clay as a function of pH for several electrolyte compositions. SGW = simulated basalt groundwater.

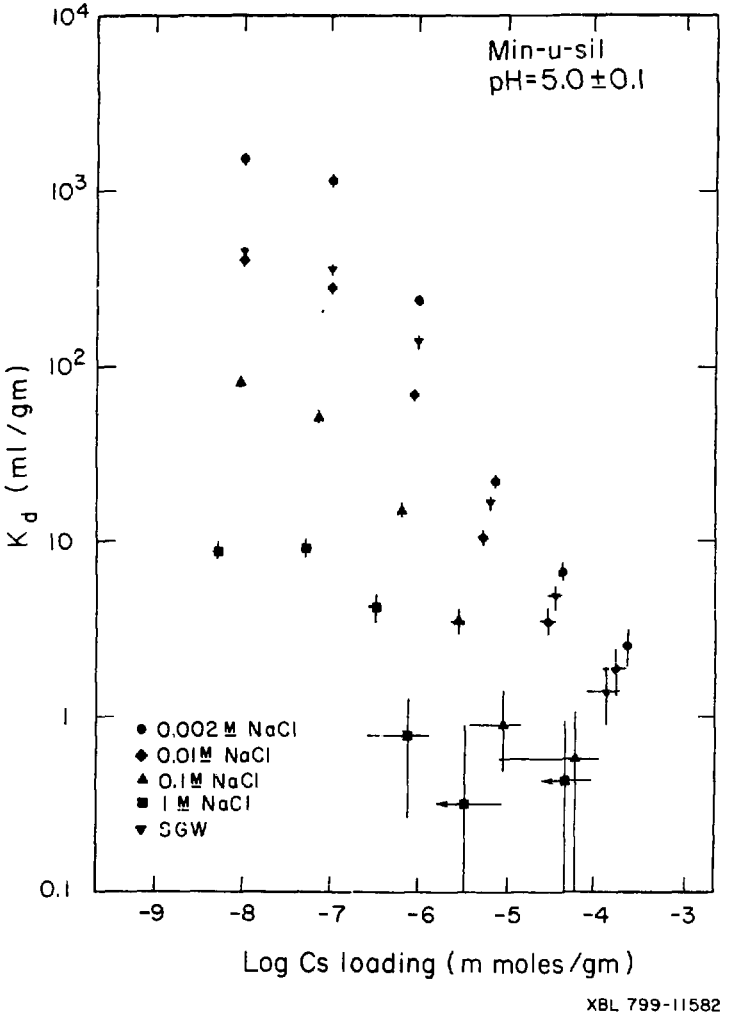

FIGURE 27. Distribution coefficients, K_d, for cesium measured at 26°C on Min-u-sil as a function of Cs loading at pH 5 for several electrolyte compositions. SGW = simulated basalt groundwater.

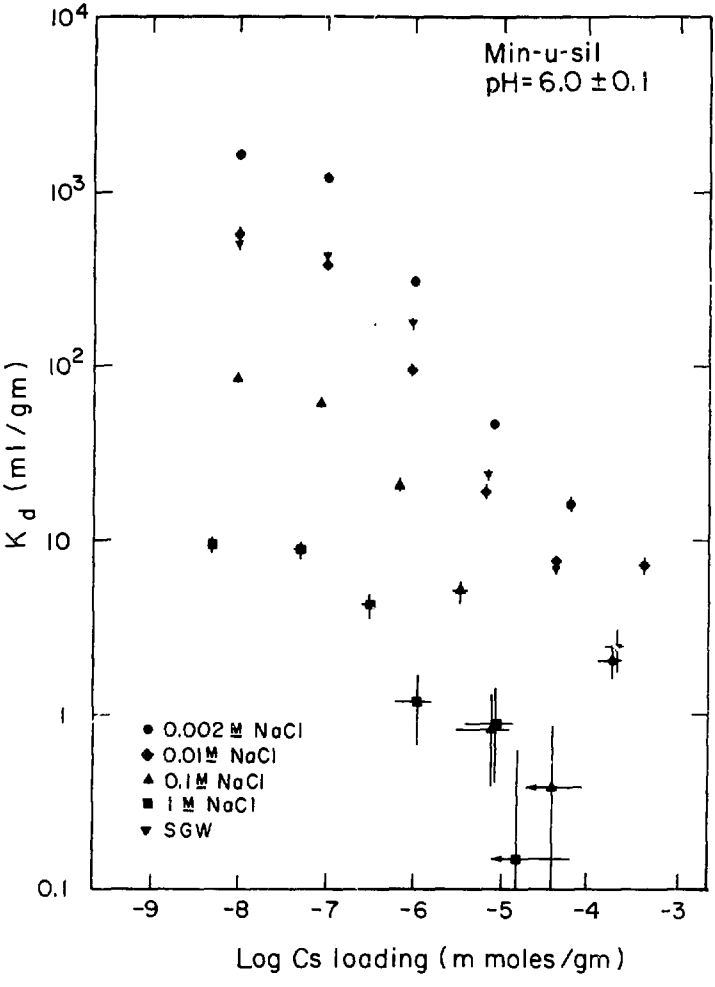

FIGURE 28. Distribution coefficients, K_d, for cesium measured at 26°C on Min-u-sil as a function of Cs loading at pH 6 for several electrolyte compositions. SGW = simulated basalt groundwater.

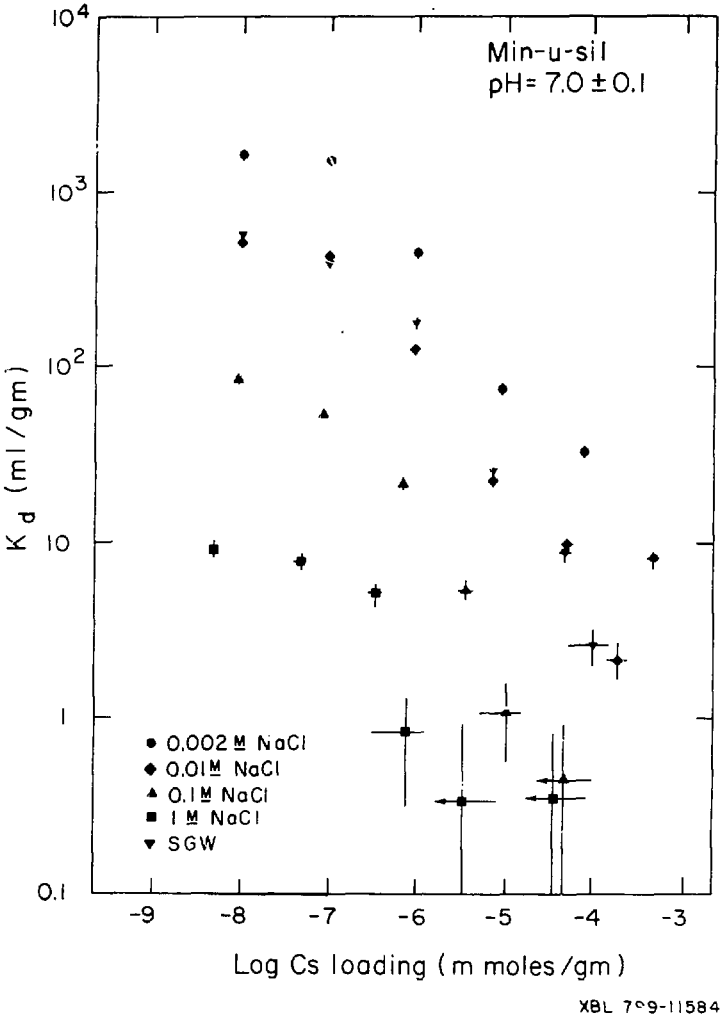

FIGURE 29. Distribution coefficients, K_d, for cesium measured at 26°C on Min-u-sil as a function of Cs loading at pH 7 for several electrolyte compositions. SGW = simulated basalt groundwater.

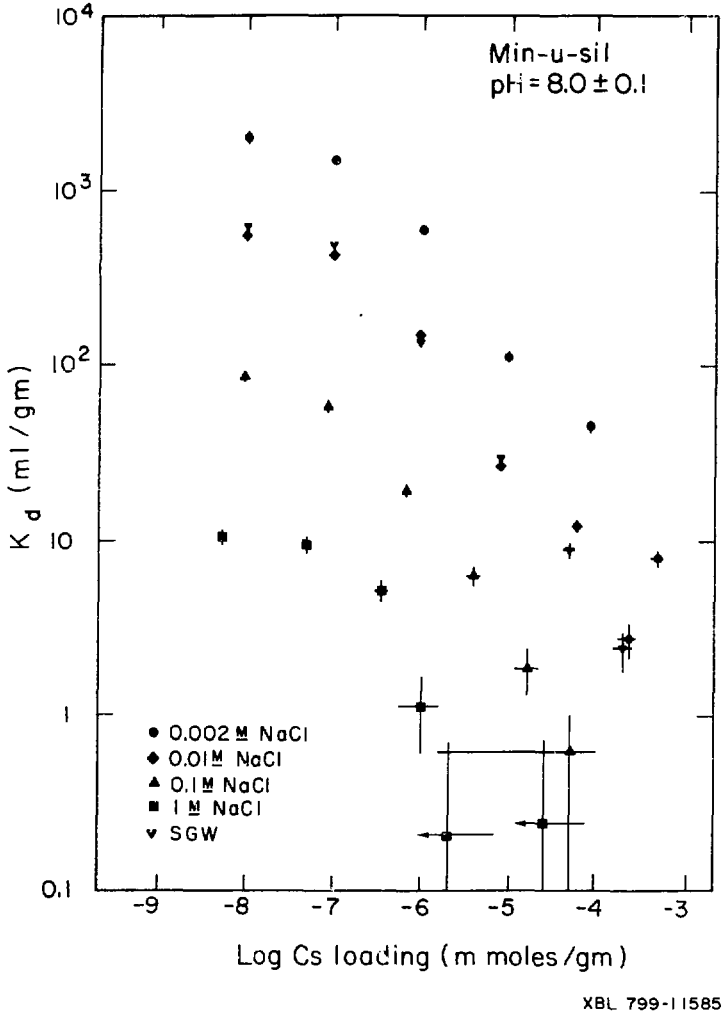

FIGURE 30. Distribution coefficients, K_d, for cesium measured at 26°C on Min-u-sil as a function of Cs loading at pH 8 for several electrolyte compositions. SGW = simulated basalt groundwater.

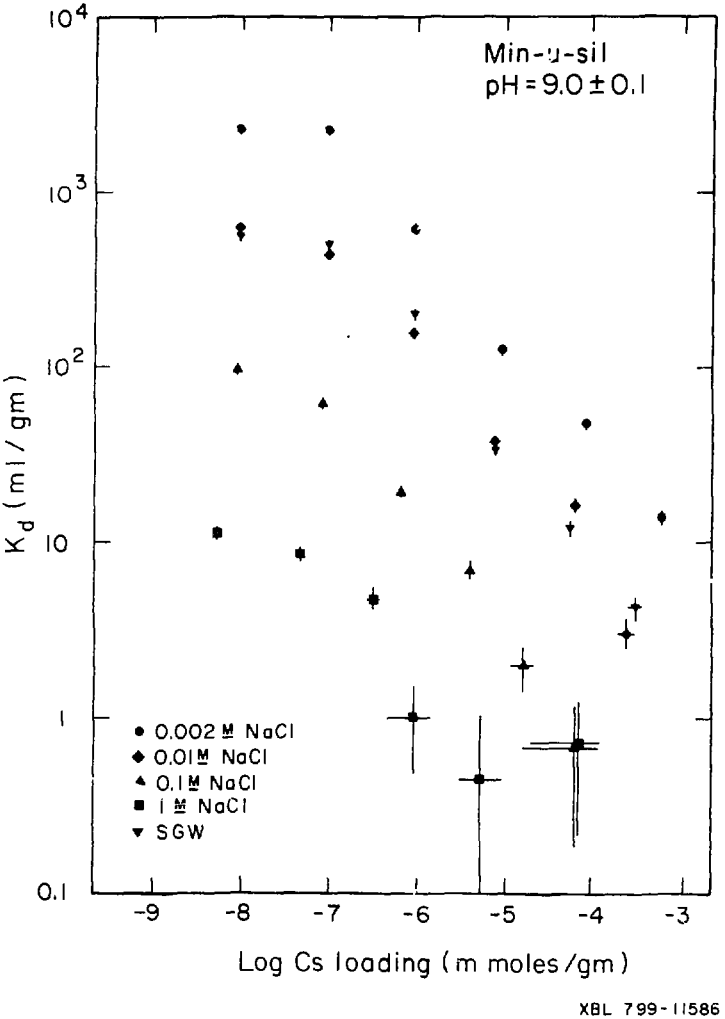

FIGURE 31. Distribution coefficients, K_d, for cesium measured at 26°C on Min-u-sil as a function of Cs loading at pH 9 for several electrolyte compositions. SGW = simulated basalt groundwater.

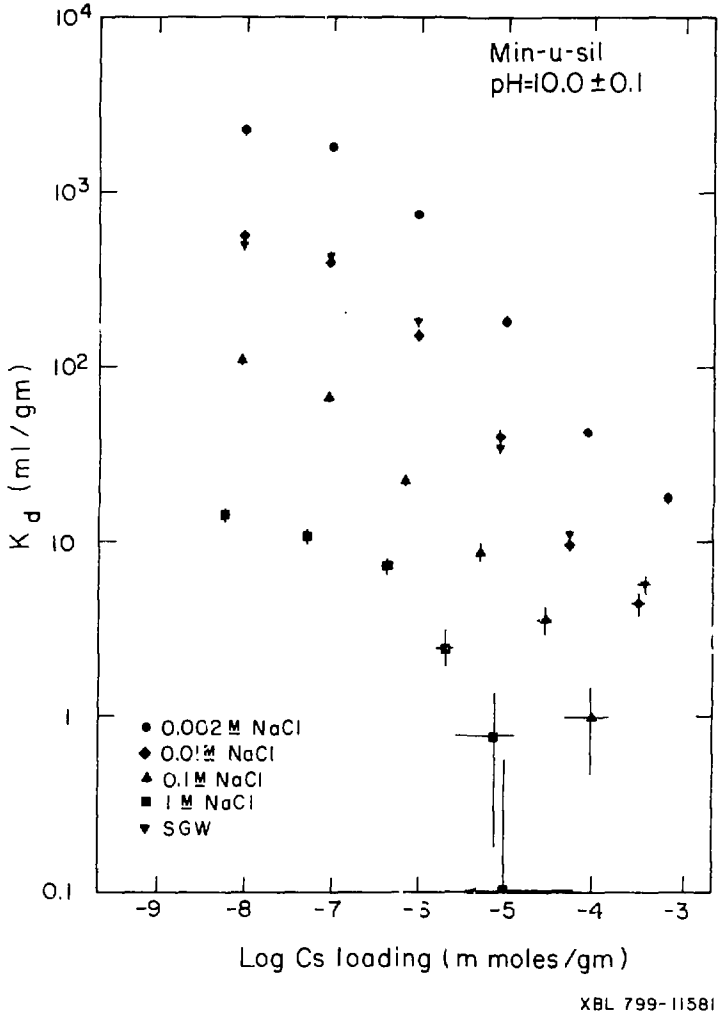

FIGURE 32. Distribution coefficients, K_d, for cesium measured at 26°C on Min-u-sil as a function of Cs loading at pH 10 for several electrolyte compositions. SGW = simulated basalt groundwater.

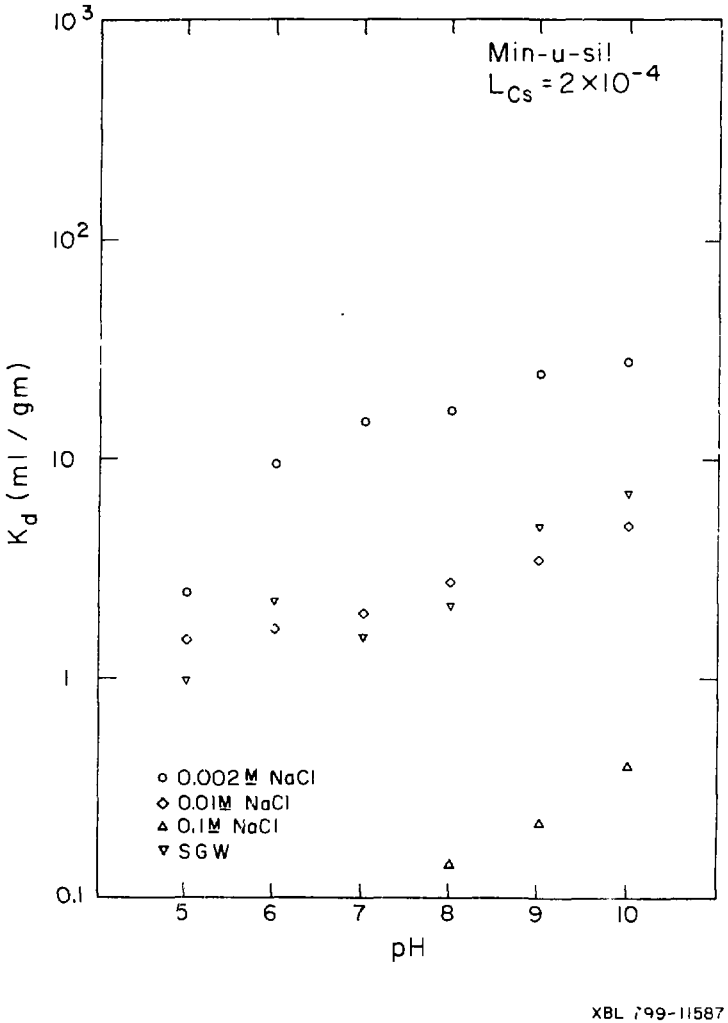

XBL 799-11587

FIGURE 33. Distribution coefficients, K_d, for cesium on Min-u-sil as a function of pH for several electrolyte compositions. SGW = simulated basalt groundwater. Open points result from slicing through smooth curves through the points given in figures 27-32 at a Cs loading of 2×10^{-4} m moles/gm.

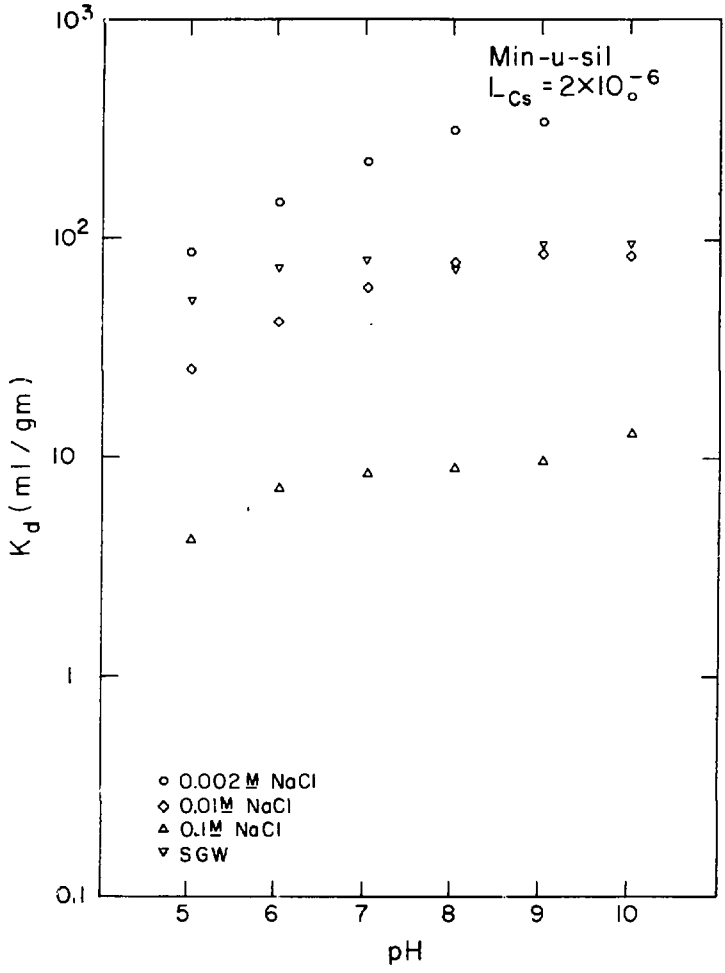

XBL 799-11588

FIGURE 34. Distribution coefficients, K_d, for cesium on Min-u-sil as a function of pH for several electrolyte compositions. SGW = simulated basalt groundwater. Open points result from slicing through smooth curves through the points given in figures 27-32 at a Cs loading of 2×10^{-6} m moles/gm.

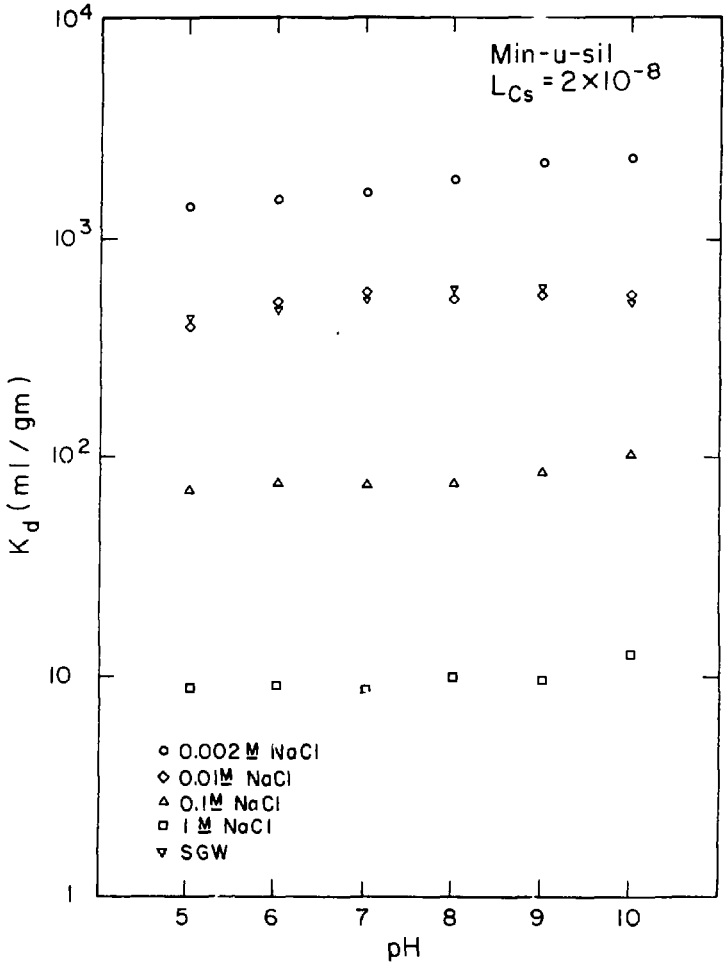

XBL 799-11589

FIGURE 35. Distribution coefficients, K_d, for cesium on Min-u-sil as a function of pH for several electrolyte compositions. SGW = simulated basalt groundwater. Open points result from slicing through smooth curves through the points given in figures 27-32 at a Cs loading of 2×10^{-8} m moles/gm.

analysis. At the higher loadings, the dependence of K_d on pH is rather large but this dependence decreases rapidly with decreased loading. For Min-u-sil, the results for the SGW are more nearly like the 0.01M NaCl solution than the 0.002M NaCl solution as was the case with the clay.

For the Belle Fourche clay, the K_d values showed only a small dependence on pH and Cs loading but a large dependence on electrolyte concentration. For the Min-u-sil, the K_d values showed a large dependence on all three parameters.

TESTING OF THE MODEL

SORPTION OF Cs ON BELLE FOURCHE CLAY

Several investigators (Garrels and Christ 1956; Blackman 1958; Truesdell and Christ 1968) have found from acid/base titrations that a single hydrogen clay behaves like a mixture of at least two distinct weak acids, i.e., two energetically different uniform sets of exchange sites. The possible nature of these sites have been discussed by Grim (Grim 1968, p.198) and James (James and Parks 1979). Our titration curves for the Belle Fourche clay also suggest the presence of two sites and, therefore, we have used a two-site model in our analysis.

Determination of MINEQL Modeling Parameters

Surface Ionization and Sodium Exchange Constants

In principle, the double extrapolation method should be applicable for determining the intrinsic surface ionization and sodium exchange constants from the titration data. As discussed previously, in practice the presence of a second site confuses the problem and long extrapolations make the results suspect. Instead, we were obliged to use a graphic method of fitting calculated curves to the titration data to obtain approximate values for these constants which ignores the changes in the constants due to surface charge. Therefore, the superscript, int, has been omitted from the symbols.

Since neither a positively charged surface nor a point of zero charge were observed for the clay in the pH region studied, the surface should be dominated by the species SO^-, TO^-, SO^-Na^+, TO^-Na^+, SOH and TOH, and the surface charge determined by the concentrations of the four charged species. For the SOH type site, we assume

$$SOH \rightleftharpoons SO^- + H^+; \quad K_{a_2} = \frac{(SO^-)(H^+)_{aq}}{(SOH)} \tag{42}$$

$$SOH + Na^+ \rightleftharpoons SO^-Na^+ + H^+; \quad {}^*K_{Na^+} = \frac{(SO^-Na^+)(H^+)_{aq}}{(SOH)(Na^+)_{aq}} \tag{43}$$

and,

$$(SO^-) + (SO^-Na^+) = \frac{K_{a_2}(SOH)}{(H^+)_{aq}} + \frac{{}^*K_{Na^+}(SOH)(Na^+)_{aq}}{(H^+)_{aq}} \tag{44}$$

or in logarithmic form,

$$\log[(SO^-) + (SO^-Na^+)] = \log(SOH) + pH + \log[K_{a_2} + {}^*K_{Na^+}(Na^+)] \tag{45}$$

Similar equations can be written for the TOH type sites.

At low pH values, little surface ionization occurs and $(SOH) \simeq N_S$, the total concentration of the SOH-type sites. In this pH region for constant Na^+ activity, a plot of $\log[(SO^-) + (SO^-Na^+)]$ versus pH should yield a curve which has a slope approaching +1 with decreasing pH. At high pH values, the surface is nearly completely ionized and $[(SO^-) + (SO^-Na^+)] \simeq N_S$. In this region, the slope of the curve should approach zero with increasing pH. The overall shape of the curve produced by plotting $\log[(SO^-) + (SO^-Na^+)]$ versus pH for a given value of Na^+ activity is independent of the actual values of N_S, K_{a_2}, and ${}^*K_{Na^+}$ (assuming they are constants) and, therefore, a generalized curve may be constructed. However, the position of the curve along the $\log[(SO^-) + (SO^-Na^+)]$ axis is determined by N_S, while the position along the pH axis is determined by $[K_{a_2} + {}^*K_{Na^+}(Na^+)]$. Thus, estimates for N_S, K_{a_2}, and ${}^*K_{Na^+}$ can be obtained by fitting the generalized curves to the experimental points calculated from the titration data.

The estimates for the surface ionization and Na exchange constants from this analysis are in actuality the fixed or average value of the reaction quotients, Q_{a_2} and ${}^*Q_{Na^+}$ of equations 9 and 10, that result in the best fit of the calculated curves to the experimental data over the entire titration range rather than the values of the quotients at zero surface charge. Therefore, one would expect these estimates to differ somewhat from the intrinsic constants.

Figures 36, 37, 38, and 39 show plots of $\log[(SO^-) + (SO^-Na^+)]$ versus pH for the four different electrolyte concentrations used in the titrations. The solid points were calculated from the titration data by assuming $[(SO^-) + (SO^-Na^+)] = \sigma_0/B$, where $[(SO^-) + (SO^-Na^+)]$ represents the sum of the contributions from both SOH and TOH sites. The solid curves, labeled SOH and TOH, are generalized curves so positioned that their sum, the dashed curves, gave the best fit to the experimental points. Since the data did not allow an accurate placement of the SOH curve along the pH axis at the low pH range for the 0.1M NaCl solution, it was arbitrarily set with the same spacing relative to the TOH curve as was observed for the other NaCl solutions, i.e., ~ 2 pH units. The limiting values that $\log[(SO^-) + (SO^-Na^+)]$ approached at high pH by the individual SOH and TOH curves, after adjusting their positions in this way, were taken as estimates for N_s for these two sites for the four different electrolyte concentrations. At one-half these limiting values, where $\log[(SO^-) + (SO^-Na^+)] = \log(SOH) = 1/2 \log N_s$, $[K_{a_2} + {}^*K_{Na^+}(Na^+)] = -pH$. Thus, estimates of the $[K_{a_2} + {}^*K_{Na^+}(Na^+)]$ can be obtained for the SOH and TOH sites for the four electrolyte concentrations from the corresponding SOH and TOH curves by identifying the pH values that satisfy this condition. The values of N_s and $[K_{a_2} + {}^*K_{Na^+}(Na^+)]$ estimated from the SOH and TOH curves are given in the figures. For each type of site, the four equations, one for each electrolyte concentration, relating K_{a_2} and ${}^*K_{Na^+}$ were solved simultaneously to give the best values for these parameters. These values are given in Table 16.

TABLE 16. MINEQL Modeling Parameters for the Belle Fourche Clay.

	SOH	TOH
N_s (meq./100 gm)	36	84
pK_{a_2}	4.0	7.1
$p^*K_{Na^+}$	0.24	2.9
$p^*K_{Cs^+}$	- 0.84	1.8

Total surface area = 800 m^2/gm

Total C.E.C. = 120 meq/gm

$K^a_{Cs/Na} = 12$

$C_1 = 500\ \mu F/cm^2$

$C_2 = 20\ \mu F/cm^2$

Site Concentrations

When using a two-site model in MINEQL, the concentrations of the two sites must be entered separately. The apparent ratio of the concentrations of SOH to TOH sites was nearly constant for the 0.001M, 0.01M and 0.1M NaCl solutions, i.e., ~ 0.43, however, the ratio for the 0.0002M NaCl solution was 0.80. A repeat of the titrations yielded essentially the same results. The reason for the difference in the (SOH) to (TOH) ratio between the 0.0002M and the other NaCl concentrations is not known. Since the Cs sorption isotherms were measured over a NaCl concentration range of 0.002M to 1M, a ratio of 0.43 was used to calculate the concentrations of the SOH and TOH sites from the C.E.C. value of 120 meq/100 gms measured for Cs and Na. These values are given in Table 16.

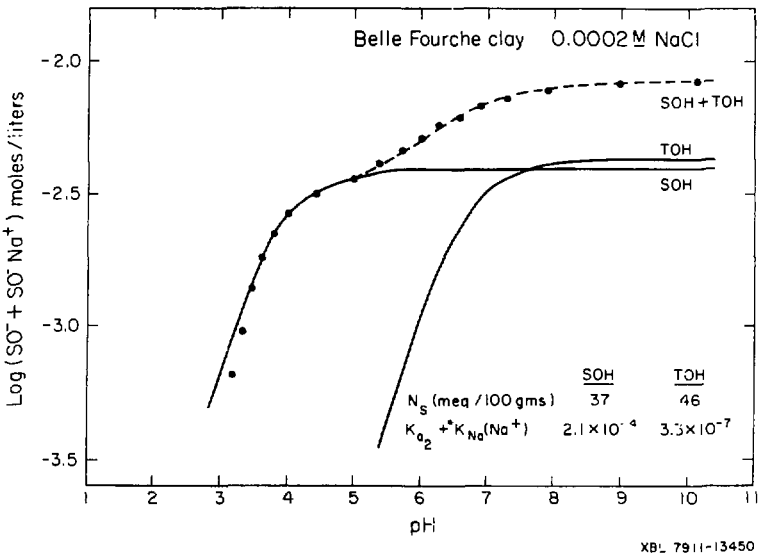

FIGURE 36. The concentration of negative sites, where $[(SO^-) + (SO^-Na^+)]$ represent contributions from both the SOH and TOH sites, as a function of pH for a NaCl electrolyte concentration of 0.0002M. The solid points were calculated from the titration data using equations 36 and 44. The lines result from the fitting of generalized curves based on equation 45 (see text for explanation). Also shown are the site concentrations, N_S, and the values of $[K_{a2} + {}^*K_{Na} + (Na+)]$ for the SOH and TOH sites that result from the fitting analysis.

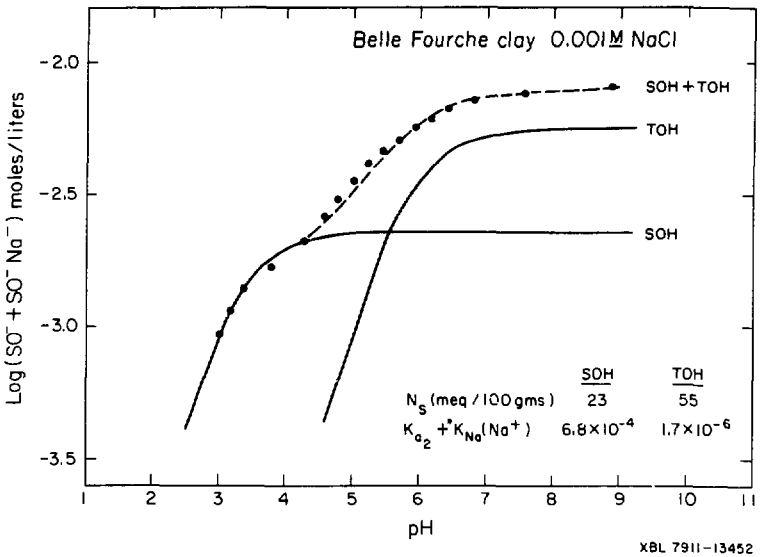

FIGURE 37. The concentration of negative sites, where $[(SO^-) + (SO^-Na^+)]$ represent contributions from both the SOH and TOH sites, as a function of pH for a NaCl electrolyte concentration of 0.001M. The solid points were calculated from the titration data using equations 36 and 44. The lines result from the fitting of generalized curves based on equation 45 (see text for explanation). Also shown are the site concentrations and the values of $[K_{a2} + K_{Na^+}(Na^+)]$ for the SOH and TOH sites that result from the fitting analysis.

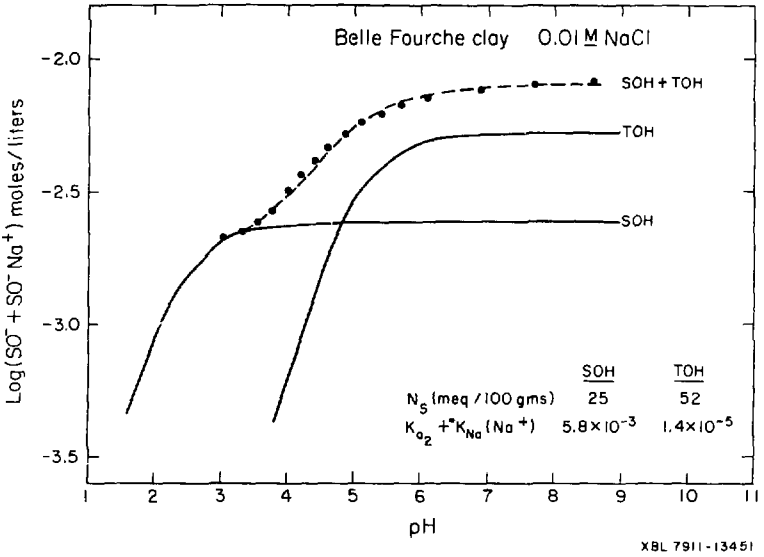

FIGURE 38. The concentration of negative sites, where $[(SO^-) + (SO^-Na^+)]$ represent contributions from both the SOH and TOH sites, as a function of pH for a NaCl electrolyte concentration of 0.01M. The solid points were calculated from the titration data using equations 36 and 44. The lines result from the fitting of generalized curves based on equation 45 (see text for explanation). Also shown are the site concentrations, N_S, and the values of $[K_{a_2} + {}^*K_{Na^+}(Na^+)]$ for the SOH and TOH sites that result from the fitting analysis.

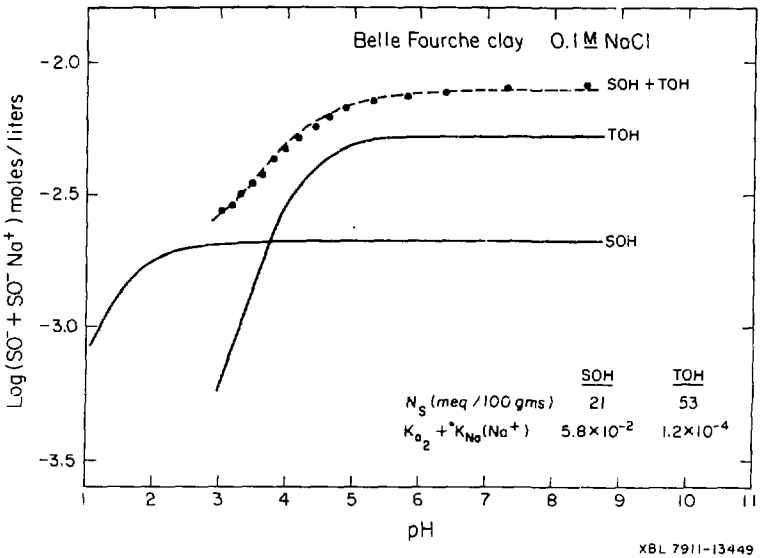

FIGURE 39. The concentration of negative sites, where $[(SO^- + SO^-Na^+)]$ represent contributions from both the SOH and TOH sites, as a function of pH for a NaCl electrolyte concentration of 0.1M. The solid points were calculated from the titration data using equations 36 and 44. The lines result from the fitting of generalized curves based on equation 45 (see text for explanation). Also shown are the site concentrations, N_S, and the values of $[K_{a_2} + {}^*K_{Na} + (Na^+)]$ for the SOH and TOH sites that result from the fitting analysis.

The Cesium Exchange Constant

Given the values of ${}^{*}K_{Na^+}$ estimated in the preceding section, the Cs exchange constant, ${}^{*}K_{Cs^+}$, can be calculated from the values of $K^{a}_{Cs/Na}$ given in Figures 8-13 through the relationship

$$\frac{{}^{*}K_{Cs^+}}{{}^{*}K_{Na^+}} = K^{a}_{Cs/Na} \qquad (46)$$

The values of $K^{a}_{Cs/Na}$ varied from 6.3 to 9.4 over the pH range 5 - 10. Using an average value of 8 and assuming that $K^{a}_{Cs/Na}$ is the same for both types of site, values for ${}^{*}K_{Cs^+}$ were calculated from the corresponding values of ${}^{*}K_{Na^+}$ for the SOH and TOH sites. The first attempts to simulate the Cs sorption isotherms for the clay using these values in MINEQL resulted in calculated K_d values consistently lower than the experimental ones by a factor of about 2 under all conditions. Better overall agreement was obtained using a value of 12 for $K^{a}_{Cs/Na}$. The values for ${}^{*}K_{Cs^+}$ given in Table 16 were obtained using this number. We do not as yet know the reason for this discrepancy.

Integral Capacitances

The integral capacitances of the electrical double layer, C_1 and C_2 in equation 20, are required as input parameters to MINEQL. A value of about 20 $\mu F/cm^2$ has been found for the diffuse layer capacitance, C_2, for Hg (Stumm 1970), AgI (Lyklema 1961), and a number of oxide surfaces (Yates 1974), and has been used successfully for simulated titrations of latexes and clays (James 1979). We have used this value for C_2 in our analysis.

The value of C_1 is customarily taken as an adjustable parameter. It affects the slope of the σ_0 versus pH curves. MINEQL calculates σ_0 for a given set of parameters and thus it is possible to obtain calculated values of σ_0 as a function of pH and electrolyte concentration. Using the other parameters given in Table 16, σ_0 was calculated for electrolyte concentrations

of 0.0002M, 0.001M, 0.01M and 0.1M as a function of pH over the range 3 to 10 for C_1 values of 120, 250, 500, and 750 $\mu F/cm^2$. The calculated curves were compared with the appropriate experimental ones shown in Figure 4. A value of 500 $\mu F/cm^2$ gave the best simulation over the pH range used in the Cs sorption measurements, i.e., 5 to 10, and was used in the subsequent calculations to simulate the Cs sorption isotherms.

Calculations of the Cs Sorption Isotherms

Using the parameters listed in Table 16, Cs sorption isotherms were calculated for the same values of initial Cs concentrations, pH and NaCl concentrations as used in the experimental measurements. The results of these calculations are shown in Figures 40 through 45 (curves) along with the experimental values (points). The solid curves were calculated without including the electrical double layer effects while the dashed curves resulted when they were included. The dashed and solid curves occur in pairs, the top-most pair corresponds to the 0.002M NaCl solution, the next lower pair to the 0.01M NaCl solution, the next lower to 0.1M NaCl, and the lowest to 1M NaCl. Where the solid and dashed curves coincide, only the solid curve is shown.

Comparisons of the calculations with the experimental data shown in the figures demonstrates that MINEQL is able to simulate the Cs sorption isotherms rather well for the most part. The data for the 0.1M and 1M NaCl solutions is fit for all Cs loadings and pH values. However, the MINEQL calculations underestimate the K_d values at the lowest pH for both the 0.002M and 0.01M NaCl solution and overestimate the K_d values for the 0.002M NaCl solution at high pH values. These trends are more easily seen in Figure 46 which shows the variation of K_d with pH for an initial Cs concentration of 10^{-7}M. Again, the points are the experimental values and the curves are the MINEQL simulations. The cause of the deviation between experiment and calculation is being investigated so that corrections can be made. The calculations with and without the inclusion of the electrical double layer effects give essentially the same results for the 0.1M and 1M NaCl solutions. There is a difference for the other NaCl concentrations but the difference decreases with increasing pH. Inclusion of the electrical double layer effects does not improve the overall

There is a difference for the other NaCl concentrations but the difference decreases with increasing pH. Inclusion of the electrical double layer effects does not improve the overall quality of the fit of the calculations to the experimental data. However, it should be remembered that the acid dissociation and sodium exchange constants were extracted from the titration data by essentially ignoring surface charge effects. They represent average values for the entire titration range rather than the actual intrinsic constants for zero surface charge, i.e., there is some average electrical double layer effect included in the constants. Other methods for obtaining the intrinsic constants from the experimental data are being investigated.

There were difficulties in obtaining values for some of the input parameters required by MINEQL in a straightforward manner and further efforts to improve our understanding of the nature of these problems is needed. However, these first attempts to use MINEQL to simulate the Cs sorption isotherms are very encouraging and further testing of the model with other substrates and radionuclides is in progress.

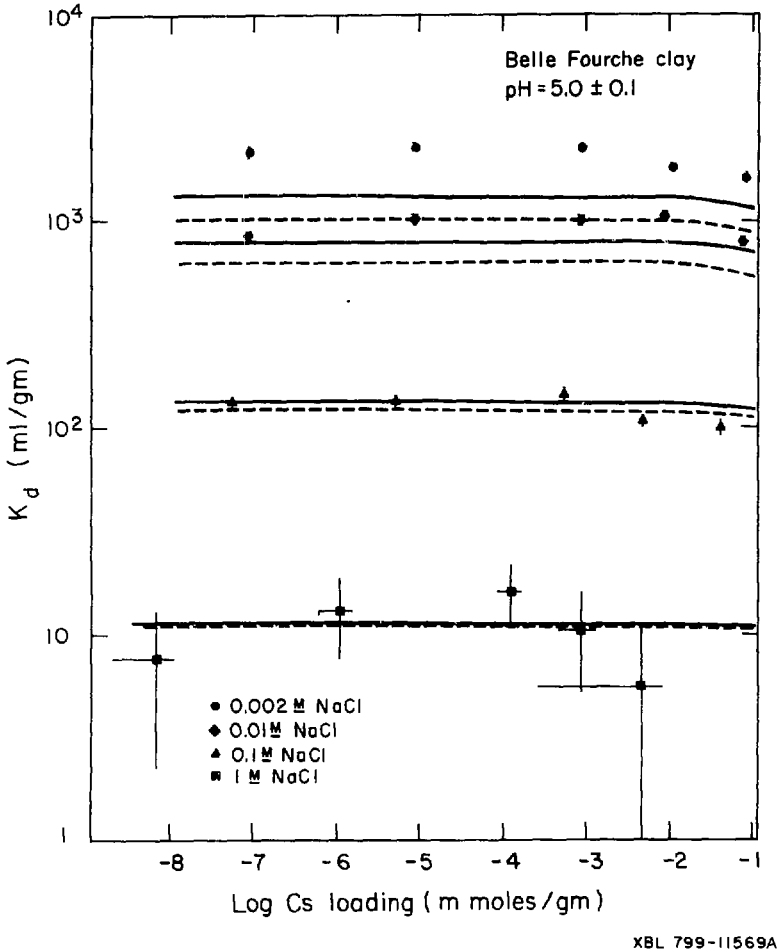

XBL 799-11569A

FIGURE 40. Cs sorption isotherms (26°C) for the Belle Fourche clay for several NaCl electrolyte concentrations at pH 5. The solid points represent the experimental data given in Table 4. The solid and dashed curves were calculated using MINEQL without and with the inclusion of the electrical double layer effects, resp. Upper most pair of solid and dashed curves for 0.002M NaCl.

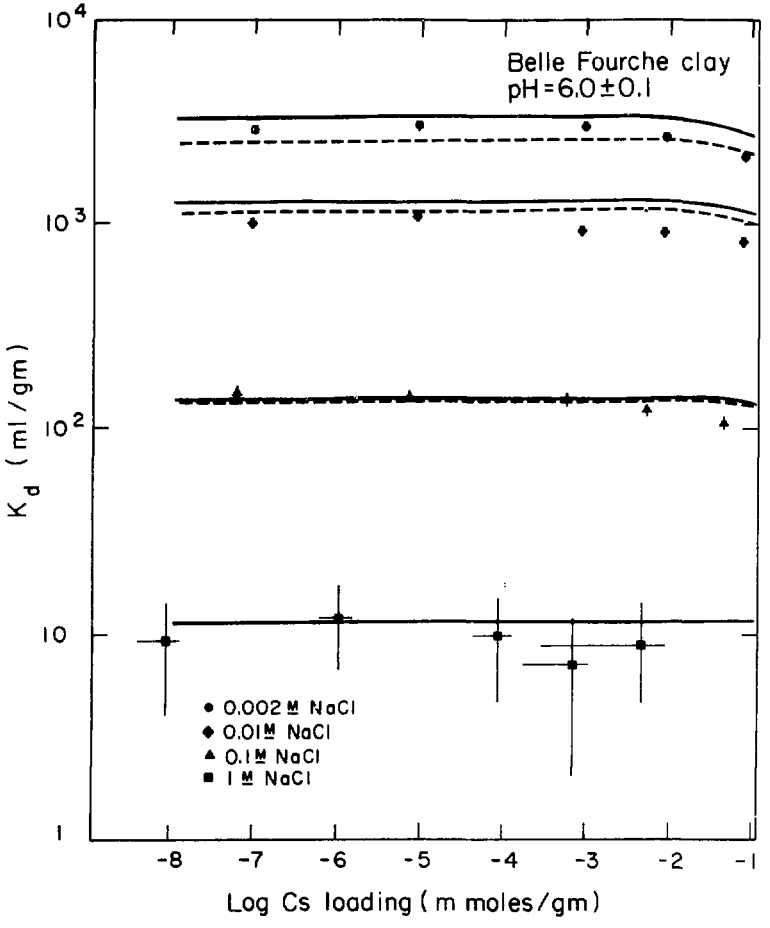

XBL 799-11570A

FIGURE 41. Cs sorption isotherms (26°C) for the Belle Fourche clay for several NaCl electrolyte concentrations at pH 6. The solid points represent experimental data given in Table 4. The solid and dashed curves were calculated using MINEQL without and with inclusion at the electrical double layer effects, resp.

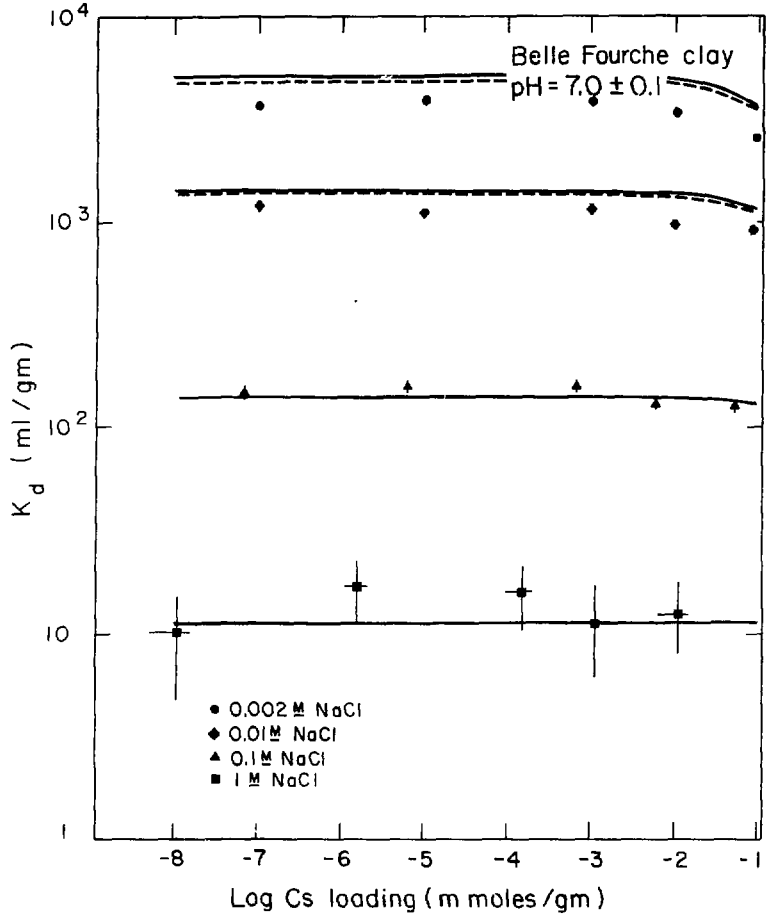

XBL 799-11576A

FIGURE 42. Cs sorption isotherms (26°C) for the Belle Fourche clay for several NaCl electrolyte concentrations at pH 7. The solid points represent experimental data given in Table 4. The solid and dashed curves were calculated using MINEQL without and with inclusion of the electrical double layer effects, resp.

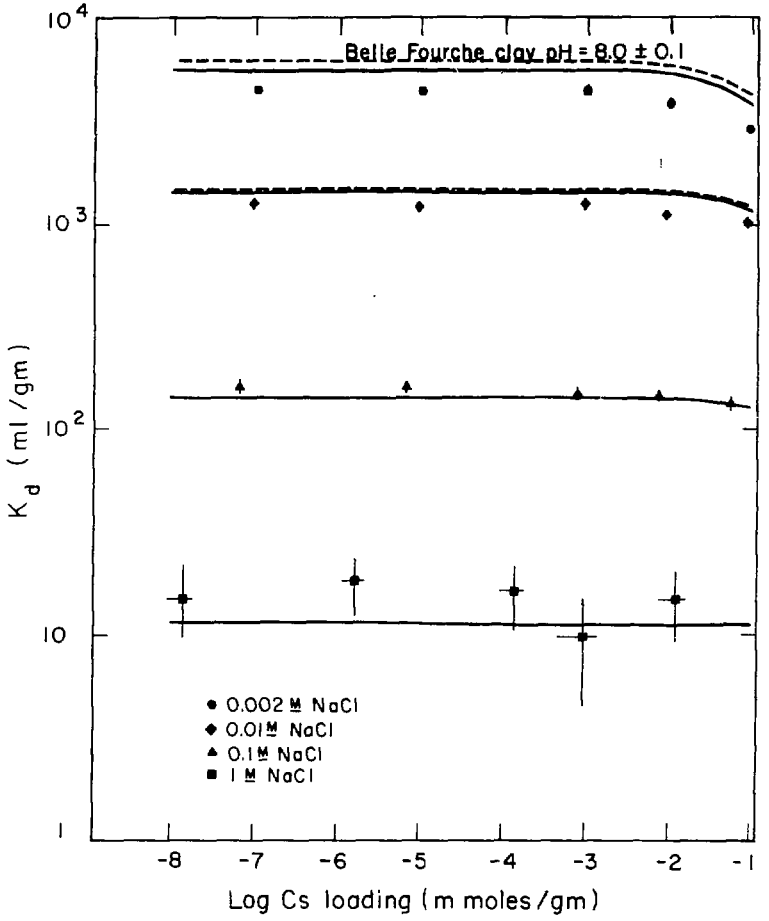

XBL 799-11577A

FIGURE 43. Cs sorption isotherms (26°C) for the Belle Fourche clay for several NaCl electrolyte concentrations at pH 8. The solid points represent experimental data given in Table 4. The solid and dashed curves were calculated using MINEQL without and with inclusion of the electrical double layer effects, resp.

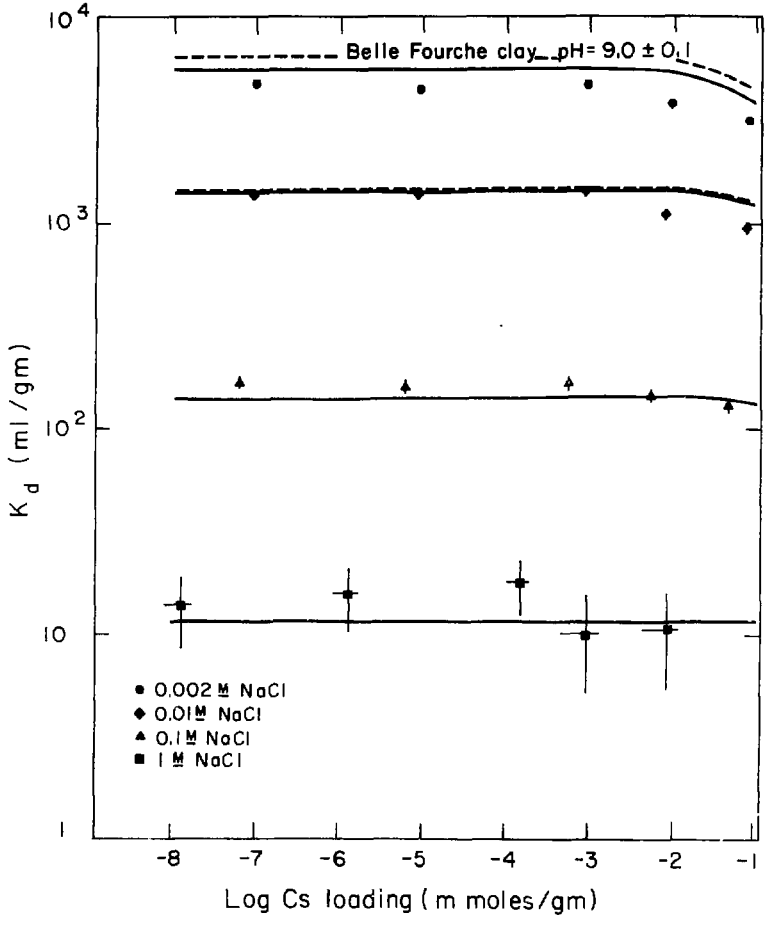

XBL 799-11578A

FIGURE 44. Cs sorption isotherms (26°C) for the Belle Fourche clay for several NaCl electrolyte concentrations at pH 9. The solid points represent experimental data given in Table 4. The solid and dashed curves were calculated using MINEQL without and with inclusion of the electrical double layer effects, resp.

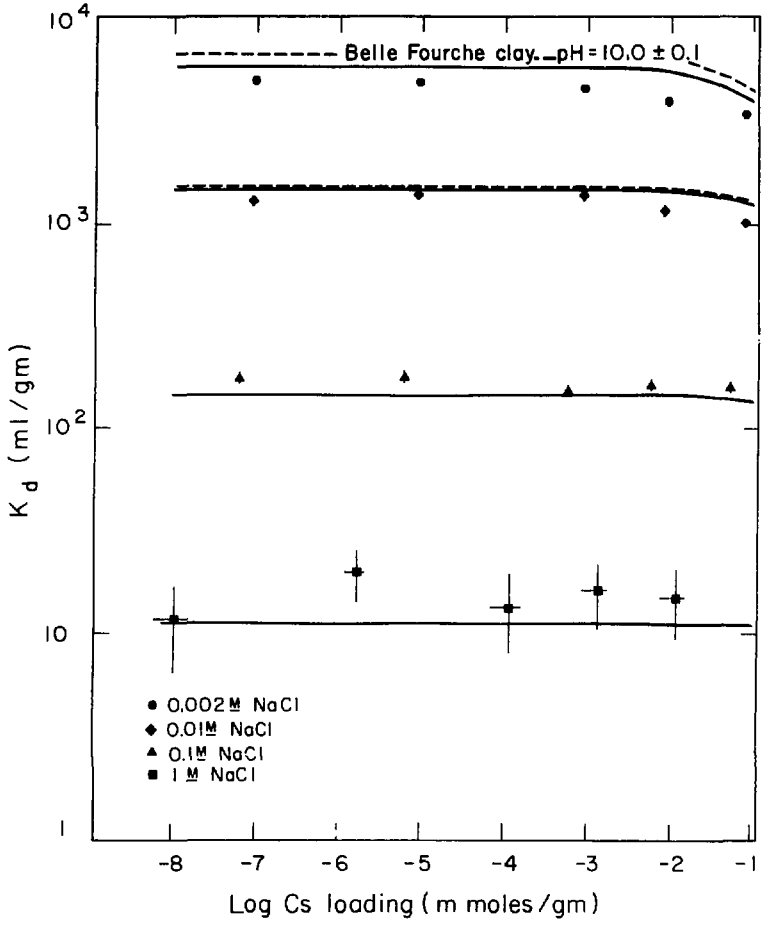

XBL 799-11579A

FIGURE 45. Cs sorption isotherms (26°C) for the Belle Fourche clay for several NaCl electrolyte concentrations at pH 10. The solid points represent experimental data given in Table 4. The solid and dashed curves were calculated using MINEQL without and with inclusion of the electrical double layer effects, resp.

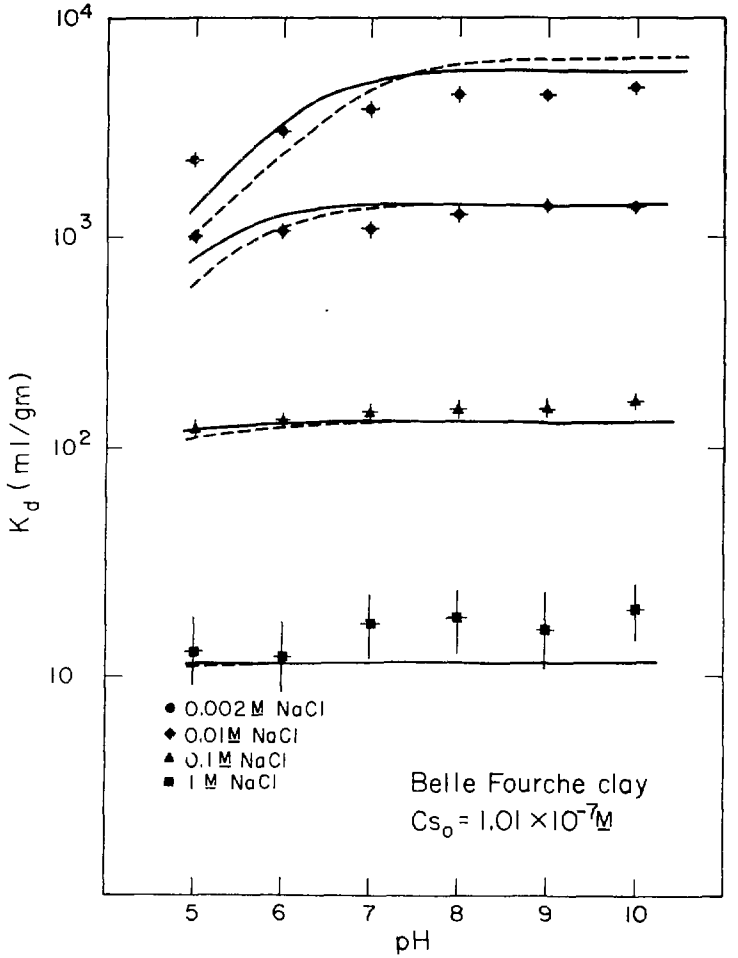

XBL 7911-13448A

FIGURE 46. Variation of distribution coefficients for cesium with pH for an initial Cs solution concentration of 1.01×10^{-7} M for several NaCl electrolyte concentrations. Solid points represent the experimental data given in Table 4. The solid and dashed curves result from calculations using MINEQL without and with the inclusion of the electrical double layer effects, resp.

BIBLIOGRAPHY

REFERENCES SITED

Allen, L. H., E. Matijevic, and L. Meites, 1971. "Exchange of Na^+ for the silanolic protons of silica." J. Inorg. Nucl. Chem. 33: 1293-1299.

Apps, J. A., J. Lucas, A. K. Mathur, and L. Tsao, 1977. Theoretical and Experimental Evaluation of Waste Transport in Selected Rocks: 1977 Annual Report. Lawrence Berkeley Laboratory Report No. 7022, Lawrence Berkeley Laboratory, Berkeley, California.

Aylmore, L. A. G., 1977. "Microporosity in montmorillonite from nitrogen and carbon dioxide sorption." Clay and Clay Minerals. 25: 148-154

Blackman, P. D., 1958. "Neutralization curves and the formulation of monovalent cation exchange properties of clay minerals." Am. J. Sci. 256: 733-743.

Butler, J. N., 1964. Ionic Equilibrium. Addison-Wesley, Reading, Mass.

Chapman, D. L., 1913. "A contribution to the theory of electrocapillarity." Phil. Mag. 25(6): 475-481.

Davis, J. A., R. O. James, and J. O. Leckie, 1978. "Surface ionization and complexation of the oxide/water interface." J. Colloid Interface Sci. 63(3):480-499.

Deer, W. A., R. A. Howie, and J. Zussman, 1963. Rock Forming Minerals. Vol. 4, Framework silicates. John Wiley, New York, N. Y.

Edwards, D. G. and H. P. Quirk, 1962. "Repulsion of chloride by montmorillonite." J. Colloid Sci. 17: 872-882.

Garrels, R. M. and C. L. Christ, 1956. "Application of cation exchange reactions to the beidellite of the putnam silt soil." Amer. Jour. Sci. 254: 372-379.

Gouy, G., 1910. "Sur la constitution de la charge electrique a' la surface d'un electrolyte." Ann. Phys. (Paris). 9(4): 457-468.

Gouy, G., 1917. "Sur la fonction electrocapillaire." Ann. Phys. (Paris). 7(9): 129-184.

Grahame, D. C., 1947. "The electrical double layer and the theory of electrocapillarity." Chem. Rev. 41: 441-501.

Greeland, D. J. and J. P. Quirk, 1962. "Adsorption of 1-n-alkylpyridinium bromides by montmorillonites." Clays and Clay Minerals. 9: 484-499.

Grim, R. E., 1968. Clay Mineralogy. McGraw-Hill, New York, New York.

Hawk, P. B., B. L. Oser, and W. H. Summerson, 1965. Practical Physiological Chemistry. McGraw-Hill, New York, New York.

Helfferich, F., 1962. Ion Exchange. McGraw-Hill, New York, New York.

Hunter, R. J. and H. J. L. Wright, 1971. "The determination of electrokinetic potential on concentration of electrolyte." J. Colloid Interface Sci. 37: 564-580.

Husler, J., 1972. Instrumental Analysis Laboratory Procedures. University of New Mexico, Department of Geology, Albuquerque, New Mexico.

Jackson, M. L., 1975. Soil Chemical Analysis - Advanced Course. published by author, Madison, Wisconsin.

James, R. O., J. A. Davis, and J. O. Leckie, 1978. "Computer simulation of the conductometric and potentiometric titrations of the surface groups on ionizable latexes." J. Colloid Interface Sci. 65(2): 331-344.

James, R. O. and G. A. Parks, 1979. "Characterization of aqueous colloids by their electrical double layer and intrinsic surface chemical properties." Submitted for publication to J. Surface and Colloid Sci.

Jones, B. F. and C. J. Bowser, 1977. "The minerology and related chemistry of lake sediments." Lakes: Chemistry, Geology, Physics, pp. 179-235, Springer Verlag, New York, New York.

Keren, R., R. G. Gast and R. I. Barnhisel, 1977. "Ion exchange reactions in nondried chambers montmorillonite hydroxy-aluminum complexes." Soil Sci. Soc. Am. J. 41: 34-39.

Koltoff, I. M., E. B. Sandell, E. J. Meeham and L. S. Bruckenstein, 1952. Quantitative Chemical Analysis, Macmillan, New York, New York.

Lyklema, J. and J. Th. G. Overbeek, 1961. "Electrochemistry of silver iodide, the capacity of the double layer at the silver iodide-water interface." J. Colloid Interface Sci. 16: 595-608.

McKeague, J. A. and J. H. Day, 1966. "Dithionite- and oxalate-extractable Fe and Al as aids in differentiating various classes of soils." Can. J. Soil Sci. 46: 13-22.

Morin, R. E. and H. S. Jacobs, 1964. "Surface area determination of soils by adsorption of ethylene glycol vapor." Proc. Am. Soil Science Soc. 28: 190-194.

Seidell, A. and W. F. Linke, 1958. Solubilities of Inorganic and Metal Organic Compounds. American Chem. Soc., Washington, D. C.

Sillen, L. G. and A. E. Martell, 1964. Stability Constants and Metal Ion Complexes, Spec. Pub. 17. The Chemical Society, London.

Silva, R. J., L. V. Benson and J. A. Apps, 1978. Theoretical and Experimental Evaluation of Waste Transport in Selected Rocks: 1978 Annual Report. Lawrence Berkeley Laboratory Report No. 8904, Lawrence Berkeley Laboratory, Berkeley, California.

Smith, R. M. and A. E. Martell, 1976. Critical Stability Constants, Vol. 4: Inorganic Complexes. Plenum, New York, New York.

Stumm, W., C. P. Huang, and S. R. Jenkins, 1970. "Specific chemical interactions affecting the stability of dispersed systems." Croat. Chem. Acta., 42: 223-225.

Stumm, W. and J. J. Morgan, 1970. Aquatic Chemistry. Wiley-Interscience, New York, New York.

Truesdell, A. H. and C. L. Christ, 1968. "Cation exchange in clay interpreted by regular solution theory." Am. J. Sci., 266: 402-412.

van Olphen, H., 1977. Clay Colloid Chemistry. Wiley-Interscience, New York, New York.

Westfall. J. C., J. I. Zachary, and F. M. M. Morel, 1976. MINEQL - A Computer Program for the Calculation of Chemical Equilibrium Composition of Aqueous Solutions. Note No. 18, EPA Grant R803738. Dept. Civil Eng., Mass. Inst. Tech. Cambridge, Massachusetts.

Yates, D. E., 1975. PhD. Thesis, Research in Collois and Surface Chemistry: The structure of the oxide/aqueous electrolyte interface. University of Melbourne, Melbourne, Australia.

Yates, D. E., S. Levine, and T. W. Healy, 1974. "Site binding model of the electrical double layer at the oxide/water interface." J. Chem. Soc. Faraday Trans. I. 170: 1807-1818.